UNIVERSIDADE FEDERAL DO RIO GRANDE DO SUL
ESCOLA DE ENGENHARIA
PROGRAMA DE PÓS-GRADUAÇÃO EM ENGENHARIA ELÉTRICA

GUSTAVO RODRIGUES GONÇALVES DA SILVA

MULTIVARIABLE DATA-DRIVEN CONTROL: NON-MINIMUM PHASE SYSTEMS, STATE-FEEDBACK AND CONTROLLER CERTIFICATION

Porto Alegre
2019

GUSTAVO RODRIGUES GONÇALVES DA SILVA

MULTIVARIABLE DATA-DRIVEN CONTROL: NON-MINIMUM PHASE SYSTEMS, STATE-FEEDBACK AND CONTROLLER CERTIFICATION

Thesis presented to Programa de Pós-Graduação em Engenharia Elétrica of Universidade Federal do Rio Grande do Sul in partial fulfillment of the requirements for the degree of Doctor in Electrical Engineering.
Area: Control and Automation

ADVISOR: Prof. Dr. Alexandre Bazanella

CO-ADVISOR: Prof[a]. Dra. Lucíola Campestrini

Porto Alegre
2019

GUSTAVO RODRIGUES GONÇALVES DA SILVA

MULTIVARIABLE DATA-DRIVEN CONTROL: NON-MINIMUM PHASE SYSTEMS, STATE-FEEDBACK AND CONTROLLER CERTIFICATION

This thesis was considered adequate for the awarding of the degree of Doctor in Electrical Engineering and approved in its final form by the Advisor and the Examination Committee.

Advisor: _____
Prof. Dr. Alexandre Bazanella, UFRGS
Doctor by the Universidade Federal de Santa Catarina – Florianópolis, BRA

Examination Committee:

Prof. Dr. Reinaldo Palhares, UFMG
Doctor by the State University of Campinas – Campinas, BRA

Prof. Dr. Júlio Elias Normey Rico, UFSC
Ph.D. by the Universidad de Sevilla – Sevilla, ESP

Prof. Dr. Luís Fernando Alves Pereira, UFRGS
Doctor by the Instituto Tecnológico de Aeronáutica – São José dos Campos, BRA

Prof. Dr. João Manoel Gomes da Silva Junior, UFRGS
Ph.D. by the Université Paul Sabatier – Toulouse, FR

Prof. Dr. Jeferson Vieira Flores, UFRGS
Doctor by the Universidade Federal do Rio Grande do Sul – Porto Alegre, BRA

Coordinator of PPGEE: _____
Prof. Dr. João Manoel Gomes da Silva Junior

Porto Alegre, October 2019.

ABSTRACT

This thesis addresses Data-Driven control methods for multivariable systems, with focus on Non-Minimum Phase systems and an approach for state-feedback in the Linear Quadratic Regulator framework. Since a fundamental assumption in Data-Driven control is that there is no model of the plant available, controllers obtained with these methods come with no guarantee to yield a stabilizing closed-loop, thus the controller certification problem is also tackled in a Data-Driven perspective. The goal is to achieve enhanced Multivariable Data-Driven control methods to cope with a variety of systems and that yield stabilizing controllers and performances similar to the ones specified. One approach is the direct extension of existent Data-Driven methods, which deal with the Model Reference control problem therefore considering transfer matrix systems representation. In this case, special attention is given to Non-Minimum Phase systems and in this work two Data-Driven methods are extended with a flexible criterion to cope with this issue and different structures of the reference model. Another option is to consider state-space systems representation and the corresponding state-feedback design. For this, an algorithm is proposed to cope with the infinite horizon Linear Quadratic Regulator problem, based on a previous predictive approach; in this case there is no issue when dealing with Non-Minimum Phase systems. Finally, a one-shot purely Data-Driven estimation of the $\mathcal{H}_\infty$-norm is proposed and applied to the controller certification problem, along with the estimation byproduct – the system's Markov parameters –, in order to solve the long-lasting stability guarantee issue in Data-Driven methods. Usage of these methods in simulation and experiments on actual systems shows the applicability and improvement of the proposed enhancements. Besides, the proposed non-parametric approach to the controller certification problem shows to outperform the system identification one. Therefore this work provides new tools and a certain level of polishing in the theory for multivariable Data-Driven control methods. Most importantly, all the proposed solutions require only one (maximum two in the noisy case) experiment on the true system.

Keywords: Data-driven control, non-minimum phase systems, controller certification, multivariable control.

RESUMO

Esta tese aborda métodos de controle baseados em dados para sistemas multivariáveis, com foco em sistemas de fase não-mínima e uma abordagem utilizando realimentação de estados dentro do escopo do Regulador Linear Quadrático. Como a hipótese principal no controle baseado em dados é que não se tem um modelo da planta, controladores obtidos com esses métodos não possuem garantias de resultar em uma malha fechada estável, então o problema de certificação do controlador também é tratado em uma abordagem baseada em dados. O objetivo é alcançar métodos aprimorados de controle multivariável baseados em dados para lidar com uma variedade de sistemas e que gerem controladores estabilizantes e com desempenho similar ao especificado. Uma abordagem é a extensão direta de métodos baseados em dados existentes, os quais lidam com o problema de controle por Modelo de Referência considerando, então, a representação por matriz de transferência. Nesse caso, atenção especial é dada para sistemas de fase não-mínima e neste trabalho dois métodos baseados em dados são estendidos com um critério flexível para lidar com esse problema e com diferentes estruturas do modelo de referência. Outra opção é considerar a representação de sistemas em espaço de estados e o respectivo projeto de realimentação de estados. Para isso, é proposto um algoritmo a fim de sintonizar um Regulador Linear Quadrático para horizonte infinito; nesse caso, não há restrições ao lidar com sistemas de fase não-mínima. Por fim, um método direto baseado em dados para estimação da norma $\mathcal{H}_\infty$ é proposto e aplicado ao problema de certificação, junto com o subproduto da estimativa (os parâmetros de Markov do sistema), a fim de resolver o problema de garantia de estabilidade em métodos baseados em dados. A aplicação desses métodos em simulação e em experimentos reais mostram a aplicabilidade e as melhorias propostas. Além disso, mostra-se que a abordagem não-paramétrica proposta para o problema de certificação supera a abordagem por identificação do sistema. Portanto, este trabalho fornece novas ferramentas e um certo nível de refinamento na teoria para métodos de controle multivariável baseados em dados. Sobretudo, todas as soluções propostas requerem apenas um experimento no sistema real (ou dois no caso com ruído).

Palavras-chave: Controle baseado em dados, sistemas de fase não-mínima, certificação de controladores, controle multivariável.

LIST OF FIGURES

LIST OF TABLES

LIST OF ABBREVIATIONS

ARMAX	Autoregressive Moving Average with Exogenous Inputs
BIBO	Bounded Input Bounded Output
BJ	Box-Jenkins
CbT	Correlation-based Tuning
DARE	Discrete-time Algebraic Riccati Equation
DD	Data-Driven
FIR	Finite Impulse Response
IFT	Iterative Feedback Tuning
IMC	Internal Model Control
LQR/LQG	Linear Quadratic (Gaussian) Regulator
LTI	Linear Time Invariant
MIMO	Multiple-Input Multiple-Output
MR	Model Reference
NMP	Non-Minimum Phase
OCI	Optimal Controller Identification
OE	Output-Error
PE	Prediction Error
PID	Proportional-Integral-Derivative
PRBS	Pseudo-Random Binary Signal
PWM	Pulse Width Modulation
SISO	Single-Input Single-Output
SNR	Signal-to-Noise Ratio
SVD	Singular Value Decomposition
THD	Total Harmonic Distortion
UPS	Uninterruptible Power Supply
VRFT	Virtual Reference Feedback Tuning

WN	White Noise
WNC	Winding Number Condition

LIST OF SYMBOLS

$\mathbb{R}$	Set of real values
$\mathbb{C}$	Set of complex values
q	Forward-shift operator
P	Controller parameters
η	Flexible Reference Model parameters
u_z	Input zero direction
y_z	Output zero direction
M_i	i-th Markov parameter
N_m	number of Markov parameter
Ψ	Additional noise model parameters
Θ	Composite controller and noise model parameters
$\beta(q)$	Controller parametrization transfer functions vector
$\vartheta(q)$	Reference Model parametrization transfer functions vector
$\psi(q)$	System pole polynomial
$\phi(q)$	System zero polynomial
$\varphi(q)$	Regression vector
l	Number of outputs
m	Number of states
p	Number of inputs
$\bar{\sigma}$	Largest Singular Value
$x(t)$	System state vector
$x_c(t)$	Internal Model Controller state vector
$u(t)$	System input vector
$y(t)$	System output vector
$v(t)$	System noise vector
$\nu(t)$	System state noise vector

$r(t)$	System reference vector
$d(t)$	System disturbance vector
$e(t)$	Reference tracking error vector
$y'(t)$	Instrumental Variable vector
$\epsilon(t, \cdot)$	Prediction error
(A, B, C, D)	State-Space matrices of an LTI system
(E, F)	State-Space matrices relating noises in an LTI system
(A_c, B_c)	Internal Model Controller State-Space matrices
K	State Feedback controller
X	DARE solution
I	Identity matrix
$U\Sigma V$	Singular Value Decomposition matrices
Q, R	LQR performance matrices
$\mathbf{M}$	Markov parameters vector
$\mathbf{O}$	Extended Observability matrix
$\mathbf{S}$	Toeplitz matrix of Markov parameters
A^T	Transpose of A
A^H	Conjugate transpose of A
a^*	Complex conjugate of a
$G_0(q)$	Transfer matrix of the plant
$H_0(q)$	Transfer matrix of the noise model
$C_d(q)$	Ideal Controller Transfer Matrix
$C(q, P)$	Parametrized Controller Transfer Matrix
$T_d(q)$	Reference Model
$T_d(q, \eta)$	Parametrized Reference Model
$L_d(q, \eta)$	Parametrized Loop Transfer Matrix
$F(q)$	Filter used in DD methods
$L_a(q)$	All-pass zero filter
$L_I(q)$	Input zero filter
$L_O(q)$	Output zero filter
$L(q)$	Loop Function
$S(q)$	Sensitivity Function
$T(q)$	Closed-loop (Complementary Sensitivity) Function
$H_{G_0,C}$	Generalized Stability Matrix

$b_{G_0,C}$	Generalized Stability Margin
δ_ν	Vinnicombe's ν-gap metric
$\mathcal{T}$	Controller Certification Objective Function
(E_i, F_i)	Right-Coprime factors
(U_i, V_i)	Left-Coprime factors
(W_i, Y_i)	Robust Performance Objective Functions
$\mathcal{E}(\cdot)$	Expectation Function
$\mathcal{B}(\cdot)$	Bias Function
$\mathcal{C}$	Controller Class
$\mathcal{R}$	Set of real-rational proper transfer functions
$\mathcal{H}_\infty$	Space of functions bounded and analytic in the complement of the closed unit disc

CONTENTS

1 INTRODUCTION

Hello, hello, Martian. Here who speaks is from Earth.

Elis Regina

Data-Driven (DD) control design methods can be understood as the solution of classical control problems – which often have model-based solutions – through data collected from the system but without deriving a mathematical model of the plant. That is, data are used to tune directly the controller parameters of a fixed structure trying to achieve some performance criteria. DD control design methods can be seen as the identification of the controller instead of the plant.

In the past two decades, a number of Data-Driven control design methods have been proposed (CAMPI; LECCHINI; SAVARESI, 2002; HJALMARSSON *et al.*, 1998; HJALMARSSON; GUNNARSSON; GEVERS, 1994; KARIMI; MIŠKOVIĆ; BONVIN, 2004; CAMPESTRINI *et al.*, 2017), where a parametrized controller structure is chosen *a priori*, and the controller tuning is based directly on input and output data collected on the plant, without the use of a model of this plant. These DD schemes are mostly derived as a solution to the classical Model Reference control problem (GOODWIN; SIN, 1984).

Assuming that one can create a universal method to tune the controller parameters – that at least leads to stable closed loop – without any knowledge of the process to be controlled is, of course, a utopia. Some prior knowledge about the process is needed, as in any control problem, mainly to strengthen tuning of stabilizing controllers; notably the process relative degree and its Non-Minimum Phase (NMP) zeros. Since these methods appear as the solution of Model Reference control, smart choices on the reference model play an important role in the success of DD control methods (BAZANELLA *et al.*, 2008), but this step seems to be overlooked in the literature (GONÇALVES DA SILVA; BAZANELLA; CAMPESTRINI, 2018).

These DD controller tuning methods may fail when the plant has NMP zeros that are not included in the desired reference model, leading possibly to an unstable closed loop. A safe way to avoid it is by including the NMP zeros in the desired reference model. Doing this *a priori*, when choosing the reference model, requires the knowledge of this zero. This issue is not related to the DD nature of the design *per se*, but is inherent

to the Model Reference approach which is the basis of these DD methods, and as such is well documented in the literature of direct adaptive control as well (see, for instance, (IOANNOU; SUN, 2012)). It is troubling enough in the SISO (single-input single-output) case, and yet it is much more serious in the MIMO (multiple-input multiple-output) case, because the transmission zeros of MIMO plants are hard to spot.

Indeed, the characteristic inverse response to a step input in SISO plants alerts the user to the presence of one NMP zero; the more crossings to the initial steady state, the more NMP zeros. In MIMO systems this does not necessarily happen, because zeros have associated input and output directions; it may even happen that one can observe an inverse response in one loop but the corresponding NMP zero is not an NMP multivariable zero (SKOGESTAD; POSTLETHWAITE, 2005). Previous work related to the NMP SISO case has been addressed in (CAMPESTRINI *et al.*, 2011) but there is still a gap for a DD method related to NMP MIMO systems.

Another classical control problem that has been tackled in a data-based perspective is the Linear Quadratic (Gaussian) Regulator (LQR/LQG) (SKELTON; SHI, 1994; AANGENENT *et al.*, 2005; FURUTA; WONGSAISUWAN, 1995). In their work however the problem is solved in order to compute directly the optimal control action at each time instant, instead of the control gain. This approach has more a predictive control than a DD control framework resemblance, as the problem is taken for finite horizon and it is assumed that the state is not measurable. In this thesis we change the perspective and drop some constraints as to better fit in the DD control scope: we assume that the state is measurable, since the control gain is fix, and because the gain is fix, we use the approach for infinite horizon LQR. An advantage of using state feedback with a performance criterion (the Q and R matrices of LQR) that is not as rigid as the Model Reference approach is that NMP plants do not pose additional issue in the implementation of the method.

Nonetheless, Data-Driven control *per se* is not restricted to controller tuning methods, and applications to fault detection and closed-loop assessment have been reported (KHAKIPOUR; SAFAVI; SETOODEH, 2017; LIU; GAO, 2017; YOUSSEF *et al.*, 2017; DU *et al.*, 2017). Some of these applications require the $\mathcal{H}_\infty$-norm estimation of a transfer matrix. A related problem regarding $\mathcal{H}_\infty$-norm estimation is the so-called controller certification (PARK; BITMEAD, 2008). The problem can be described as follows: given an initial stabilizing controller operating in closed-loop with an un-modeled system and a second controller that is to be put in place of the initial controller, how can we assure that this new controller will also, at least, stabilize the plant based on data collected from the closed-loop? The solution to this problem usually involves the distance between the two controllers and the $\mathcal{H}_\infty$-norm estimation of a given generalized stability function. The $\mathcal{H}_\infty$-norm estimation itself is an issue to be dealt with and approaches using interpolation of some frequency response points (PARK, 2008; CHEONG; BITMEAD, 2012) or the system Markov parameters (OOMEN *et al.*, 2014) have been reported.

Main approaches to the certification problem derives from (VINNICOMBE, 1993), where the ν-gap metric has been introduced and showed to satisfy a sufficient condition to guarantee certification, and has since then been used as the standard tool in controller certification procedures (PARK; BITMEAD, 2004, 2007; CHEONG; BITMEAD, 2012). However, when the plant is unknown this constraint is hard to be validated and can also be too conservative. A different closed-loop configuration is proposed in (DEHGHANI *et al.*, 2009), in order to collect data and certify the new controller, circumventing the test via the ν-gap criterion. The proposed data-based approach however requires many experiments, as the constraint studied depends on the frequency response of a given transfer function.

In this work we bring their mappings to the standard closed-loop configuration, not only for stability purposes, but also for robust performance assessment. We also show that a similar procedure applies when data are collected in open-loop (i.e., there is no initial stabilizing controller), given that the plant is open-loop stable. All these tests are based on an $\mathcal{H}_\infty$-norm criterion of given transfer functions, thus we present an algorithm to estimate the respective $\mathcal{H}_\infty$-norm directly from data obtained from *one single experiment*, without identifying a respective parametrized transfer function (matrix). We also show that our non-parametric approach outperforms the system identification one.

The contributions of this thesis are: extensions to two one-shot data-driven methods to cope with unknown NMP transmission zeros; a data-driven approach to the infinite horizon LQR control; a one-shot data-driven controller certification procedure with robust stability assessment. Accordingly, the innovative aspects treated here are: direct identification of the NMP transmission zeros location and direction ratio without identifying the whole MIMO system; one-shot $\mathcal{H}_\infty$-norm estimation; purely data-driven controller certification procedure.

The thesis is divided as follows: a brief overview of multivariable systems and the data-driven control approach are presented in Chapter 2. Contributions are divided in the following chapters. In Chapter 3 the extensions of two DD methods to cope with unknown NMP transmission zero are presented with some illustrative examples. The main results of this chapter have been published in (GONÇALVES DA SILVA; CAMPESTRINI; BAZANELLA, 2016, 2018). Chapter 4 deals with a different control approach: the LQR control, so it is meant to be self-contained. This chapter resulted in the article (GONÇALVES DA SILVA *et al.*, 2019). Finally, a one-shot data-driven controller certification and robust performance assessment approach is presented Chapter 5. At the moment, these results have been accepted in an article sent to *ISA Transactions*, but not yet published. Concluding remarks are then given in Chapter 6.

2 MULTIVARIABLE SYSTEMS AND DATA-DRIVEN CONTROL

Everybody 1, 2, step. We about to get it on.

Ciara

This chapter presents the basic definitions and tools which will be used along this thesis. We start by giving two different system representations and their equivalence, followed by the definitions of poles, zeros and their directions for MIMO systems described as transfer matrix. These definitions apply to SISO systems as they can be seen as 1×1 matrix. In the three subsequent sections the control problem approached in this work is stated, two existing direct DD methods are presented and finally closed-loop stability is discussed.

2.1 System representations

Consider a linear time-invariant discrete-time multiple-input multiple-output (MIMO) process

$$\begin{aligned} y(t) &= G_0(q)u(t) + v(t) \\ &= G_0(q)u(t) + H_0(q)w(t), \end{aligned} \tag{1}$$

where q is the forward-shift operator, such that $qx(t) = x(t+1)$, $u(t)$ is a p-dimension input vector, $y(t)$ an l-dimension output vector and $w(t)$ is a zero mean white noise p-dimension vector with co-variance $\sigma^2_{w_i}$. $G_0(q)$ is a transfer matrix representing the process and $H_0(q)$ is the noise model.

System representation (1) gives the direct relation between the system's input and output. Another description of the system, which considers its internal variables, namely its *state vector*, is given by

$$\begin{aligned} x(t+1) &= Ax(t) + Bu(t) + Ew(t) \\ y(t) &= Cx(t) + Du(t) + Fw(t) \end{aligned} \tag{2}$$

where $x(t)$ is an m-dimension state vector. System matrices are of size $A \in \mathbb{R}^{m\times m}$, $B \in \mathbb{R}^{m\times p}$, $E \in \mathbb{R}^{m\times p}$, $C \in \mathbb{R}^{l\times m}$, $D \in \mathbb{R}^{l\times p}$ and $F \in \mathbb{R}^{l\times p}$.

The relation between $G_0(q)$ and the system (A, B, C, D) is given by:

$$G_0(q) = C(qI - A)^{-1}B + D, \tag{3}$$

with I the identity matrix, and for the noise model we have

$$H_0(q) = C(qI - A)^{-1}E + F. \tag{4}$$

For the remaining of this thesis we shall consider, unless pointed out differently, $p = l \triangleq n$, i.e., both $G_0(q)$ and $H_0(q)$ are *square* $n \times n$ matrices whose elements are proper rational transfer functions.

2.2 Poles, zeros, directions and Markov parameters

Definitions of poles and zeros of a linear time-invariant system and their respective directions are introduced in this section. We also review the concept of the system Markov parameters and their relation with the system impulse response.

2.2.1 Poles

The following definition gives the poles corresponding to the system's minimal realization directly from the transfer matrix $G_0(q)$.

Definition 2.1. (MACFARLANE; KARCANIAS, 1976) *The pole polynomial $\phi(q)$ corresponding to a transfer matrix $G_0(q)$ is the least common denominator of all non-identically null minors of all orders of $G_0(q)$.*

Example 2.1. *Consider the 2×3 system*

$$G_0(q) = \begin{bmatrix} \dfrac{1}{(q-0.9)} & 0 & \dfrac{(q-1.2)}{(q-0.9)(q-0.8)} \\ \dfrac{-1}{(q-1.2)} & \dfrac{1}{(q-0.8)} & \dfrac{1}{(q-0.8)} \end{bmatrix}.$$

The rank of the system is 2, since the third column can be obtained by multiplying the first column by $\frac{q-1.2}{q-0.8}$ and adding the second column multiplied by 2. The minors of order 1 from the elements different from zero are:

$$\frac{1}{q-0.9}, \ \frac{q-1.2}{(q-0.9)(q-0.8)}, \ \frac{-1}{q-1.2}, \ \frac{1}{q-0.8}, \ \frac{1}{q-0.8}.$$

The minors of order 2 are

$$\frac{-(q-1.2)}{(q-0.9)(q-0.8)^2}, \ \frac{2}{(q-0.9)(q-0.8)}, \ \frac{1}{(q-0.9)(q-0.8)}.$$

Considering all minors, the least common denominator is

$$\phi(q) = (q - 1.2)(q - 0.9)(q - 0.8)^2.$$

Thus, the system has four poles: one at $q = 1.2$*, one at* $q = 0.9$ *and two at* $q = 0.8$*.*

From the example above, it can be noticed that the poles of MIMO systems are essentially the poles of the elements. However it is not possible to determine their multiplicity by only looking at the matrix elements.

2.2.2 Zeros and transmission zeros

The zeros of a system arise when internal effects compete such that the output is identically null even when the inputs (and the states) are not themselves identically null. For a SISO system, the zeros z_i are solution of $G_0(z_i) = 0$. Overall, we can argue that zeros are the values of q for which $G_0(q)$ looses rank (from rank 1 to rank 0 for SISO systems). However, this definition includes values of q equal to the poles and values at infinity. In order to avoid further misunderstanding, the term *zero* will be used for the zeros in each matrix element and the terms *transmission zero* and *multivariable zero* for the zeros defined in the following definition.

Definition 2.2. (MACFARLANE; KARCANIAS, 1976) *The **finite** transmission zeros polynomial* $\psi(q)$ *of a system* $G_0(q)$ *is the greatest common divisor of all numerators of all minors of order* n_r *of* $G_0(q)$*, where* n_r *is the normal rank of* $G_0(q)$*, once these minors have been adjusted as to have the pole polynomial* $\phi(q)$ *as their denominator.*

The normal rank of $G_0(q)$ is defined as the rank of $G_0(q)$ in all values of q except for a finite number of singularities (which are the transmission zeros). For SISO systems, zeros and transmission zeros are equivalent. The transmission zeros can be interpreted as the (discrete) exponentials which, when present in the input signal, are blocked in the output. Transmission zeros whose module are greater than 1 are called Non-Minimum Phase (NMP).

Example 2.2. *Consider the following* 2×2 *system,* ***which will be extensively worked around throughout this thesis****:*

$$G_0(q) = \begin{bmatrix} \dfrac{(q - 0.7)}{(q - 0.9)(q - 0.8)} & \dfrac{2}{(q - 0.8)} \\ \dfrac{1.25}{(q - 0.8)} & \dfrac{1.5}{(q - 0.8)} \end{bmatrix}, \tag{5}$$

and whose response to a sequence of steps is portrayed in Figure 1.

The normal rank of $G_0(q)$ *is* 2 *and the minor of order* 2 *is the determinant*

$$det(G_0(q)) = \frac{1.5(q - 0.7) - 2.5(q - 0.9)}{(q - 0.9)(q - 0.8)^2} = \frac{-(q - 1.2)}{(q - 0.9)(q - 0.8)^2}.$$

Figure 1 – Open-loop response of the NMP system (5) to a sequence of steps.

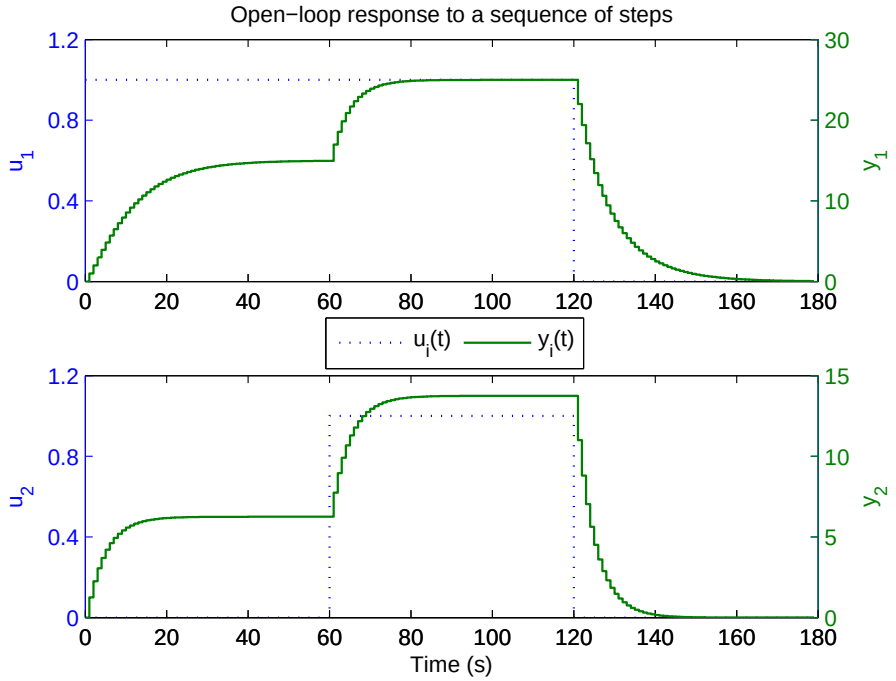

Source: author.

From Definition 2.1 the pole polynomial is $\phi(q) = (q - 0.9)(q - 0.8)^2$ *so the transmission zero polynomial is* $\psi(q) = -(q - 1.2)$*. Thus,* $G_0(q)$ *has an NMP transmission zero at* $q = 1.2$*.*

This example illustrates that, in general, multivariable zeros have no direct relation to the zeros of the transfer matrix elements, unlike the poles. Notice also that the usual inverse response effect due to NMP zero is not apparent in Figure 1. This is due to zero directions, which will be discussed next.

If $G_0(q)$ is a square matrix then the following is usually true:

$$\frac{\psi(q)}{\phi(q)} = \det\left(G_0(q)\right). \tag{6}$$

There are particular cases where pole-zero cancellation in (6) does not *necessarily* yield the system poles and transmission zeros, as in triangular systems (SKOGESTAD; POSTLETHWAITE, 2005).

2.2.3 Poles and zeros directions

In multivariable systems, poles and multivariable zeros have directions associated to them. These directions give an indication on how much a mode is excited by the inputs and how much they are expressed at the output.

Theorem 2.1. (HAVRE; SKOGESTAD, 1996) (ZERO DIRECTIONS) *If* $G_0(q)$ *has a transmission zero for* $q = z_i \in \mathbb{C}$*, then there exist non-null vectors called zero input*

direction $u_{z_i} \in \mathbb{C}^p$ *and zero output direction* $y_{z_i} \in \mathbb{C}^l$*, such that* $u_{z_i}^H u_{z_i} = 1$*,* $y_{z_i}^H y_{z_i}$*=1, and*

$$G_0(z_i)u_{z_i} = 0 \quad \textit{and} \tag{7}$$

$$y_{z_i}^H G_0(z_i) = 0. \tag{8}$$

From a practical point of view, the zero output direction y_{z_i} is usually of greater importance, since y_{z_i} gives an information of what (combination of) output is harder to control. It also imposes a constraint for closed-loop stability when the transmission zero is NMP, as will be discussed later. The input direction is the direction of inputs for which the usual inverse response effect is more apparent in the output response.

Theorem 2.2. (HAVRE; SKOGESTAD, 1996) (POLE DIRECTIONS) *If* $G_0(q)$ *has a pole for* $q = p_i \in \mathbb{C}$*, then there exist non-null vectors called pole input direction* $u_{p_i} \in \mathbb{C}^p$ *and pole output direction* $y_{p_i} \in \mathbb{C}^l$*, such that* $u_{p_i}^H u_{p_i} = 1$*,* $y_{p_i}^H y_{p_i}$*=1, and*

$$G_0(p_i)u_{p_i} = \infty \quad \textit{and} \tag{9}$$

$$y_{p_i}^H G_0(p_i) = \infty. \tag{10}$$

The zero directions u_{z_i} and y_{z_i} can be obtained from the Singular Value Decomposition (SVD) of $G_0(z_i) = U\Sigma V^H$. We have that u_{z_i} is the *last* column of V (corresponding to the singular value zero) and y_{z_i} is the *last* column of U. As for the pole directions, since the gain is infinite, then one can not compute the directions directly by $G_0(p_i)$, as for the zeros. In this case consider $G_0(p_i + \varepsilon)$, with $\varepsilon \to 0$. Thus u_{p_i} is the *first* column of V (corresponding to the singular value "infinite") and y_{p_i} is the *first* column of U (SKOGESTAD; POSTLETHWAITE, 2005). Besides, if the inverse of $G_0(p_i)$ exists then the pole direction can be computed as the zero directions of $G_0^{-1}(p_i)y_{p_i} = 0$. Notice that for SISO systems all these direction vectors equal to 1.

We highlight that the procedure above applies when poles and multivariable zeros are distinct, otherwise there will be more than one singular value equal to zero (or infinite) and one can not assure the chosen vectors are correct. For the case of poles and transmission zeros with multiplicity greater than 1 a generalized eigenvalue problem can be solved using the system state space representation (HAVRE, 1998). For the scope of this work, pole and zero directions will be of importance only when the respective poles and transmission zero are outside the unit circle. In this case, most of actual systems behave in a way that usually there are not two equal unstable modes. Also, only the output direction will be of interest for closed-loop stability purposes as will be seen in Section 2.5.

Example 2.3. *Consider the system in Example 2.2, which has a multivariable zero at* $z_i = 1.2$*, one pole at* $p_i = 0.9$ *and two poles at* $p_i = 0.8$*. The input and output directions of the elements with multiplicity* 1 *are determined using the SVD. For the transmission*

zero we have:

$$G_0(z_i) = G_0(1.2) = \begin{bmatrix} \frac{25}{6} & 5 \\ \frac{25}{8} & \frac{15}{4} \end{bmatrix} = \begin{bmatrix} -0.8 & -0.6 \\ -0.6 & 0.8 \end{bmatrix} \begin{bmatrix} \frac{25\sqrt{61}}{24} & 0 \\ 0 & 0 \end{bmatrix} \begin{bmatrix} \frac{-5\sqrt{61}}{61} & \frac{-6\sqrt{61}}{61} \\ \frac{-6\sqrt{61}}{61} & \frac{5\sqrt{61}}{61} \end{bmatrix}^H$$

The input and output directions are associated to the singular value zero, thus $u_{z_i} = \begin{bmatrix} \frac{-6\sqrt{61}}{61} \\ \frac{5\sqrt{61}}{61} \end{bmatrix}$ *and* $y_{z_i} = \begin{bmatrix} -0.6 \\ 0.8 \end{bmatrix}$. *For the input-output direction of the pole at* 0.9, *consider:*

$$G_0(p_i + \varepsilon) = G_0(0.9 + \varepsilon) = \begin{bmatrix} \frac{0.2+\varepsilon}{\varepsilon(0.1+\varepsilon)} & \frac{2}{0.1+\varepsilon} \\ \frac{1.25}{0.1+\varepsilon} & \frac{1.5}{0.1+\varepsilon} \end{bmatrix} =_{\varepsilon \to 0} \begin{bmatrix} -1 & 0 \\ 0 & 1 \end{bmatrix} \begin{bmatrix} \frac{2}{\varepsilon} & 0 \\ 0 & 0 \end{bmatrix} \begin{bmatrix} -1 & 0 \\ 0 & 1 \end{bmatrix}^H$$

The input and output directions are associated to the singular value $2/\varepsilon$, *thus* $u_{p_i} = \begin{bmatrix} -1 \\ 0 \end{bmatrix}$ *and* $y_{p_i} = \begin{bmatrix} -1 \\ 0 \end{bmatrix}$.

We omit here the procedure for the poles at 0.8 *as it is out of the scope of this thesis.*

To complete the example, Figure 2 shows the system response to an input $u(t) = -2 \begin{bmatrix} \frac{-6\sqrt{61}}{61} \\ \frac{5\sqrt{61}}{61} \end{bmatrix}$, *which is multiple of the transmission zero input direction. Notice that now*

Figure 2 – Open-loop response of the NMP system (5) to an input multiple of the NMP transmission zero input direction.

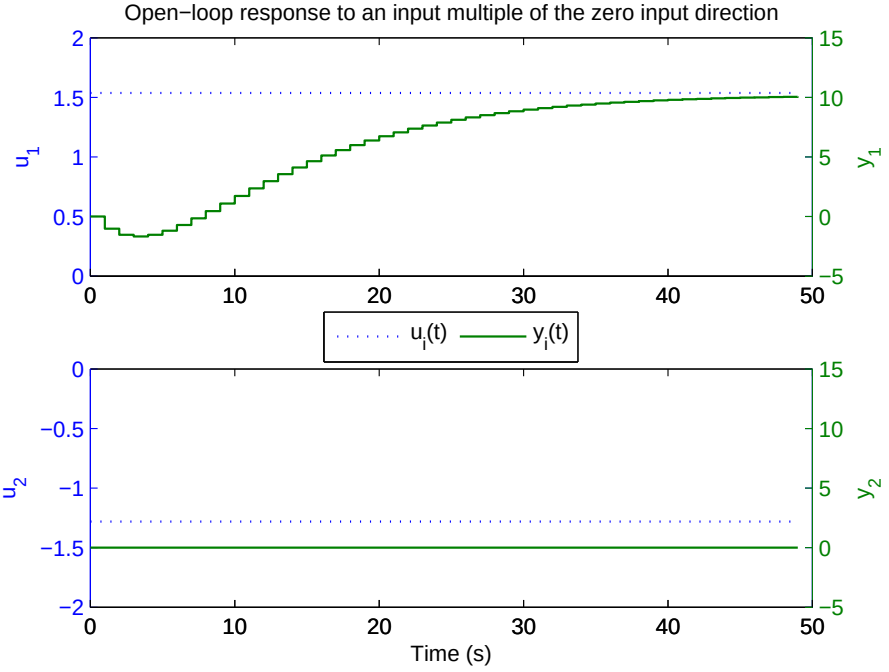

Source: author.

we observe an inverse response in output 1, *whereas output* 2 *remains at zero. This is a typical response when the input is in the same direction of the zero.*

2.2.4 All-pass factorization of transfer function matrices

The following formulation was based on the one given in (SKOGESTAD; POSTLETHWAITE, 2005), albeit a discrete-time formulation has been used to fit the scope of this work. These MIMO filters are all-pass in the sense that all singular values equal 1 for $q = e^{j\omega T_s},\ \forall\omega \in \mathbb{R}$.

Consider a plant model $G_0(q)$ with N_z NMP transmission zeros at z_{nm_i} (where the index *nm* means non-minimum) and associated input and output directions $u_{z_{nm_i}}$ and $y_{z_{nm_i}}$, respectively. Then $G_0(q)$ can be factored as follows:

$$G_0(q) = G_0^1(q)L_1(q) \tag{11}$$

$$z_{nm_1}L_1(q) = I + \left(\frac{|z_{nm_1}|}{z_{nm_1}}\frac{z_{nm_1} - q}{z^*_{nm_1}q - 1} - 1\right)\widehat{u}_{z_{nm_1}}\widehat{u}^H_{z_{nm_1}} \tag{12}$$

where $\widehat{u}_{z_{nm_1}}$ is the input zero direction of z_{nm_1} and $z^*_{nm_1}$ is the complex conjugate of z_{nm_1}. With this factorization, z_{nm_1} is not a transmission zero of $G_0^1(q)$, as it is reflected inside the unit circle becoming $1/z_{nm_1}$. By repeated application of (12) on $G_0^i(q)$, $i = 1 \ldots N_z$, $G_0(q)$ can be factored into a minimum phase part and an all-pass filter as

$$G_0(q) = G_0^{mi}(q)L_I(q) \tag{13}$$

$$L_I(q) = \prod_{i=1}^{N_z}\left(I + \left(\frac{|z_{nm_i}|}{z_{nm_i}}\frac{z_{nm_i} - q}{z^*_{nm_i}q - 1} - 1\right)\widehat{u}_{z_{nm_i}}\widehat{u}^H_{z_{nm_i}}\right) \tag{14}$$

In (13), $G_0^{mi}(q)$ is minimum phase with NMP transmission zeros of $G_0(q)$ reflected inside the unit circle and $L_I(q)$ is an all-pass filter. Note that except for the direction associated with the multivariable zero factored first, $\widehat{u}_{z_{nm_i}}$ differs from $u_{z_{nm_i}}$, as it is calculated based on $G_0^{(i-1)}(q)$ and not $G_0(q)$. The NMP transmission zeros can be alternatively factored at system's output similarly

$$G_0(q) = L_O(q)G_0^{mo}(q) \tag{15}$$

$$L_O(q) = \prod_{i=N_z}^{1}\left(I + \left(\frac{|z_{nm_i}|}{z_{nm_i}}\frac{z_{nm_i} - q}{z^*_{nm_i}q - 1} - 1\right)\widehat{y}_{z_{nm_i}}\widehat{y}^H_{z_{nm_i}}\right) \tag{16}$$

Example 2.4. *Consider the system given by*

$$G_0(q) = \begin{bmatrix} \dfrac{-6.5(q - 121/130)}{(q - 0.9)(q - 0.8)} & \dfrac{2}{(q - 0.9)} \\ \dfrac{-7}{(q - 0.8)} & \dfrac{2(q - 0.6)}{(q - 0.9)(q - 0.7)} \end{bmatrix}. \tag{17}$$

This system has NMP transmission zeros at $z_1 = 1.2$ *with* $y_{z_1} = [-0.76822\ \ 0.64018]^T$ *and* $z_2 = 1.3$ *with* $y_{z_2} = [-0.75926\ \ 0.65079]^T$. *Factoring first* z_1 *yield*

$$L_1(q) = \begin{bmatrix} \dfrac{0.90164(q - 1.033)}{(q - 0.8333)} & \dfrac{0.081967(q + 1)}{(q - 0.8333)} \\ \dfrac{0.081967(q + 1)}{(q - 0.8333)} & \dfrac{0.93169(q - 0.9677)}{(q - 0.8333)} \end{bmatrix} \tag{18}$$

$$G_0^{(1)}(q) = L_1^{-1}(q)G_0(q) = \begin{bmatrix} \dfrac{-6.5787(q-0.9077)}{(q-0.9)(q-0.8)} & \dfrac{2.0393(q-0.6672)}{(q-0.9)(q-0.7)} \\ \dfrac{-6.9344(q-0.918)}{(q-0.9)(q-0.8)} & \dfrac{1.9672(q-0.6267)}{(q-0.9)(q-0.7)} \end{bmatrix}. \quad (19)$$

System (19) *now has an NMP transmission zero at* $z_2 = 1.3$ *but with a different output direction* $\widehat{y}_{z_2} = [-0.71627 \quad 0.69783]^T$. *This is the direction that should be used for computing the respective output filter, which is given by*

$$L_2(q) = \begin{bmatrix} \dfrac{0.88161(q-1.007)}{(q-0.7692)} & \dfrac{0.11535(q+1)}{(q-0.7692)} \\ \dfrac{0.11535(q+1)}{(q-0.7692)} & \dfrac{0.88762(q-0.9932)}{(q-0.7692)} \end{bmatrix}. \quad (20)$$

The minimum-phase factor of (17) *is given by*

$$G_0^{mo}(q) = (L_1(q)L_2(q))^{-1}G_0(q) = \begin{bmatrix} \dfrac{-6.5514(q-0.9156)}{(q-0.9)(q-0.8)} & \dfrac{2.0582(q-0.6519)}{(q-0.9)(q-0.7)} \\ \dfrac{-6.961(q-0.9106)}{(q-0.9)(q-0.8)} & \dfrac{1.9488(q-0.642)}{(q-0.9)(q-0.7)} \end{bmatrix}, \quad (21)$$

which has only transmission zeros at $1/1.3$ *and* $1/1.2$.

The filters (14) and (16) are known as *Blaschke products*. For more on Blaschke products and filters computation the reader is referred to (HAVRE; SKOGESTAD, 1996; HAVRE, 1998).

2.2.5 System Markov parameters

Another concept in system theory is the system impulse response. It can be used to infer about the system stability and to determine the system output to any given input (CHEN, 1999). In discrete-time, the impulse matrix response associated with a state-space model is called the Markov parameter M_i sequence. It can be found by direct calculation using (2) (with the noise terms $E = F = 0$), and where the input $u(t) = \underline{\delta}(t) = \delta(t)I_{p\times p}$ is a $p \times p$ matrix having the impulse signal $\delta(t)$ along the diagonal and zeros elsewhere:

$$
\begin{aligned}
M_0 &= Cx(0) + D\underline{\delta}(0) = D \\
x(1) &= Ax(0) + B\underline{\delta}(0) = B \\
M_1 &= Cx(1) + D\underline{\delta}(1) = CB \\
x(2) &= Ax(1) + B\underline{\delta}(1) = AB \\
M_2 &= Cx(2) + D\underline{\delta}(2) = CAB \\
x(3) &= Ax(2) + B\underline{\delta}(2) = A^2B \\
M_3 &= Cx(3) + D\underline{\delta}(3) = CA^2B \\
&\vdots \\
M_i &= CA^{(i-1)}B, \;\; i > 0.
\end{aligned}
$$

Note that $x(0) = 0$, i.e., zero initial state or zero initial conditions. Since the system input is a $p \times 1$ vector, one may regard $\underline{\delta}(t)$ as a sequence of p successive input vectors, each providing an impulse at one of the input components.

The impulse response of the state-space model can be summarized as

$$
M_i = \begin{cases} D, & i = 0 \\ CA^{i-1}B, & i > 0 \end{cases} \tag{22}
$$

Notice that each "sample" of the impulse response M_i is an $l \times p$ matrix. Therefore, it is not a feasible output signal, unless $p = 1$. It can be viewed as a sequence of l outputs, each $p \times 1$. Furthermore, M_i is the inverse z-transform of the matrix transfer-function of system (1). The Markov parameters are widely used in subspace identification theory (VAN OVERSCHEE; DE MOOR, 2012), for FIR filter synthesis, and also play an important role in system stability assessment (CHEN, 1999), as will be discussed in Section 2.5.

2.3 Model Reference control

Model Reference is a classical control design paradigm, which is particularly well suited for adaptive and data-driven control design. In the framework of DD control, as well as in the so-called direct adaptive control, there is no model of the plant and none is expected to be obtained. Instead, input-output data from the plant are directly mapped into controller parameters that, at least ideally, yield the specified performance. The performance specification is made by stating what is the desired closed-loop transfer matrix. In this design approach, the *designer's* task consists essentially in the choice of this transfer matrix, which is called the reference model.

The design task is to tune the parameter vector $P \in \mathbb{R}^z$ of a linear time-invariant controller $C(q, P)$ in order to achieve a desired closed-loop response. We assume that this controller belongs to a given user-specified controller class $\mathcal{C}$ such that all elements of the loop transfer matrix $L(q) = G_0(q)C(q, P)$ have positive relative degree for all $C(q, P) \in \mathcal{C}$. The controller class $\mathcal{C}$ is generically defined as

$$\mathcal{C} = \{C(q, P) : P \in \mathbb{R}^z\}. \tag{23}$$

The control action $u(t)$ is given by

$$u(t) = C(q, P)(r(t) - y(t)), \tag{24}$$

where $r(t)$ is the reference signal, which is assumed to be quasi-stationary and uncorrelated with the noise $v(t)$, that is $\bar{\mathcal{E}}\left[r(t)v(s)\right] = 0 \ \forall t, s$, and

$$\bar{\mathcal{E}}[f(t)] \triangleq \lim_{N\to\infty} \frac{1}{N} \sum_{t=1}^{N} \mathcal{E}[f(t)]$$

with $\mathcal{E}[\cdot]$ denoting expectation (LJUNG, 1999). The system (1)-(24) in closed loop becomes

$$\begin{aligned}
y(t, P) &= T(q, P)r(t) + S(q, P)v(t) && (25)\\
S(q, P) &= [I + G_0(q)C(q, P)]^{-1} && (26)\\
T(q, P) &= [I + G_0(q)C(q, P)]^{-1}G_0(q)C(q, P) = S(q, P)G_0(q)C(q, P) && (27)\\
I &= T(q, P) + S(q, P) && (28)
\end{aligned}$$

where the dependence on the controller parameter vector P is now made explicit in the output signal $y(t, P)$. The function $S(q, P)$ is called sensitivity function and $T(q, P)$ is called complementary sensitivity function or closed-loop function. The closed-loop system is depicted in Figure 3.

Figure 3 – Block diagram of the closed-loop system.

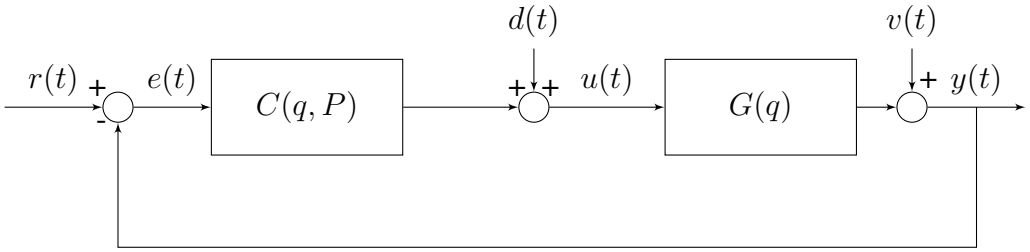

Source: author.

Here, we have already introduced the disturbance signal $d(t)$ in the block diagram as its implication on closed-loop stability will be discussed later. However, for the discussion presented next, consider $d(t) = 0$.

The idea behind Model Reference (MR) control is that closed-loop performance is specified through a "desired" closed-loop transfer matrix $T_d(q)$, which is known as *reference model*, and describes the relation between the reference signal and the desired closed-loop output $y_d(t)$:

$$y_d(t) = T_d(q)r(t).$$

The controller parameters can be tuned by solving the Reference Model optimization problem

$$\begin{cases} \min\limits_{P} J^{MR}(P) & (29) \\ J^{MR}(P) \triangleq \bar{\mathcal{E}}||(T(q,P) - T_d(q))r(t)||_2^2. & (30) \end{cases}$$

The *optimal controller* is defined as $C(q, P^{MR})$ with

$$P^{MR} = \arg\min_{P} J^{MR}(P).$$

This optimization is usually a nonconvex one, even in the easiest case of a linearly parametrized SISO controller (CAMPESTRINI *et al.*, 2011; BAZANELLA; CAMPESTRINI; ECKHARD, 2011). We will be concerned with the properties of the optimal P^{MR}, supposing it can be found by a data-driven approach. Besides, the choice of $T_d(q)$ also influences the difficulty in solving the optimization (GONÇALVES DA SILVA; BAZANELLA; CAMPESTRINI, 2018).

The ideal controller $C_d(q)$ is the one that makes the closed-loop behave exactly as the chosen reference model. We have that

$$T_d(q) = [I + G_0(q)C_d(q)]^{-1}G_0(q)C_d(q), \tag{31}$$

and rewriting (31) for $C_d(q)$, the *ideal controller* is given by

$$\begin{aligned} C_d(q) &= G_0(q)^{-1}L_d(q), & (32) \\ L_d(q) &\triangleq T_d(q)[I - T_d(q)]^{-1}. & (33) \end{aligned}$$

Ideally, one wants to find P^{MR} such that $C(q, P^{MR}) = C_d(q)$, and the theory developed for Model Reference control starts from this assumption, i.e., $C_d(q) \in \mathcal{C}$.

If $G_0(q)$ is known and the controller has no structure constraint then one can apply (32) directly to obtain the ideal controller. However, actual systems usually behave as to not satisfy these assumptions. First, in most cases $G_0(q)$ is unknown and must be obtained through modeling and/or via some identification method. Errors due to noise and the chosen structure for $G(q)$ will appear so the obtained controller via (32) will not necessarily make the closed-loop behave exactly as the reference model previously chosen. Finally, the structure of the controllers used is rarely flexible enough to guarantee that (32) can be used. The controller structure is usually fixed and only its gains can be adjusted.

In this case, the optimal controller can be found minimizing criterion (29), which can be achieved considering designs of optimal control (GOODWIN; GRAEBE; SALGADO, 1984), adaptive control (LANDAU *et al.*, 2011) or data-driven control (BAZANELLA; CAMPESTRINI; ECKHARD, 2011). Here, we will concern ourselves with the latter.

2.4 Data-Driven control

Amongst the Data-Driven control methods developed in the last decades there are the iterative ones, in which a batch of experiments is required such that the optimal controller is obtained after a sequence of controllers is put in closed-loop with the actual plant. And there are the direct methods, based on only one experiment. Both approaches use a controller structure defined *a priori* and the controller tuning is based directly on input and output data collected from the plant, without a direct use of a complete model of the system. Some of the methods have both SISO and MIMO versions.

Among the iterative methods, stands out the *Iterative Feedback Tuning* (IFT), proposed for the SISO case in (HJALMARSSON; GUNNARSSON; GEVERS, 1994; HJALMARSSON *et al.*, 1998) and for the MIMO case in (DE BRUYNE, 1997; HJALMARSSON; BIRKELAND, 1998). Also, initially iterative, the *Correlation-based Tuning* (CbT) was proposed for the SISO case in (KARIMI; MIŠKOVIĆ; BONVIN, 2004) and an extension to the MIMO case can be found in (MIŠKOVIĆ *et al.*, 2007). A non-iterative version of the CbT-SISO is presented in (KARIMI; VAN HEUSDEN; BONVIN, 2007). This version is extended to multivariable systems in (YUBAI; USAMI; HIRAI, 2009). One of the major problems encountered in these works for the multivariable case is the need to perform as many experiments as the number of parameters to be identified or, given a re-parametrization, the number of extra experiments is equal to $p \times l$ for the noisy case.

Recently a new direct method has been proposed for the SISO case, the *Optimal Controller Identification* (OCI) (CAMPESTRINI *et al.*, 2017). In OCI, the input-output system model is substituted from the beginning by an equivalent description involving only the parameters that are function of the MR optimal controller parameters. Thus, the controller identification is inserted in a classical identification problem by prediction error framework. A MIMO-OCI version was applied to a simulated refrigerator system in (HUFF; GONÇALVES DA SILVA; CAMPESTRINI, 2018) and has been further developed in (HUFF *et al.*, 2019).

The *Virtual Reference Feedback Tuning* (VRFT) (CAMPI; LECCHINI; SAVARESI, 2002) is one of the most known and applied method. The main advantage of this method is that the optimal MR controller can be estimated as the solution of a least-squares problem for noise-free data (or using Instrumental Variables otherwise) and linear in the parameters controller. Unstable and NMP plants also bring about issues when applying the VRFT. In

(CAMPESTRINI *et al.*, 2011) a flexible VRFT criterion is proposed to cope with SISO NMP plants where the NMP zero is estimated into the reference model together with the optimal controller.

A formal MIMO extension of the VRFT is presented in (FORMENTIN; SAVARESI, 2011) although some constraints are imposed such as an equal desired performance for each loop via a *diagonal* reference model. This might not be a problem when the process variables are of the same type, but the method will not yield good results otherwise. An extension without this constraint is given in (CAMPESTRINI *et al.*, 2016) and applied in (BOEIRA *et al.*, 2018).

The properties of a data-driven design are strongly dependent on how well the controller class can represent the ideal controller, so let us formalize this concept. When the controller structure $\mathcal{C}$ is such that it can represent exactly the ideal controller $C_d(q)$ for some set of parameters – say, P_d –, we say that *the ideal controller belongs to the controller class*.

Assumption 2.1. *$C_d(q) \in \mathcal{C}$: There is a parameter vector P_d such that $C(q, P_d) = C_d(q)$.*

In general, this is not the case because the chosen controller structure is restrictive with respect to the reference model choice. That is, the ability of the controller class to represent exactly the ideal controller depends on the choice of the reference model. The choice of the reference model plays an important role in the success of DD methods and a detailed work on this subject can be found in (GONÇALVES DA SILVA; BAZANELLA; CAMPESTRINI, 2018; GONÇALVES DA SILVA; CAMPESTRINI; BAZANELLA, 2016). Some of these choices will be reviewed in this thesis when necessary. In the next subsections the most common controller parametrizations are reviewed and the VRFT and OCI methods are presented.

2.4.1 Controller structure

Data-Driven control methods can be used to estimate a variety of controllers. Some methods however, such as VRFT, are tailored for when the controller is linear in the parameters, which is the case of Proportional-Integral-Derivative (PID) controllers with fixed derivative pole. Moreover, the integral action of these controllers yields null steady-state error, which is a concern when the controller is designed for constant reference tracking.

Within the controller class $\mathcal{C}$ (23), the structure of the controller to be designed is defined as

$$C(q,P) = \begin{bmatrix} C_{11}(q,\rho_{11}) & C_{12}(q,\rho_{12}) & \cdots & C_{1n}(q,\rho_{1n}) \\ \vdots & \vdots & \ddots & \vdots \\ C_{n1}(q,\rho_{n1}) & C_{n2}(q,\rho_{n2}) & \cdots & C_{nn}(q,\rho_{nn}) \end{bmatrix} \tag{34}$$

and $P = [\rho_{11}^T \;\; \rho_{12}^T \;\; \dots \;\; \rho_{n1}^T \;\; \dots \;\; \rho_{nn}^T]^T$.

In the case of PID controllers with fixed derivative pole each element of the controller matrix $C(q, P)$ in (34) has the following parametrized structure

$$C_{ij}(q, \rho_{ij}) = [kp_{ij}\ ki_{ij}\ kd_{ij}] \begin{bmatrix} 1 \\ \frac{T_s q}{q-1} \\ \frac{q-1}{T_s(q-p_{d_{ij}})} \end{bmatrix} \triangleq \rho_{ij}^T\ \beta_{ij}(q). \tag{35}$$

where $kp,\ ki,\ kd$ are the proportional, integral and derivative gains, respectively, $p_{d_{ij}}$ is the derivative pole, and T_s is the sampling time. When the derivative pole is set *a priori*, then we say that (35) is linear in the parameters; in general, $p_{d_{ij}} = 0, \forall i, j$. It is also possible to incorporate $p_{d_{ij}}$ in P, adding a new parameter to be identified. With the choice of $\beta_{ij}(q)$ in (35), P is the vector having exactly the continuous time gains of the PID controller that the operator wants to find (GONÇALVES DA SILVA; CAMPESTRINI; BAZANELLA, 2014).

2.4.2 Virtual Reference Feedback Tuning – VRFT

The VRFT method is a one-shot (i.e., not iterative) data-driven design method, that is, with one batch of input-output data, the method searches for a controller that makes the closed-loop system as close as possible to the reference model. The user defines the reference model $T_d(q)$ and the controller structure, then the controller parameters are found through a least squares minimization. The MIMO-VRFT approach was formally presented in (FORMENTIN; SAVARESI; DEL RE, 2012), and applications have been reported, such as to diesel engines and waste-water treatment systems (ROJAS *et al.*, 2012). A MIMO approach derived directly from SISO-VRFT has been presented in (CAMPESTRINI *et al.*, 2016), where it has been applied to level control of a two tank process.

Consider the noise-free case, that is, $w(t) = 0$ in (1), and that the system has the same number n of inputs and outputs. In (CAMPESTRINI *et al.*, 2016), the controller parameters are obtained by the solution of the following optimization problem:

$$\begin{aligned} &\min_P J^{VR}(P) \\ &J^{VR}(P) = \sum_{t=1}^{N} \|F(q)[u(t) - C(q, P)(T_d^{-1}(q) - I)y(t)]\|_2^2. \end{aligned} \tag{36}$$

where $F(q)$ is a filter that can be used as an additional degree of freedom and the remaining variables have been previously defined.

The properties of this MIMO method are similar to those of the SISO-VRFT (CAMPI; LECCHINI; SAVARESI, 2002). When the signals are noise free and the ideal controller $C_d(q)$ belongs to the chosen controller class, that is, Assumption 2.1 is satisfied, the ideal controller parameter vector is the minimum of $J^{VR}(P)$, no matter which filter $F(q)$ is chosen. When Assumption 2.1 is not satisfied, *the filter is chosen to approximate the*

minima of $J^{VR}(P)$ *and* $J^{MR}(P)$, which is the performance criterion that one really wants to optimize. An implementable filter that performs this task is given by (CAMPESTRINI *et al.*, 2016)

$$F(q) = T_d(q)(I - T_d(q)). \tag{37}$$

Besides, if $C(q, P)$ is linearly parametrized then $J^{VR}(P)$ is quadratic in the parameters and a closed form solution to the optimization problem is given by

$$\hat{P} = \left(\sum_{t=1}^{N} \phi(t)\phi^T(t) \right)^{-1} \sum_{t=1}^{N} \phi(t) u_F(t), \tag{38}$$

where

$$\begin{gathered} u_F(t) = F(q)u(t), \quad \phi(t) = [A_1 \; A_2 \; \cdots \; A_n], \\ A_x = \begin{bmatrix} F_{x1}(q)E_x(t) \\ F_{x2}(q)E_x(t) \\ \vdots \\ F_{xn}(q)E_x(t) \end{bmatrix}, \quad E_x(t) = \begin{bmatrix} \beta_{x1}(q)\bar{e}_1(t) \\ \beta_{x2}(q)\bar{e}_2(t) \\ \vdots \\ \beta_{xn}(q)\bar{e}_n(t) \end{bmatrix} \end{gathered} \tag{39}$$

for $x = 1, 2, \ldots, n$, where $\bar{e}(t) = (T_d^{-1}(q) - I)y(t)$ is the *virtual error*, $\bar{e}_i(t)$ is the $i - th$ component of $\bar{e}(t)$ and $F_{ij}(q)$ is the (i, j) element of the filter $F(q)$.

In the more practical situation in which the signals are noisy, the solution (38) is biased and an instrumental variable technique should be used to eliminate the bias. An extra signal $y'(t)$, which is correlated to $y(t)$ but not correlated to the noise present in output, should be obtained and the *instrumental variable* $\zeta(t)$ is defined as $\zeta(t) = [A'_1 \;\; A'_2 \;\; \cdots \;\; A'_n]^T$, where $A'_x, x = 1, 2, \ldots, n$ is similar to A_x (from $\phi(t)$), but formed with the signal $y'(t)$ *in lieu* of $y(t)$. The solution of VRFT with the instrumental variable approach is

$$\hat{P}_{IV} = \left(\sum_{t=1}^{N} \zeta(t)\phi(t)^T \right)^{-1} \sum_{t=1}^{N} \zeta(t) u_F(t). \tag{40}$$

2.4.3 Optimal Controller Identification – OCI

Using the concept of the ideal controller (32), it is possible to turn the Model Reference control design problem into an identification problem of the controller, without using a model for the process. This data-driven design method was presented in (CAMPESTRINI *et al.*, 2017) for SISO systems and is extended for MIMO processes in (HUFF *et al.*, 2019). The core idea is to rewrite the input-output system (1) in terms of the ideal controller $C_d(q)$, which is done by inverting the relation (32), i.e.,

$$G_0(q) = T_d(q) \left(I - T_d(q)\right)^{-1} C_d^{-1}(q). \tag{41}$$

Then a model for the plant can be written in terms of the controller parameters as

$$G(q, P) \triangleq T_d(q) \left(I - T_d(q)\right)^{-1} C^{-1}(q, P) \tag{42}$$

and the task will be to identify an estimate $C(q, \hat{P})$ of the ideal controller $C_d(q)$ within the parametrized controller class defined by $\mathcal{C}$. In other words, this corresponds to an identification of a plant model $G(q, P)$ with a fixed part, which is a function of the reference model $T_d(q)$, and a parametrized part, which is a function of the controller inverse. Thus, (1) can be rewritten as

$$y(t, \Theta) = G(q, P)u(t) + H(q, \Theta)w(t) \tag{43}$$

where $\Theta = \begin{bmatrix} P^T & \Psi^T \end{bmatrix}^T$ and $\Psi \in \mathbb{R}^c$ is an additional parameter vector that appears in the noise model.

From N measured input-output data, the parameter vector estimate $\hat{\Theta}_N = \begin{bmatrix} \hat{P}_N^T & \hat{\Psi}_N^T \end{bmatrix}^T$ is defined as (CAMPESTRINI *et al.*, 2017):

$$\hat{\Theta}_N = \arg\min_{\Theta} V(\Theta) \tag{44}$$

where

$$V(\Theta) = \frac{1}{N} \sum_{t=1}^{N} \|\epsilon(t, \Theta)\|_2^2 , \tag{45}$$

$\epsilon(t, \Theta)$ is the prediction error

$$\epsilon(t, \Theta) \triangleq y(t) - \hat{y}(t|t-1, \Theta) \tag{46}$$

and

$$\hat{y}(t|t-1, \Theta) = H^{-1}(q, \Theta)T_d(q) \left(I - T_d(q)\right)^{-1} C^{-1}(q, P)u(t) + \left[I - H^{-1}(q, \Theta)\right] y(t) \tag{47}$$

is the one-step ahead predictor for model (43), where $G(q, P)$ has been replaced by (42). The predictor is now a function of the noise model $H(q, \Theta)$ and the inverse of the controller $C^{-1}(q, P)$.

Instead of minimizing $J^{MR}(P)$, which depends on the unknown plant $G_0(q)$, the design is made by minimizing the cost function $V(\Theta)$, which is purely data-dependent and no model of the plant $G_0(q)$ is used. Since the estimation of the optimal Model Reference controller has been transformed into a Prediction Error (PE) identification problem, all properties of PE identification theory apply. Specifically, the estimate in (44) converges, under mild conditions, to the optimal vector $\Theta^* = \begin{bmatrix} P^{*T} & \Psi^{*T} \end{bmatrix}^T$ defined as follows:

$$\hat{\Theta}_N \to \Theta^* = \arg\min_{\Theta} \bar{V}(\Theta) \tag{48}$$

where

$$\bar{V}(\Theta) = \bar{\mathcal{E}} \|\epsilon(t, \Theta)\|_2^2 . \tag{49}$$

It is worth mentioning that, since the object of interest is the optimal controller only, and not the plant model, the identification of $H_0(q)$ is of no interest for the controller

design. It is well known from PE identification theory that if Assumption 2.1 is satisfied, informative enough data set is collected in open-loop and $G(q, P)$ and $H(q, \Theta)$ are parametrized independently (that is, $\frac{\partial H(q,\Theta)}{\partial P} = 0$), then, for $N \to \infty$ (LJUNG, 1999):

$$C(q, \hat{P}_N) \to C_d(q). \tag{50}$$

If Assumption 2.1 is satisfied but data are collected in closed-loop, then (50) holds provided that $\exists\Theta_0$ such that $H(q, \Theta_0) = H_0(q)$.

It is often the case that one imposes some fixed part in the controller, the most common instance of this fact probably being the imposition of a pole at $q = 1$ to guarantee zero steady-state error for constant references and disturbances. This fixed part does not need to be identified. So, we call $C_F(q)$ this fixed part and rewrite the controller transfer function as

$$C(q, P) = C_F(q)C_I(q, P). \tag{51}$$

Using (51) and (42), (43) can be written as

$$y(t, \Theta) = \underbrace{T_d(q)\left(I - T_d(q)\right)^{-1} C_F^{-1}(q)}_{F(q)} \underbrace{C_I^{-1}(q, P)}_{\tilde{C}(q,P)} u(t) + H(q, \Theta)w(t) \tag{52}$$

where $F(q)$ is a fixed transfer matrix formed by the fixed part of $G(q, P)$. Notice that in the SISO case, or if $T_d(q)$ is a scalar function times the identity matrix and $C_F(q)$ is also a scalar function, then $F(q)$ commutes with $\tilde{C}(q, P)$ and (52) can be written as

$$\begin{aligned} y(t, \Theta) &= \underbrace{C_I^{-1}(q, P)}_{\tilde{C}(q,P)} \times \underbrace{T_d(q)\left(I - T_d(q)\right)^{-1} C_F^{-1}(q)u(t)}_{\tilde{u}(t)} + H(q, \Theta)w(t) \\ &= \tilde{C}(q, P)\tilde{u}(t) + H(q, \Theta)w(t). \end{aligned} \tag{53}$$

Identification of Θ in (53) can be easily obtained through available toolboxes. However, in most MIMO cases the matrices in (52) do not commute and a dedicated optimization solution should be used in order to minimize (45). In (HUFF *et al.*, 2019), it is proposed to apply an optimization procedure combining *steepest descent* and *quasi-Newton* algorithms with an initial controller provided by the VRFT method. In the next section this solution is detailed for the case where $H(q, \Theta) = I$, so the predictor (47) is reduced to

$$\hat{y}(t, P) = G(q, P)u(t). \tag{54}$$

It is worth mentioning tough that a noise model $H(q, \Theta)$ could also be estimated, with the burden of solving more complex equations on the optimization solution presented next.

2.4.3.1 Optimization problem solution

At first, the *steepest descent method* is used to minimize the cost function (45) because of its large region of attraction to a local minimum. In this case, the recursion formula is

given by (BAZANELLA; CAMPESTRINI; ECKHARD, 2011)

$$P_{i+1} = P_i - \gamma_i \nabla V(P_i) \tag{55}$$

where, for each iteration i, γ_i is a positive scalar and $\nabla V(P_i)$ is the gradient of the cost function V evaluated at the parameter vector P_i. Quantity γ_i is increased by 1% if $V(P_i) < V(P_{i-1})$. Otherwise, it is decreased by 1% and one has $P_i = P_{i-1}$.

The *Levenberg-Marquardt method* is used next, whose convergence is faster, but its region of attraction tends to be smaller than that of the steepest descent method's. The recursion in this case is given by

$$P_{i+1} = P_i - \left(\nabla^2 V(P_i) + \lambda_i I\right)^{-1} \nabla V(P_i) \tag{56}$$

where $\nabla^2 V(P_i)$ is an *approximation* of the Hessian of the cost function. When λ_i is zero, the search direction corresponds to that of Gauss-Newton method. As $\lambda_i \to \infty$, the search direction tends towards the steepest descent one, and the magnitude of the step tends to zero.

To apply this sequence of numerical method, one needs to compute both the gradient and the Hessian of the cost function $V(\Theta)$. In the case where the noise model is *not* identified in parallel with the controller, (45) becomes a function of the controller parameter P only, as

$$V(P) = \frac{1}{N} \sum_{t=1}^{N} \|\epsilon(t,P)\|_2^2 \tag{57}$$

$$= \frac{1}{N} \sum_{t=1}^{N} \left(y(t) - \hat{y}(t,P)\right)^T \left(y(t) - \hat{y}(t,P)\right) \tag{58}$$

whose partial derivative with respect to the kth element of P is

$$\frac{\partial V(P)}{\partial P_k} = \frac{2}{N} \sum_{t=1}^{N} \left(\hat{y}(t,P) - y(t)\right)^T \frac{\partial \hat{y}(t,P)}{\partial P_k} \tag{59}$$

where

$$\hat{y}(t,P) = F(q)\tilde{C}(q,P)u(t) \tag{60}$$

$$\frac{\partial \hat{y}(t,P)}{\partial P_k} = F(q)\frac{\partial \tilde{C}(q,P)}{\partial P_k}u(t). \tag{61}$$

The partial derivative of $\tilde{C}(q,P) = C_I^{-1}(q,P)$ is given by

$$\begin{aligned} \frac{\partial \left[C_I^{-1}(q,P)\right]}{\partial P_k} =& \frac{1}{\det\left(C_I(q,P)\right)} \frac{\partial \left[\text{cof}^T\left(C_I(q,P)\right)\right]}{\partial P_k} \\ -& \frac{1}{\det^2\left(C_I(q,P)\right)} \text{cof}^T\left(C_I(q,P)\right) \frac{\partial \left[\det\left(C_I(q,P)\right)\right]}{\partial P_k} \end{aligned} \tag{62}$$

where $\det(\cdot)$ is the determinant and $\text{cof}(\cdot)$ is the cofactor matrix. The gradient of the cost function is calculated by using (59)-(62) for $k = 1\,, 2\,, \ldots\,, z$.

In order to apply the *Levenberg-Marquardt* method, the Hessian of the cost function needs to be calculated, which is obtained through the partial derivatives of (59) with respect to the l-th component of P for $k\,, l = 1\,, 2\,, \ldots\,, p$, as shown below:

$$\frac{\partial^2 V(P)}{\partial P_k \partial P_l} = \frac{2}{N}\sum_{t=1}^{N}\left(\frac{\partial \hat{y}(t,P)}{\partial P_l}\right)^T \frac{\partial \hat{y}(t,P)}{\partial P_k} + (\hat{y}(t,P) - y(t))^T \frac{\partial^2 \hat{y}(t,P)}{\partial P_k \partial P_l}. \tag{63}$$

Ignoring the second term in the right-hand side of (63), which involves second order derivatives, we have

$$\frac{\partial^2 V(P)}{\partial P_k \partial P_l} \cong \frac{2}{N}\sum_{t=1}^{N}\left(\frac{\partial \hat{y}(t,P)}{\partial P_l}\right)^T \frac{\partial \hat{y}(t,P)}{\partial P_k}. \tag{64}$$

2.4.3.2 PID estimation

The methodology presented in this work can be used to estimate any class of controllers, whether linear in the parameters or not. For instance, consider a 2×2 PID controller $C(q,P) = C_F(q)C_I(q,P)$ where

$$C_F(q) = \frac{1}{q(q-1)} \tag{65}$$

$$C_I(q,P) = \begin{bmatrix} a_{11}q^2 + b_{11}q + c_{11} & a_{12}q^2 + b_{12}q + c_{12} \\ a_{21}q^2 + b_{21}q + c_{21} & a_{22}q^2 + b_{22}q + c_{22} \end{bmatrix} \tag{66}$$

and $P = [a_{11}\ b_{11}\ c_{11}\ a_{12}\ \ldots\ a_{21}\ \ldots\ a_{22}\ \ldots\ c_{22}]^T$. In this case, the adjugate matrix is

$$\text{cof}^T\left(C_I(q,P)\right) = \begin{bmatrix} a_{22}q^2 + b_{22}q + c_{22} & -(a_{12}q^2 + b_{12}q + c_{12}) \\ -(a_{21}q^2 + b_{21}q + c_{21}) & a_{11}q^2 + b_{11}q + c_{11} \end{bmatrix} \tag{67}$$

and its determinant is

$$\begin{aligned} \det\left(C_I(q,P)\right) = &\left(a_{11}q^2 + b_{11}q + c_{11}\right)\left(a_{22}q^2 + b_{22}q + c_{22}\right) \\ &- \left(a_{12}q^2 + b_{12}q + c_{12}\right)\left(a_{21}q^2 + b_{21}q + c_{21}\right). \end{aligned} \tag{68}$$

The partial derivatives of (67) and (68) with respect to the parameter a_{11}, for instance, are given by

$$\frac{\partial\left[\text{cof}^T\left(C_I(q,P)\right)\right]}{\partial a_{11}} = \begin{bmatrix} 0 & 0 \\ 0 & q^2 \end{bmatrix}, \tag{69}$$

$$\frac{\partial\left[\det\left(C_I(q,P)\right)\right]}{\partial a_{11}} = a_{22}q^4 + b_{22}q^3 + c_{22}q^2. \tag{70}$$

Similar equations are obtained for each element of P in order to compute (62), (61) and then (59) so the estimate can be obtained by the steepest descent method. The same quantities are used to compute (63) in the quasi-Newton minimization.

Now, since the first step of the optimization solution is obtained through (55), an initial controller parameter vector that *stabilizes* (42) is needed. The closer the initial controller $C(q, P_0)$ is to $C(q, P^*)$, the greater are the chances that the algorithm actually results in $C(q, P^*)$, and not in a local minimum. Furthermore, it has been shown that this formulation can also be applied to identify a PID controller where the derivative pole is not fixed, even for the MIMO case, but with the burden to computing more complex derivatives. Finally, it is important to note that this formulation casts the controller estimation into a prediction error identification framework, which makes the method less susceptible to noisy signals.

This formulation has been applied to the control of a (simulated) refrigeration system in (HUFF; GONÇALVES DA SILVA; CAMPESTRINI, 2018) as part of a challenge proposed in the 3rd IFAC Conference on Advances in Proportional-Integral-Derivative Control. It has been reported in that conference to be the formulation that led to the lowest cost among 20 other papers on the same subject.

2.5 Closed-loop stability

In this section we will discuss the overall stability of the feedback system presented in Figure 3. The system's input and output can be written as

$$u(t) = C(q,P)S(q)(r(t) - y(t) - v(t)) + (I + C(q,P)G_0(q))d(t) \tag{71}$$

$$y(t) = T(q)r(t) + S(q)G_0(q)d(t) + S(q)v(t). \tag{72}$$

We then have the following theorem.

Theorem 2.3. (SKOGESTAD; POSTLETHWAITE, 2005)(modified) Internal Stability: *The feedback system in Figure 3 is* ***internally stable*** *iff the transfer matrix*

$$H(G_0, C) = \begin{bmatrix} T(q) & S(q)G_0(q) \\ C(q,P)S(q) & (I + C(q,P)G_0(q)) \end{bmatrix} \tag{73}$$

is stable.

Each transfer matrix in (73) is stable if all poles lie strictly inside the unit circle in the q-plane. Let (A, B, C, D) be a minimal state-space realization of $H(G_0, C)$. Internal stability means the matrix A has all eigenvalues strictly inside the unit circle in the q-plane.

The Markov parameters (22) associated with a realization also play their role when inferring about stability. In the SISO case, these parameters correspond to the system's impulse response and if they vanish for $N_m \to \infty$, then the impulse response is absolutely summable, thus the system is BIBO-stable (Bounded Input Bounded Output). In the MIMO case, if every sequence in each entry of the impulse response matrix is absolutely summable, then the system is BIBO-stable (CHEN, 1999).

Now, if the ideal controller $C_d(q)$ were put in the control loop, the objective function $J^{MR}(P)$ would evaluate to zero, providing the ideal input-output performance. However, it is clear from (32) that the plant's zeros turn into poles of the ideal controller, which will result in internal instability for plants that possess NMP zeros, unless the NMP zeros appearing in the denominator (32) are canceled by a proper choice of the reference model, as specified in the following theorem.

Theorem 2.4 ((HAVRE; SKOGESTAD, 1996)). *If $G_0(q)$ has an NMP transmission zero at z_{nm} with output direction $y_{z_{nm}}$, then for internal stability of the feedback system with the ideal controller, the following constraint must apply:*

$$y_{z_{nm}}^H T_d(z_{nm}) = 0. \tag{74}$$

It is clear – but still worth a remark – that constraint (74) is a function of the *transmission zeros* of $G_0(q)$ and has no direct relation with the zeros of the elements of $G_0(q)$. Theorem 2.4 states that in order to obtain internal stability, the reference model $T_d(q)$ must have the same NMP transmission zeros of $G_0(q)$ in the same output directions. So if the system has non-minimum phase transmission zeros the user needs to know at least their location (just like in the SISO case (CAMPESTRINI *et al.*, 2011; BAZANELLA; CAMPESTRINI; ECKHARD, 2011)) in order to choose a reference model satisfying (74). As for the transmission zeros directions, there are two possibilities. One is to chose the reference model such that its NMP transmission zero has the same direction as in the plant's transfer function; this of course requires knowledge of the zero direction in addition to knowledge of its value. Another choice is to put the NMP transmission zero in n linearly independent directions in the reference model, which is obtained by putting it as a zero of each one of the elements in a diagonal $T_d(q)$, for instance. This second choice does not require knowledge of the NMP transmission zero's direction, but spreads its (usually nasty) effect on the performance throughout all the outputs (GONÇALVES DA SILVA; CAMPESTRINI; BAZANELLA, 2016). The reader is referred to references (GONÇALVES DA SILVA; CAMPESTRINI; BAZANELLA, 2016, 2018; GONÇALVES DA SILVA; BAZANELLA; CAMPESTRINI, 2018) for a thorough synthesis of the reference model, as this thesis is concerned with data-driven methods themselves, even though we briefly review these choices in Chapter 3.

2.6 Chapter conclusions

In this Chapter we revised some fundamental concepts of multivariable systems and data-driven control. Transfer matrix representation, NMP transmission zero issues, Model Reference and data-driven control are concepts used in Chapter 3 to deal with NMP systems using feedback control in a DD perspective. State-space representation and Markov parameters are used in Chapter 4 to derive a solution to the LQR problem using data

only. In Chapter 5 we use both system representations, definition of poles and Markov parameters, and closed-loop stability to set a DD approach to the controller certification problem. Finally, it is also important that the reader has some basis on system identification, for which we refer to (LJUNG, 1999) and (VAN OVERSCHEE; DE MOOR, 2012).

3 DATA-DRIVEN CONTROL FOR NON-MINIMUM PHASE SYSTEMS

Denying the appearances, disguising the evidence.

Chitãozinho & Xororó

As in any model reference design, Data-Driven methods often result in an internally unstable closed-loop when the process is NMP and the reference model does not include the NMP transmission zeros. Also, instability is more usual with NMP zeros that come from actual NMP behavior in continuous-time (which have positive real part) than with those which arise as a discretization phenomenon (which have negative real part).

One possible approach to this problem is to perform a process identification before proceeding to the controller design, and if the process is NMP, then include the identified NMP transmission zero, and possibly its direction, in the reference model. A rough identification might be enough, since only the NMP zeros are required, and unstable singularities tend to be identified more accurately (MÅRTENSSON; HJALMARSSON, 2009).

However, Data-Driven designs are most advantageous precisely because they do not require the identification of a model. ***Since no process model is known, one can not assume prior knowledge of the NMP transmission zeros' locations, let alone their directions.*** As a consequence, direct application of such data-driven methods to NMP plants, whether SISO or MIMO, tends to fail because the reference model will lack the inclusion of the unknown NMP zeros. An alternative solution to this issue was presented for the SISO case in (CAMPESTRINI *et al.*, 2011) using the VRFT, in which the use of a *flexible reference model* provides the NMP transmission zeros together with the controller parameters.

The situation in the MIMO case is similar to the SISO case, but presents additional challenges; let us briefly discuss some of them. In a SISO plant, the existence of an NMP zero is usually easy to detect from the plant's step response, since the NMP characteristic causes an inverse response in the first moments after the step.[1] This is not the case for

[1]This is true for plants with natural NMP behavior, but not necessarily when an NMP zero appears in $G_0(q)$ as a result of sampling phenomena.

NMP-MIMO plants, unless the input is applied close to the NMP transmission zero's direction – a rare occurrence. Moreover, a step input in the MIMO case may produce an inverse response in a system that has **no** NMP transmission zeros.

Another difficulty peculiar to the MIMO case is the one expressed in Theorem 2.4 and discussed in the paragraph following it: the reference model must consider not only the location of the NMP transmission zero in the complex plane, but also its direction. Conceiving an appropriate reference model $T_d(q)$ is also more involved in the MIMO case. Since the ideal controller is a function of $G_0(q)$ and $T_d(q)$ (see (32)), a suitable choice on $T_d(q)$ should, at least ideally, allow the ideal controller to belong to the controller class. More realistically, the model reference may be chosen so that the ideal controller has a structure, which is not too far from the class $\mathcal{C}$ (GONÇALVES DA SILVA; BAZANELLA; CAMPESTRINI, 2018). For instance, if the controller has a centralized structure, then the reference model can be a decentralized one, i.e., setting all nondiagonal elements equal to zero and then to selecting SISO reference models for each output, or even a block-triangular one; in case the controller is decentralized, then a proper choice of the reference model structure would be centralized one. A thorough discussion on the choice of the reference model can be found in (GONÇALVES DA SILVA; BAZANELLA; CAMPESTRINI, 2018). Finally, a MIMO controller is bound to have a much larger number of parameters than a SISO controller, which raises numerical issues.

Contributions of this chapter are presented as follows: the approach when the NMP transmission zero and its output direction are known *a priori* is detailed in Subsection 3.1.1 for the VRFT; this has been published in (GONÇALVES DA SILVA; CAMPESTRINI; BAZANELLA, 2016). The extension using a flexible criterion, so the NMP transmission zero is also identified, to the MIMO case of VRFT is presented in Section 3.2; this has been published in (GONÇALVES DA SILVA; CAMPESTRINI; BAZANELLA, 2018). This solution however has a drawback: the reference model must be diagonal. To alleviate this constraint we propose a similar approach using the OCI in Section 3.3.

3.1 *A priori* knowledge of NMP transmission zeros and their output directions

In this section we discuss briefly the modifications needed on the studied DD methods when the process' NMP transmission zeros are already included in the reference model. There will be no discussion on how the information needed was obtained, as the focus is on the methods themselves.

3.1.1 Extended VRFT cost function

Assume the user has knowledge of the system's NMP transmission zeros and their output direction and he/she is decided to use the VRFT method to tune the controller pa-

rameters. From (36), it is clear that if the NMP transmission zeros information is added to the reference model, as suggested by Theorem 2.4, then the method will fail because it depends on the inverse of the reference model $T_d^{-1}(q)$, which will be an unstable filter. Notice that aside from the Model Reference problem regarding NMP zeros, in this case there is also an issue from the DD method point of view. Thus, the problem tackled in this Subsection is: given all *a priori* knowledge regarding the system's NMP transmission zeros, how can the user use the MIMO-VRFT method and still identify the optimal controller. The main parts of the results presented here were published in (GONÇALVES DA SILVA; CAMPESTRINI; BAZANELLA, 2016).

Inversion of $T_d(q)$ in (36) yields an unstable filter when $T_d(q)$ has an NMP transmission zero. The key-idea is then to add an all-pass filter, as presented in Subsection 2.2.4, which reflects this zero inside the unit circle, so the inversion yields a stable filter without altering the minimum of (36). For the non-minimum phase case, we will discuss the solutions based on some choices for the reference model. Our choices will consider that we are aiming to tune a *centralized* PID controller (35) with fixed derivative pole at zero.

3.1.1.1 Case 1*: diagonal reference model*

Let us consider first the case where a diagonal reference model has been chosen, that is

$$T_d(q) = \begin{bmatrix} T_{d_{11}}(q) & 0 & \dots & 0 \\ 0 & T_{d_{22}}(q) & \dots & 0 \\ \vdots & \vdots & \ddots & \vdots \\ 0 & 0 & \dots & T_{d_{nn}}(q) \end{bmatrix}, \tag{75}$$

where each element has the form

$$T_{d_{ii}}(q) = \frac{\frac{(1-p_{1ii})(1-p_{2ii})}{(1-z_{nm})}(q - z_{nm})}{(q - p_{1ii})(q - p_{2ii})}. \tag{76}$$

Since it can be seen as a choice of n SISO models, we can use the same approach as in (GONÇALVES DA SILVA; CAMPESTRINI; BAZANELLA, 2014) for the choice of the elements.

- If no overshoot is allowed, choose $p_{1ii} = e^{-4/n_s}$ and set $p_{2ii} = \frac{z_{nm}(1-p_{1ii})}{(z_{nm}-p_{1ii})}$.
- If some overshoot is allowed, then choose complex values for $p_{1,2}$, with $\text{Re}\{p\} = \frac{|p|^2+z_{nm}}{2z_{nm}}$ and $|p| = e^{-4/n_s}$.

Here, n_s is the desired number of samples in the settling time. The choice proposed for the second pole of the reference model elements yield, when computing the filter $L_d(q)$ (33) – which is a function of the reference model only –, the poles of a PID controller (35) with derivative pole at zero when computing the ideal controller (see (32)).

Notice that the NMP transmission zero is present in each element of (75). Thus, for a diagonal structure of the reference model one does not need to be concerned with the zero output direction, since constraint (74) will be satisfied because $T_d(z_{nm}) = 0$. On the other hand, the nasty effects of the NMP transmission zero are spread out to all outputs.

To apply the VRFT method, we need to add a filter $L_a(q)$ to (36) that both reflects the zero inside the unit circle and does not change the minimum of (36). In order to cope with the second necessity, we define

$$J^{VR}(P) = \sum_{t=1}^{N} ||F(q)L_a(q)[u(t) - C(q,P)(T_d^{-1}(q) - I)y(t)]||_2^2. \tag{77}$$

Also, in order to commute the filter $L_a(q)$ with $C(q,P)$ so we can multiply it with $T_d^{-1}(q)$ in (77), then $L_a(q)$ must be a scalar function multiplying the identity matrix and it must cope with the first necessity (zero reflection into the unit circle).

Since every element $T_{d_{ii}}(q)$ of $T_d(q)$ has the plant's NMP transmission zeros, we must reflect every zero inside the unit circle, which can be properly achieved with a scalar function times the identity matrix. The scalar function is a well-known Blaschke function given by

$$f(q) = \frac{|z_{nm}|}{z_{nm}} \frac{z_{nm} - q}{z_{nm}^* q - 1},$$

where z_{nm}^* is the complex conjugate of z_{nm}, and a generalized filter that considers every NMP transmission zero in the system is given by

$$L_a(q) = I \prod_{i=1}^{N_z} \frac{|z_{nm_i}|}{z_{nm_i}} \frac{z_{nm_i} - q}{z_{nm_i}^* q - 1}\ , \tag{78}$$

where N_z is the number of different NMP transmission zeros. Notice that this filter is a special case of filters (14)–(16) with $uu^H = yy^H = I$.

Let

$$\overline{T}_d(q) \triangleq T_d(q)L_a(q)^{-1}. \tag{79}$$

Then

$$J^{VR}(P) = \sum_{t=1}^{N} ||F(q)[L_a(q)u(t) - C(q,P)(\overline{T}_d^{-1}(q) - L_a(q))y(t)]||_2^2, \tag{80}$$

and due to the addition of $L_a(q)$, the implementable filter $F(q)$ is given by

$$F(q) = [T_d(q)(I - T_d(q))]L_a^{-1}(q). \tag{81}$$

3.1.1.2 Case 2: non-diagonal reference model

Consider now the case where the reference model is not diagonal but satisfies (74). In this case, each NMP transmission zero *of the reference model* will have an output direction

(74) equal to the process, but its input direction will be different of the process zero input direction.

One special case is when the reference model has a block-triangular structure. This structure allows a design where we can move the effect of the NMP transmission zero to a specific output. Let k be this output and consider the case with only one NMP transmission zero. Thus, the reference model can be defined as

$$T_d(q) = \begin{bmatrix} T_{d_{11}}(q) & 0 & 0 & 0 & \dots & 0 \\ 0 & T_{d_{22}}(q) & 0 & 0 & \dots & 0 \\ \vdots & \vdots & \ddots & \vdots & \dots & \vdots \\ T_{d_{k1}}(q) & T_{d_{k2}}(q) & \dots & T_{d_{kk}}(q) & \dots & T_{d_{kn}}(q) \\ 0 & 0 & 0 & 0 & \ddots & 0 \\ 0 & 0 & 0 & 0 & \dots & T_{d_{nn}}(q) \end{bmatrix}. \tag{82}$$

The elements $T_{d_{jj}}(q), j \neq k$, can be chosen according to the desired performance using models of first or second-order. The element $T_{d_{kk}}(q)$ must have the NMP transmission zeros and its poles are chosen according to performance criteria. The other elements of row k should be chosen so that the ideal controller matches the PID class, or at least is closer to it. Using (82), filter (33) is given by

$$L_d(q) = \begin{bmatrix} \frac{T_{d_{11}}(q)}{1-T_{d_{11}}(q)} & 0 & 0 & 0 & \dots & 0 \\ 0 & \frac{T_{d_{22}}(q)}{1-T_{d_{22}}(q)} & 0 & 0 & \dots & 0 \\ \vdots & \vdots & \ddots & \vdots & \dots & 0 \\ \frac{T_{d_{k1}(q)}}{\text{den}(L_{d_{jk}}(q))} & \frac{T_{d_{k2}}(q)}{\text{den}(L_{d_{jk}}(q))} & \dots & \frac{T_{d_{kk}}(q)}{1-T_{d_{kk}}(q)} & \dots & \frac{T_{d_{kn}}(q)}{\text{den}(L_{d_{jk}}(q))} \\ 0 & 0 & 0 & 0 & \ddots & 0 \\ 0 & 0 & 0 & 0 & \dots & \frac{T_{d_{nn}}(q)}{1-T_{d_{nn}}(q)} \end{bmatrix}$$

where $\text{den}(L_{d_{jk}}(q)) = (1 - T_{d_{jj}}(q))(1 - T_{d_{kk}}(q))),\ j = 1, \dots, n$ and $j \neq k$.

Since $C_d(q) = G_0^{-1}(q)L_d(q)$, the elements of $L_d(q)$ should at least contain the poles of the PID controller. To simplify the discussion, assume $T_{d_{kk}}(q)$ as a second-order model with the NMP zero and $T_{d_{jj}}(q)$ as a first-order model, both without delays. Then

$$L_{d_{jj}}(q) = \frac{1 - p_{1jj}}{q - 1}, \tag{83}$$

$$L_{d_{kj}}(q) = \frac{T_{d_{kj}}(q)}{\frac{(q-1)}{(q-p_{1jj})} \frac{(q-1)\left(q - \frac{z_{nm}(1-p_{1kk}-p_{2kk})+p_{1kk}p_{2kk}}{1-z_{nm}}\right)}{(q-p_{1kk})(q-p_{2kk})}}. \tag{84}$$

Notice that a proper choice of $T_{d_{kj}}(q)$ and $T_{d_{kk}}(q)$ will make (84) present the poles of a PID controller. More specifically, $T_{d_{kj}}(q)$ should have the poles of both $T_{d_{jj}}(q)$ and $T_{d_{kk}}(q)$, a zero at one and also the expression $\frac{z_{nm}(1-p_{1kk}-p_{2kk})+p_{1kk}p_{2kk}}{1-z_{nm}}$ should evaluate to the derivative pole; if it is zero, the result is as the one proposed in the diagonal reference model.

Consider the following choice for $T_{d_{kj}}(q)$:

$$\begin{aligned} T_{d_{kj}}(q) &= K_j \frac{(q-1)(q-z_{kj})}{(q-p_{1jj})(q-p_{1kk})(q-p_{2kk})} \\ &= K_j(q-z_{kj})\overline{T}_{d_{kj}}(q), \end{aligned} \tag{85}$$

where variables K_j and z_{kj} are (dependent) degrees of freedom that can be used to satisfy $y_{z_{nm}}^H T_d(z_{nm}) = 0$. This can be achieved as follows: choose a value for K_j (we recommend a value near the ratio between directions $|y_j/y_k|$); compute z_{kj} using

$$z_{kj} = z_{nm} + \frac{y_j T_{d_{jj}}(z_{nm})}{y_k K_j \overline{T}_{d_{kj}}(z_{nm})}. \tag{86}$$

There is a compromise between choices of K_j and z_{kj} and the maximum value expected at the output of $T_{d_{kj}}(q)$. Moreover, it is easier to move the effect of the NMP zero to the output where directionality is larger. If k is this output, then one can expect a lower interaction. Also, it is expected that with the recommended choice for K_j, expression (86) would result in a zero z_{kj} inside the unit circle, so the output is less deteriorated. Furthermore, since $\overline{T}_{d_{kj}}(q)$ has the poles of both $T_{d_{jj}}(q)$ and $T_{d_{kk}}(q)$, if every loop j is "faster" or have the same speed as loop k, then one can also expect lower interaction. If we consider time-delay, then a similar approach can be applied, and again the user must be aware that the ideal controller will not be in the PID controller class.

As for the VRFT criterion, we would like to add a filter to the left of (80), in order to keep the minimum unchanged and to maintain the orders of operators and signals. Since the criterion involves the inverse of a minimum phase factor of $T_d(q)$ (i.e. $\overline{T}_d^{-1}(q)$), the input factorization $L_I(q)$ (see Subsection 2.2.4) of the reference model is a suitable choice.

Nevertheless, this filter is not diagonal so it can not be commuted in (80). Thus, we use the filter $L_a(q)$ *along with* the input-factor filter $L_I(q)$. The criterion to be minimized is defined by

$$J^{VR} = \sum_{t=1}^{N} ||F(q)L_I(q)[L_a(q)u(t) - C(q,P)(\overline{T}_d^{-1}(q) - L_a(q))y(t)]||_2^2, \tag{87}$$

where $L_a(q)$ is given by (78) and $L_I(q)$ is given by (14).

Due to the addition of both $L_a(q)$ and $L_I(q)$, the implementable filter $F(q)$ is given by

$$F(q) = [T_d(q)(I - T_d(q))][L_I(q)L_a(q)]^{-1}. \tag{88}$$

The cost function (87) is a more complete version of (36): if the NMP transmission zeros have been added to the reference model without the direction information, then $L_I(q) = I$ and we obtain (80); if the reference model does not include any NMP transmission zero, then $L_a(q) = L_I(q) = I$ and we obtain (36).

3.2 Joint identification of NMP transmission zeros: VRFT with flexible criterion

The solution presented previously, although feasible, requires *a priori* knowledge of the NMP transmission zero, which in most practical situations would be obtained in a system identification approach. This contrasts with the philosophy of DD control methods that no plant model is supposed to be obtained. Thus, a more interesting solution would be one in which only the NMP transmission zero is identified and included in the reference model.

In (CAMPESTRINI *et al.*, 2011) a method has been developed, inspired by previous work in IFT (LECCHINI; GEVERS, 2002), to deal with this issue in SISO plants. The method consists of a parametrized reference model numerator which is to be identified along with the controller parameters in an iterative procedure using the same batch of data for both steps. A practical application of this method was presented in (SCHEID FILHO *et al.*, 2016).

Here we apply a similar approach to the design of MIMO controllers. The plant's transmission zeros are estimated along with optimal controller parameters, by means of a parametrized decoupled reference model; this is the first step of a two-step procedure. Once the NMP transmission zero(s) is (are) identified and included in the reference model, a second step can be performed where the reference model is then fixed and the VRFT method is applied only to estimate new controller parameters that will provide enhanced performance.

3.2.1 The flexible performance criterion

The core idea of the proposed method is to let the reference model be a parametrized transfer matrix:

$$T_d(q) = T_d(q, \eta) \tag{89}$$

where $\eta \in \mathbb{R}^c$ is a vector of free parameters of the numerator of each element in $T_d(q, \eta)$. In so doing, we are not specifying the whole transfer function; instead, degrees of freedom are left in its specification which can accommodate the inclusion of the necessary transmission zeros in the reference model. Using this parametrized transfer matrix in the performance criterion (36), we have the following *flexible criterion*:

$$J^{VR}(\eta, P) = \sum_{t=1}^{N} ||F(q, \eta)[u(t) - C(q, P)(T_d^{-1}(q, \eta) - I)y(t)]||_2^2. \tag{90}$$

The optimization of the flexible criterion $J^{VR}(\eta, P)$ is now made with respect to the controller parameters as well as the η parameters, which will provide the appropriate zeros in the reference model. The critical Assumption 2.1 must be adapted for this case, as follows.

Assumption 3.1. *There exists a pair (η^*, P^*) such that $J^{VR}(\eta^*, P^*) = 0$ or, equivalently,*

$$\exists \eta^*, P^* : C(q, P^*) = G_0^{-1}(q) T_d(q, \eta^*)[I - T_d(q, \eta^*)]^{-1}. \tag{91}$$

The parametrization to be chosen for the reference model will be the one most appropriate to the design method to be applied. In order to be able to apply a VRFT scheme similar to the one in (CAMPESTRINI *et al.*, 2011), we will need the following assumption on this parametrization.

Assumption 3.2. *The flexible reference model is chosen as*

$$T_d(q, \eta) = \eta^T \vartheta(q) I, \tag{92}$$

where $\eta \in \mathbb{R}^c$ is a vector of free parameters and $\vartheta(q)$ is a c-vector of proper rational functions.

Notice that (92) implies that the same closed-loop behavior is specified for every input-output pair, which may be a restrictive performance choice. However, this drawback can be solved in a two-step procedure, which will be described later. On the other hand, this parametrization will allow us to keep the attractive VRFT solution via least-squares.

Under Assumptions 3.1 and 3.2, it follows that

$$(\eta^*, P^*) = \underset{\substack{\eta, P \\ (\eta, P) \neq \{0,\, 0\}}}{\arg\min}\ \tilde{J}^{VR}(\eta, P) \tag{93}$$

$$\tilde{J}^{VR}(\eta, P) = \sum_{t=1}^{N} ||\bar{F}(q) T_d(q, \eta) u(t) - \bar{F}(q) C(q, P)(I - T_d(q, \eta)) y(t)||_2^2 \tag{94}$$

$$\bar{F}(q) = (I - T_d(q, \hat{\eta})). \tag{95}$$

The criterion $\tilde{J}^{VR}(\eta, P)$ in (94) is obtained by approximating the filter (37) as $F(q) = T_d(q, \eta)\bar{F}(q)$, which has a term that is a function of the unknown η, and a term that is a function of an estimated $\hat{\eta}$. Under Assumption 3.2, $T_d(q, \eta)$ commutes with all matrices and can be estimated in the procedure that will be described in the following. On the other hand, by using a term that uses an estimated $\hat{\eta}$, the filter used to approximate the minima of $J^{VR}(\eta, P)$ and $J^{MR}(P)$ is a known quantity. Optimization of $\tilde{J}^{VR}(\eta, P)$ will be easier because it depends on $T_d(q, \eta)$ and not on its inverse, thus all the parameters to be identified appear in its numerator. Given the linear parametrization of both the controller and the reference model, then $\tilde{J}^{VR}(0, 0) = 0$. Thus, the multiplication by $T_d(q, \eta)$ has created an additional – and undesired – global minimum at the origin, which is the reason why the right hand side of (94) is subjected to a constraint that excludes $(\eta, P) = \{0,\, 0\}$. In most control applications, a natural constraint exists which automatically does that: the reference model must have steady-state gain $T_d(1, \eta) = I$.

3.2.2 Sequential least-squares

Since the argument in (94) is bilinear in η and P, the minimization of $\tilde{J}^{VR}(\eta, P)$ can be treated as a sequence of least squares problems (LJUNG, 1999):

$$\hat{\eta}^{(i)} = \arg\min_{\eta} \quad \tilde{J}^{VR}(\eta, \hat{P}^{(i-1)}) \tag{96}$$

$$\hat{P}^{(i)} = \arg\min_{P} \quad \tilde{J}^{VR}(\hat{\eta}^{(i)}, P), \tag{97}$$

where we assume knowledge of one quantity (η or P) to obtain the other and the use of a known filter $\bar{F}(q)$. Assume that $C(q, \hat{P})$ is a known transfer matrix and insert (92) in (94). This gives

$$\begin{aligned}\tilde{J}^{VR}(\eta, \hat{P}) &= \sum_{t=1}^{N} ||\eta^T \vartheta(q)[\bar{F}(q)u(t) + \bar{F}(q)C(q, \hat{P})y(t)] - \bar{F}(q)C(q, \hat{P})y(t)||_2^2 \\ &= \sum_{t=1}^{N} ||\eta^T \vartheta(q)\bar{F}(q)[u(t) + C(q, \hat{P})y(t)] - \bar{F}(q)C(q, \hat{P})y(t)||_2^2. \end{aligned} \tag{98}$$

where $\bar{F}(q)$ can be obtained using the estimate of η obtained in the previous iteration, that is $\hat{\eta}^{(i-1)}$. Least-squares solution of (98) with respect to η is given by

$$\hat{\eta} = \left[\sum_{t=1}^{N} (\vartheta(q)b(t))^T (\vartheta(q)b(t))\right]^{-1} \left[\sum_{t=1}^{N} (\vartheta(q)b(t))^T \tilde{u}(t)\right] \tag{99}$$

where $b(t) = \bar{F}(q)[u(t) + C(q, \hat{P})y(t)]$ and $\tilde{u}(t) = \bar{F}(q)C(q, \hat{P})y(t)$.

Now, assume that $T(q, \hat{\eta})$ is a known transfer matrix. Then (94) can be rewritten as

$$\begin{aligned}\tilde{J}^{VR}(\hat{\eta}, P) &= \sum_{t=1}^{N} ||T(q, \hat{\eta})\bar{F}(q)u(t) - F(q)C(q, P)y(t) + \bar{F}(q)C(q, P)T(q, \hat{\eta})y(t)||_2^2 \\ &= \sum_{t=1}^{N} ||T(q, \hat{\eta})\bar{F}(q)u(t) - \bar{F}(q)C(q, P)(I - T(q, \hat{\eta}))y(t)||_2^2. \end{aligned} \tag{100}$$

Least-squares solution to (100) is the same as (38) but with

$$u_F(t) = T(q, \hat{\eta})\bar{F}(q)u(t) \;\text{ and }\; \bar{e}(t) = (I - T(q, \hat{\eta}))y(t)$$

The formulation presented above is to be used when signals are noise free. In this case, when Assumption 3.2 is satisfied, then the algorithm is able to identify the NMP transmission zeros and the ideal controller. However, when data is corrupted with noise, the solution of the algorithm is biased. Just like the standard VRFT, the flexible criterion makes use of instrumental variables when data is affected by noise to provide unbiased estimates (BAZANELLA; CAMPESTRINI; ECKHARD, 2011; CAMPESTRINI *et al.*, 2016). Moreover, we highlight that the sequential least squares procedure is only guaranteed to converge to a local minimum (LJUNG, 1999).

3.2.3 Important remarks

Since the procedure is iterative, initial values for $C(q, P^{(0)})$ and/or $T_d(q, \eta^{(0)})$ must be given. The procedure is well fit for when data are collected in closed-loop as the initial controller parameters are given, which is the case of a controller redesign, so in the first iteration we already try to identify the transmission zero. If data are collected in an open-loop experiment, then the user could start by identifying the controller based on an initial reference model. One possible choice for the initial $T_d(q, \eta)$ is to use a reference model that does not take account of the NMP transmission zeros, with a fixed numerator, and that provides a slow closed-loop response. However, there is no guarantee that this choice leads to a stable closed-loop with the identified controller.

If data are collected in closed-loop then the first step of the sequential least squares is to identify the reference model. Remember that filter $\bar{F}(q)$ is a function of an estimate of η, which is unknown. In this case, we suggest to start the algorithm by using $\bar{F}(q) = I$ to obtain $\eta^{(1)}$ and then update the filter at each step using the obtained estimates of η.

Finally it is important to highlight that, just as in the SISO case, even though the minimization algorithm is iterative, the data from the system are collected just once, thereby keeping the "one-shot" property of the VRFT method.

3.2.4 Two-step procedure

It has been shown in (93), (94) and (95) that the global minimum of the flexible criterion $\tilde{J}^{VR}(\eta, P)$ corresponds to a diagonal reference model that contains the NMP transmission zeros of the plant, if any. The two-step procedure can then be described as follows.

Step 1: Minimize $\tilde{J}^{VR}(\eta, P)$; call $(\hat{\eta}, \hat{P})$ the minimizing parameters and check the step response of $T_d(q, \hat{\eta})$. If it is satisfactory, apply $C(q, \hat{P})$ to the system. If not, go to *Step 2*.

Step 2: If the obtained $T_d(q, \hat{\eta})$ has NMP transmission zeros, then keep these zeros and change the reference model poles according to a desired response; if not, change poles and zeros accordingly. Apply the standard MIMO-VRFT (see Subsection 3.1.1).

Notice that while *Step 1* is used to identify the NMP transmission zeros, *Step 2* is used to eliminate the drawback of having the same desired response for every loop. However, we cannot eliminate the NMP effect from every output since we do not know their direction.

3.3 Joint identification of NMP transmission zero and output direction ratio: OCI with flexible criterion

The VRFT method with a flexible criterion presented in the previous section has a drawback: in order to identify the NMP transmission zero together with the optimal controller, the flexible reference model must be such as to have the NMP transmission zero in all outputs. Moreover, it has been shown in Subsection 3.1.1 that with a proper choice of the reference model structure, one can move the NMP transmission zero effect to one output. Thus, in this section we bring these ideas together in order to develop a flexible criterion for the OCI so as to avoid addition of NMP transmission zeros in the closed-loop.

3.3.1 The flexible performance criterion

Recall that for the VRFT, the core idea of the flexible criterion was to let the reference model be a parametrized transfer matrix. A similar approach is used here, but instead of parametrizing the reference model, we will use a parametrization directly on the filter $L_d(q)$ (33), i.e.,

$$L_d(q) = L_d(q, \eta) \tag{101}$$

where $\eta \in \mathbb{R}^c$ is a vector of free parameters of the numerators in $L_d(q, \eta)$. More specifically, in light of the argument opening this section, let the reference model have a block-triangular structure (82). Also, for instance, consider a 2×2 system where we want to move the zero effect to output $k = 2$, so the parametrized loop function is of the form

$$L_d(q, \eta) = \begin{bmatrix} \frac{T_{d_{11}}(q)}{1-T_{d_{11}}(q)} & 0 \\ \frac{T_{d_{21}}(q)}{(1-T_{d_{11}}(q))(1-T_{d_{22}}(q)))} & \frac{T_{d_{22}}(q)}{1-T_{d_{22}}(q)} \end{bmatrix} = \begin{bmatrix} L_{d_{11}}(q) & 0 \\ L_{d_{21}}(q, \eta) & L_{d_{22}}(q, \eta) \end{bmatrix}, \tag{102}$$

where we made clear that only the elements of the reference model with respect to the output k to which we want to move the NMP transmission zero effect need to be parametrized. We shall see next that with the choices proposed in Subsection 3.1.1.2 this will lead to a MISO (multiple-input single-output) least-squares identification with constraints. Assume the ideal form of the elements of the reference model

$$T_{d_{11}}(q) = \frac{1 - p_1}{q - p_1}$$

$$T_{d_{22}}(q) = \frac{\frac{(1-p_{1_{22}})(1-p_{2_{22}})}{1-z_{nm}}(q - z_{nm})}{(q - p_{1_{22}})(q - p_{1_{22}})} \quad T_{d_{21}}(q) = \frac{K(q-1)(q - z_{21})}{(q - p_1)(q - p_{1_{22}})(q - p_{1_{22}})}$$

We then have

$$L_d(q) = \begin{bmatrix} \frac{1 - p_1}{q - 1} & 0 \\ \frac{K(q - z_{21})}{(q-1)(q - \frac{z_{nm}(1-p_{1_{22}}-p_{2_{22}})+p_{1_{22}}p_{2_{22}}}{1-z_{nm}})} & \frac{\frac{(1-p_{1_{22}})(1-p_{2_{22}})}{1-z_{nm}}(q - z_{nm})}{(q-1)(q - \frac{z_{nm}(1-p_{1_{22}}-p_{2_{22}})+p_{1_{22}}p_{2_{22}}}{1-z_{nm}})} \end{bmatrix} \tag{103}$$

and a parametrized model of (103) can be described by

$$L_d(q,\eta) = \begin{bmatrix} 1-p_1 & 0 \\ \dfrac{\eta_1 q - \eta_2}{q-\eta_5} & \dfrac{\eta_3 q - \eta_4}{q-\eta_5} \end{bmatrix} \frac{1}{q-1}. \tag{104}$$

Notice that only row 2 needs to be identified, and since the elements have a common denominator, that can be achieved with a MISO least-squares identification with constraints as follows.

Let $C(q,\hat{P})$ be a *fixed* controller, then (42) can be rewritten in terms of the parametrized $L_d(q,\eta)$ as

$$G(q,\eta) = L_d(q,\eta)C^{-1}(q,\hat{P}). \tag{105}$$

Define

$$\tilde{u}(t) = \left(\frac{1}{q-1}C^{-1}(q,\hat{P})\right) u(t) \tag{106}$$

$$\eta = [\eta_1 \;\; \eta_2 \;\; \eta_3 \;\; \eta_4 \;\; \eta_5]^T \tag{107}$$

$$\varphi(t) = [\tilde{u}_1(t) \;\; \tilde{u}_1(t-1) \;\; \tilde{u}_2(t) \;\; \tilde{u}_2(t-1) \;\; -y_2(t-1)]^T \tag{108}$$

so the simplified predictor (54) of the *second* row can be rewritten as

$$\hat{y}_2(t,\eta) = \eta^T\varphi(t). \tag{109}$$

Predictor (109) is put in a classical least-squares form and can be solved as such. It is important however to be aware of some constraints:

- Recall that the gain K and the zero z_{21} are related via (86). This degree of freedom can lead to bad conditioning when solving the least-squares problem. We recommend to choose K (i.e., fixing η_1) and let the zero be identified.
- The element $T_{d_{22}}(q)$ must satisfy $T_{d_{22}}(1) = 1$ for constant reference tracking. Under the assumption that we want to identify a PID and that the ideal controller belongs to the PID controller class, then η_5 should evaluate to zero and, to satisfy $T_{d_{22}}(1) = 1$, then $\eta_3 + \eta_4 = (1-p_{1_{22}})(1-p_{2_{22}})$.
- Notice that in terms of reconstructing the reference model from η, η_5 is not used at all and the other terms are directly the reference model parameters.

These ideas can be put together in the following minimization problem

$$\begin{aligned} \min_{\eta} \quad & \frac{1}{2}||\eta^T\varphi(t) - y(t)||^2 \\ \text{subject to} \quad & \begin{bmatrix} 1 & 0 & 0 & 0 & 0 \\ 0 & 0 & 1 & 1 & 0 \end{bmatrix} \eta = \begin{bmatrix} K \\ (1-p_{1_{22}})(1-p_{2_{22}}) \end{bmatrix} \end{aligned} \tag{110}$$

We remark that we presented the formulation considering output $k = 2$ and the PID controller with derivative pole at zero (35), but it can be easily rewritten for other outputs and/or controller structures. In terms of which output to choose to move the zero, a practical situation would be the output less important of the process, such as level control that acts like buffering either for production or to reduce variability of the cascaded processes.

3.3.2 Sequential optimization

In Subsection 2.4.3 we presented the formulation for the MIMO-OCI to find the optimal controller parameters when the reference model is fixed and in Subsection 3.3.1 we changed the formulation in order to identify some reference model parameters to accommodate the system NMP transmission zeros when the controller is fixed.

Based on the idea of a sequential least-squares given for the VRFT, we apply a similar procedure now using the OCI. Having in mind that the proposed formulation requires an initial controller, the most natural step to take next is to proceed with the identification of the free parameters in the reference model. The sequential optimization can be described as

1. Given an initial controller $C(q, P_0)$, select the output k to which the NMP transmission zero effect is to be moved and choose an *a priori* value for K_{jk}. Let $i = 1$.

2. Solve (110) and find $\eta^{(i)}$. Fix the reference model $T_d(q, \hat{\eta}^{(i)})$.

3. Apply the standard MIMO-OCI method to find $P^{(i)}$. Fix the controller $C(q, \hat{P}^{(i)})$.

4. Increase $i = i + 1$. Repeat steps 2–3 until some convergence criterion is achieved.

As in the VRFT method, the same batch of data is used throughout the sequential optimization thus keeping the "one-shot" characteristic of the method.

3.4 Illustrative examples

In this section we present simulation studies using the flexible VRFT scheme with the two-step procedure. We apply the proposed procedure to an NMP process with one NMP transmission zero, first for the case without noise, then for a case where noise is present at the output. We also consider the cases where Assumption 3.1 is satisfied and where it is not. The idea is to explore the applicability of the proposed methodology from the ideal case (when all assumptions are satisfied) to the most practical case. In Sub-Section 3.4.4 we provide an illustrative example using the OCI methodology.

3.4.1 Process with one NMP transmission zero

Consider again the process of Example 2.2, repeated here for convenience:

$$G_1(q) = \begin{bmatrix} \dfrac{(q-0.7)}{(q-0.9)(q-0.8)} & \dfrac{2}{(q-0.8)} \\ \dfrac{1.25}{(q-0.8)} & \dfrac{1.5}{(q-0.8)} \end{bmatrix}, \tag{111}$$

which has an NMP transmission zero at $q = 1.2$ with $y_{z_{nm}} = [-0.6 \;\; 0.8]^T$. The plant's open-loop response to a sequence of steps was portrayed in Figure 1, where no inverse response is observed though the process is NMP.

Since the output has no inverse response and prior to any knowledge about the system's model, one might be tricked to choose a reference model without considering the NMP transmission zero, like the following desired reference model:

$$T_d(q) = \begin{bmatrix} \dfrac{0.2}{(q-0.8)} & 0 \\ 0 & \dfrac{0.2}{(q-0.8)} \end{bmatrix}.$$

Applying the standard VRFT criterion with this reference model and using the open-loop data collected to tune a PID controller yields

$$C(q,\hat{P}) = \begin{bmatrix} \dfrac{0.234(q+0.2037)(q-0.9073)}{q(q-1)} & \dfrac{-0.1911(q+0.2666)(q-0.8616)}{q(q-1)} \\ \dfrac{-0.195(q+0.2037)(q-0.9073)}{q(q-1)} & \dfrac{0.2926(q+0.1493)(q-0.8377)}{q(q-1)} \end{bmatrix}, \tag{112}$$

which causes the closed-loop to be unstable, as the corresponding closed-loop transfer matrix will have a pole at $q = 1.0105$. As pointed out in (CAMPESTRINI *et al.*, 2011), the system instability is not caused by an unstable pole-zero cancellation between a controller pole and the NMP zero of $G_1(q)$, since the controller poles are fixed. Notice that in practice the model is unavailable, so an unstabilizing controller would have been put in closed loop; this is why the subject of Chapter 5 is of ultimate importance.

We thus use the proposed two-step procedure. First, the loop is closed with an initial stabilizing proportional controller given by

$$C(q,P^{(0)}) = \begin{bmatrix} 0.5 & 0 \\ 0 & 0.5 \end{bmatrix}. \tag{113}$$

and data is collected in closed-loop with the reference signal being a sequence of steps – the same sequence applied to the process input in the open-loop experiment presented in Figure 1. For the remaining of this Section, we consider the tuning of a centralized PID controller class (35) with fixed derivative pole at zero.

3.4.1.1 Assumption 3.1 is not satisfied

Consider the following flexible reference model

$$T_d(q,\eta) = \frac{\eta_1 q + \eta_2}{(q-0.8)^2} I = \underbrace{[\eta_1 \;\; \eta_2]}_{\eta^T} \underbrace{\begin{bmatrix} \dfrac{q}{(q-0.8)^2} \\ \dfrac{1}{(q-0.8)^2} \end{bmatrix}}_{\vartheta(q)} I, \tag{114}$$

for which Assumption 3.1 is not satisfied for a centralized PID controller class (35), which is the most common situation when the process is unknown.

Minimizing (90) using the iterative procedure (96)–(97) yields the following results at iteration 30:

$$T_d(q,\hat{\eta}^{(30)}) = \begin{bmatrix} \dfrac{-0.1884(q-1.212)}{(q-0.8)^2} & 0 \\ 0 & \dfrac{-0.1884(q-1.212)}{(q-0.8)^2} \end{bmatrix},$$

$$C(q,\hat{P}^{(30)}) = \begin{bmatrix} \dfrac{0.4057(q-0.7139)(q-0.9168)}{q(q-1)} & \dfrac{-0.5166(q-0.6879)(q-0.922)}{q(q-1)} \\ \dfrac{-0.3166(q-0.6876)(q-0.9205)}{q(q-1)} & \dfrac{0.2805(q-0.6451)(q-0.797)}{q(q-1)} \end{bmatrix}. \tag{115}$$

The closed-loop response of plant (111) with controller (115) is shown in Figure 4. Some coupling between loops appears in the actual response, specially from input 2 to output 1, which represents a mismatch between the obtained response and the desired one, which specified a decoupled behavior. This was to be expected, since the controller's structure is not complex enough to provide exactly the desired response for this plant. For this case the performance measure (30) is evaluated as $J^{MR}(\hat{P}^{(30)}) = 0.27$.

One might be satisfied with this result and stop the design at this point. Nonetheless, as indicated in (GONÇALVES DA SILVA; CAMPESTRINI; BAZANELLA, 2016), once the NMP transmission zero has been identified, if one is aiming for the matched case, then a proper choice of the second pole based on the NMP transmission zero can be done (see also Sub-Subsection 3.1.1.1, p. 42). A suitable reference model choice in this case would be

$$T_d(q) = \begin{bmatrix} \dfrac{-0.388(q-1.212)}{(q-0.588)(q-0.8)} & 0 \\ 0 & \dfrac{-0.388(q-1.212)}{(q-0.588)(q-0.8)} \end{bmatrix}, \tag{116}$$

Figure 4 – Closed-loop response of system (111) with controller (115).

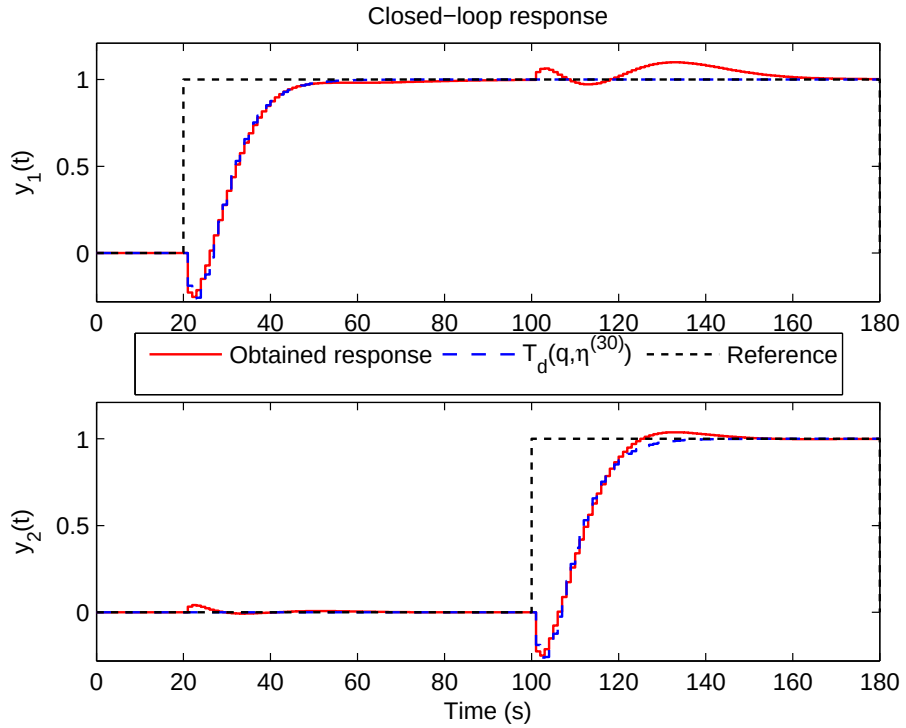

Source: author.

to which the minimization of (80) yields the controller

$$C(q,\hat{P}) = \begin{bmatrix} \dfrac{0.6081(q-0.8094)(q-0.8997)}{q(q-1)} & \dfrac{-0.8038(q-0.8048)(q-0.9006)}{q(q-1)} \\ \dfrac{-0.5068(q-0.8094)(q-0.8997)}{q(q-1)} & \dfrac{0.4112(q-0.7227)(q-0.7897)}{q(q-1)} \end{bmatrix}. \tag{117}$$

The closed-loop response of plant (111) with controller (117) is shown in Figure 5, and the comparison of the closed-loop control action with controllers (115) and (117) is shown in Figure 6. With this simple change of the second pole, coupling has been much reduced, with only a small change in the control action, and we obtained $J^{MR}(\hat{P}) = 0.043$, which is much smaller than obtained previously. Notice that we only changed the reference model whereas the data were the same – no additional experiment was required for the redesign.

The main point of discussion here is that even when the flexible reference model does not allow to achieve the matching condition (91), the NMP transmission zero can still be identified with good precision. The quality of the estimate depends on the choice of the reference model poles and, since NMP transmission zeros impose some limitations on closed-loop bandwidth (SKOGESTAD; POSTLETHWAITE, 2005), the dominant pole of the reference model should be chosen to provide a response that is only moderately faster than in open-loop.

Figure 5 – Closed-loop response of system (111) with controller (117).

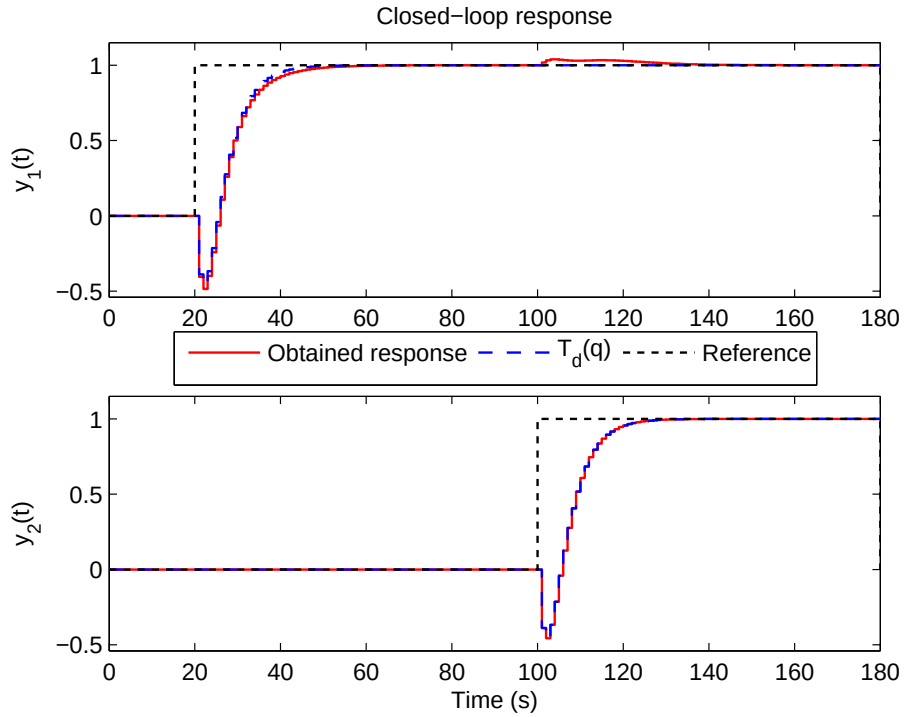

Source: author.

Figure 6 – Control action of the closed-loop response with controllers (115) (red line) and (117) (dashed blue line).

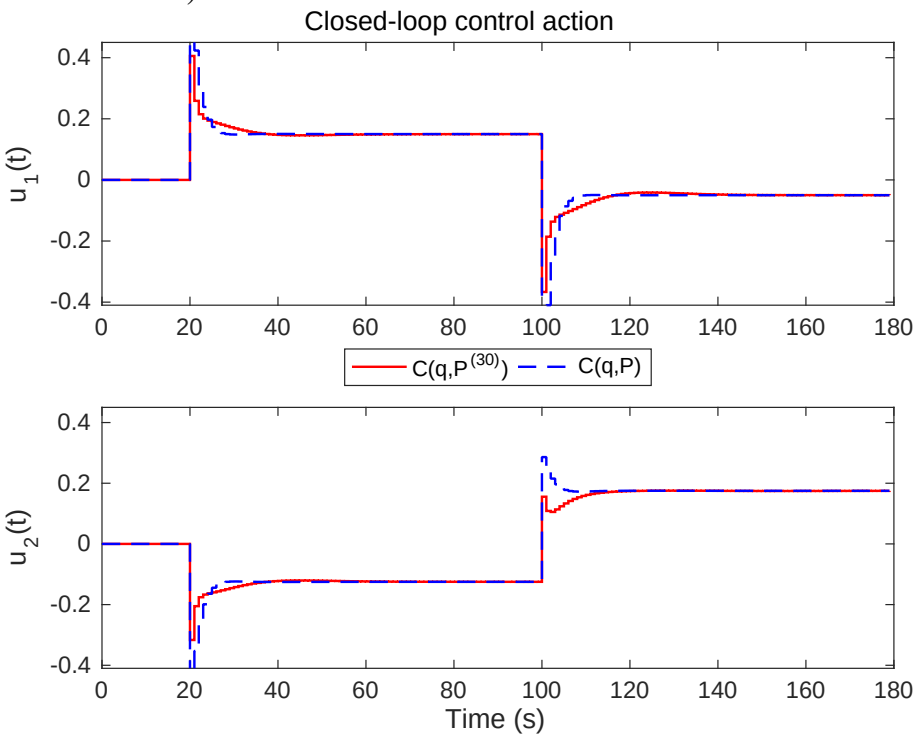

Source: author.

3.4.1.2 Assumption 3.1 is satisfied

Consider the following flexible reference model

$$T_d(q,\eta) = \frac{\eta_1 q + \eta_2}{(q-0.8)(q-0.6)} I = \underbrace{[\eta_1 \;\; \eta_2]}_{\eta^T} \underbrace{\begin{bmatrix} \dfrac{q}{(q-0.8)(q-0.6)} \\ \dfrac{1}{(q-0.8)(q-0.6)} \end{bmatrix}}_{\vartheta(q)} I, \tag{118}$$

which satisfies Assumption 3.1 for a PID controller class. That is, reference model (118) allows minimization of (90) to achieve the matching condition (91) for some (η^*, P^*) pair.

We minimize again (90) using the iterative procedure (96)–(97). Table 1 shows the evolution of the estimated reference model parameters for some iterations, as well as the intermediate cost $\tilde{J}^{VR}(\hat{\eta}, \hat{P}^{(i-1)})$ and the final cost $\tilde{J}^{VR}(\hat{\eta}^{(i)}, \hat{P})$. The controller parameters have been omitted. Notice that in the first iteration, when the reference model does not have the NMP transmission zero, the cost was $\tilde{J}^{VR}(\hat{\eta}^{(1)}, \hat{P}) = 6.50$, significantly higher compared to the result of the last iteration, when the NMP transmission zero was correctly identified and the cost was reduced to $\tilde{J}^{VR}(\hat{\eta}^{(30)}, \hat{P}) = 1.0 \times 10^{-4}$.

Table 1 – Evolution of estimated num($T_d(q)$) and VRFT cost function

i	num($T_d(q)$)	$\tilde{J}^{VR}(\hat{\eta}, \hat{P}^{(i-1)})$	$\tilde{J}^{VR}(\hat{\eta}^{(i)}, \hat{P})$
1	$0.13004(q-0.3848)$	67.764	6.497
2	$0.06105(q+0.3103)$	8.786	6.450
3	$-0.01139(q-8.0194)$	8.731	6.181
4	$-0.08420(q-1.9501)$	8.332	5.641
10	$-0.35951(q-1.2225)$	1.945	1.019
30	$-0.4(q-1.2000)$	2.1×10^{-4}	1.0×10^{-4}

The obtained $T_d(q, \hat{\eta}^{(30)})$ and $C(q, \hat{P}^{(30)})$ at iteration 30 are:

$$T_d(q, \hat{\eta}^{(30)}) = \begin{bmatrix} \dfrac{-0.4(q-1.2)}{(q-0.6)(q-0.8)} & 0 \\ 0 & \dfrac{-0.4(q-1.2)}{(q-0.6)(q-0.8)} \end{bmatrix},$$

$$C(q, \hat{P}^{(30)}) = \begin{bmatrix} \dfrac{0.6(q-0.8)(q-0.9)}{q(q-1)} & \dfrac{-0.8(q-0.8)(q-0.9)}{q(q-1)} \\ \dfrac{-0.5(q-0.8)(q-0.9)}{q(q-1)} & \dfrac{0.4(q-0.7)(q-0.8)}{q(q-1)} \end{bmatrix}.$$

A good estimate of the NMP transmission zero is already obtained at iteration $i = 10$. This observation is coherent with the findings of (MÅRTENSSON; HJALMARSSON,

2009) for the SISO case where it is shown that NMP zeros are easier to be estimated than minimum phase ones. Suppose now we would like to make loop 2 slower than loop 1, with a pole at $q = 0.9$. Since now we know the NMP transmission zero location, we can properly choose the reference model as

$$T_d(q) = \begin{bmatrix} \dfrac{-0.4(q-1.2)}{(q-0.6)(q-0.8)} & 0 \\ 0 & \dfrac{-0.3(q-1.2)}{(q-0.4)(q-0.9)} \end{bmatrix}, \tag{119}$$

and proceed with Step 2 of the proposed methodology. Minimizing (80) yields the controller

$$C(q,\hat{P}) = \begin{bmatrix} \dfrac{0.6(q-0.8)(q-0.9)}{q(q-1)} & \dfrac{-0.6(q-0.8)(q-0.9)}{q(q-1)} \\ \dfrac{-0.5(q-0.8)(q-0.9)}{q(q-1)} & \dfrac{0.3(q-0.7)(q-0.8)}{q(q-1)} \end{bmatrix}. \tag{120}$$

Figure 7 shows the evolution of the reference model choices and the closed-loop response of system (111) with controller (120), which has exactly the desired behavior (119) specified in Step 2.

Figure 7 – Closed-loop response of system (111) with controller (120).

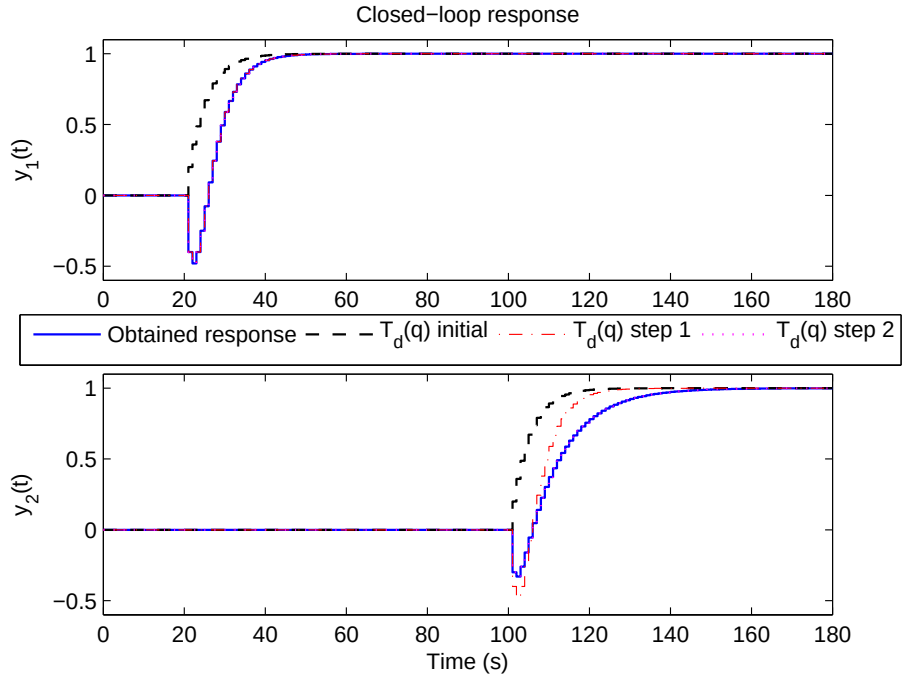

Source: author.

3.4.2 Process with one minimum phase transmission zero

Consider a process described by

$$G_2(q) = \begin{bmatrix} \dfrac{25/24(q-0.7)}{(q-0.9)(q-0.8)} & \dfrac{0.625}{(q-0.8)} \\ \dfrac{0.4}{(q-0.8)} & \dfrac{1.2(q-0.78)}{(q-0.9)(q-0.8)} \end{bmatrix} \tag{121}$$

which has a minimum phase transmission zero at $q = 0.6$ with $y_z = [-0.75517 \ 0.65553]^T$. A batch of data is obtained from a closed-loop experiment, where the reference signal is a PRBS and the controller is the same as (113).

3.4.2.1 Assumption 3.1 is satisfied

Let the flexible reference model be

$$T_d(q,\eta) = \frac{\eta_1 q + \eta_2}{(q-0.85)(q+0.36)} I, \tag{122}$$

which satisfies Assumption 3.1. Minimization of (90) with 30 iterations resulted in:

$$T_d(q,\hat{\eta}^{(30)}) = \begin{bmatrix} \dfrac{0.52827(q-0.6138)}{(q-0.85)(q+0.36)} & 0 \\ 0 & \dfrac{0.52827(q-0.6138)}{(q-0.85)(q+0.36)} \end{bmatrix},$$

$$C(q,\hat{P}^{(30)}) = \begin{bmatrix} \dfrac{0.63249(q-0.902)(q-0.7804)}{q(q-1)} & \dfrac{-0.32986(q^2-1.805q+0.8145)}{q(q-1)} \\ \dfrac{-0.2113(q^2-1.807q+0.817)}{q(q-1)} & \dfrac{0.54892(q-0.9023)(q-0.6994)}{q(q-1)} \end{bmatrix}. \tag{123}$$

Notice that the identified transmission zero is not precisely $q = 0.6$, though it is not an NMP transmission zero; it took actually 150 iterations to converge to $q = 0.6$. Closed-loop response with controller (123) is shown in Figure 8.

Although it is a well known result in control theory that zeros of a system can not be relocated with feedback control, so they should appear in the reference model anyway, minimum phase zeros do not impose fundamental stability constraints. Also, the shape of the response due to a pole at $q = -0.36$ might be disregarded by the user. Thus, he/she could go for a simpler reference model – say, first order diagonal elements – and still achieve a closed-loop with good resemblance to the reference model. We will retake this discussion in the next subsection.

3.4.2.2 Assumption 3.1 is not satisfied

Let the flexible reference model be

$$T_d(q,\eta) = \frac{\eta_1 q + \eta_2}{(q-0.85)(q-0.4)} I, \tag{124}$$

Figure 8 – Closed-loop response of system (121) with controller (123).

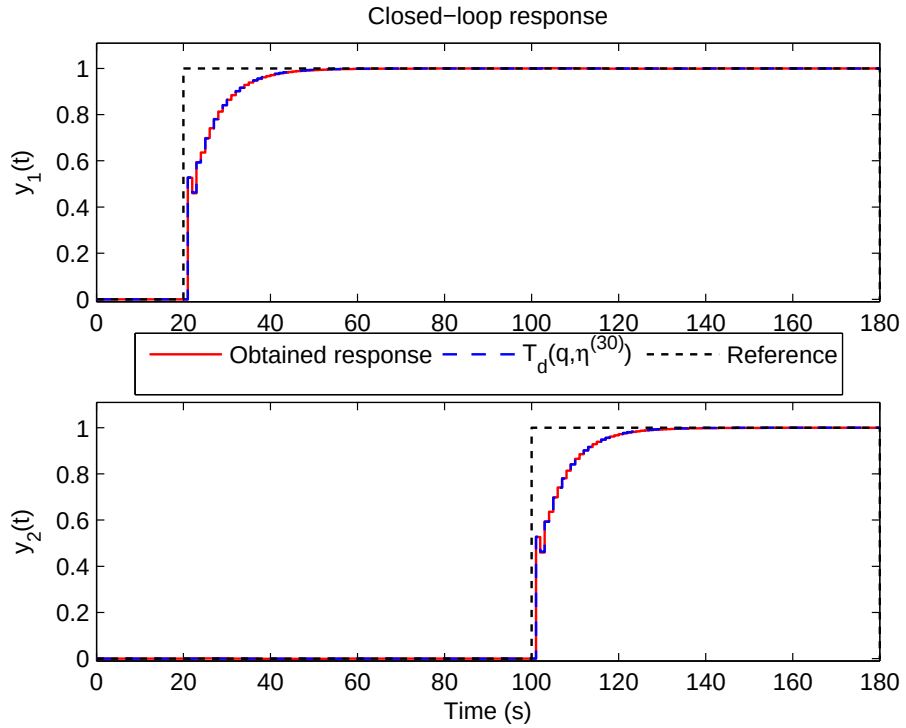

Source: author.

which does not satisfies Assumption 3.1 for the centralized PID controller class. Minimization of (94) with 30 iterations resulted in:

$$T_d(q,\hat{\eta}^{(30)}) = \begin{bmatrix} \dfrac{0.65615(q-0.8628)}{(q-0.85)(q-0.4)} & 0 \\ 0 & \dfrac{0.65615(q-0.8628)}{(q-0.85)(q-0.4)} \end{bmatrix},$$

$$C(q,\hat{P}^{(30)}) = \begin{bmatrix} \dfrac{0.78828(q-0.9543)(q-0.131)}{q(q-1)} & \dfrac{-0.4107(q-1.033)(q-0.2054)}{q(q-1)} \\ \dfrac{-0.26299(q-1.037)(q-0.2008)}{q(q-1)} & \dfrac{0.68378(q-0.9056)(q-0.07865)}{q(q-1)} \end{bmatrix}.$$

The difference between the identified transmission zero here and the one identified previously is remarkable, even though it is still minimum phase. Even after 150 iterations the transmission zero identification converged to $q = 0.865$, which is far from 0.6. If one would aim for a matched-case with the identified zero and keeping the dominant pole at $q = 0.85$, the second pole should be chosen as $q = 9.75$ which would lead to an unstable choice for the reference model. The point here is that the identification of minimum phase transmission zeros can be misleading if neither the controller structure nor the reference model's are flexible enough to identify them, as was already pointed out for the SISO case in (MÅRTENSSON; HJALMARSSON, 2009).

Since the identified transmission zero is minimum phase (as it was in the matched case), we will proceed to Step 2 with a model of reduced order:

$$T_d(q) = \begin{bmatrix} \dfrac{0.15}{(q-0.85)} & 0 \\ 0 & \dfrac{0.15}{(q-0.85)} \end{bmatrix} \tag{125}$$

to which minimization of (36) yields the controller

$$C(q,\hat{P}) = \begin{bmatrix} \dfrac{0.19949(q-0.9324)(q-0.3619)}{q(q-1)} & \dfrac{-0.14721(q-0.9753)(q-0.5473)}{q(q-1)} \\ \dfrac{-0.069296(q-0.984)(q-0.4976)}{q(q-1)} & \dfrac{0.21888(q-0.9171)(q-0.1977)}{q(q-1)} \end{bmatrix}. \tag{126}$$

Figure 9 shows the closed-loop response of system (121) with controller (126). The desired response was achieved almost exactly in both outputs, but we notice that the performance was just a little worse in output 1 where y_z is larger.

Figure 9 – Closed-loop response of system (121) with controller (126).

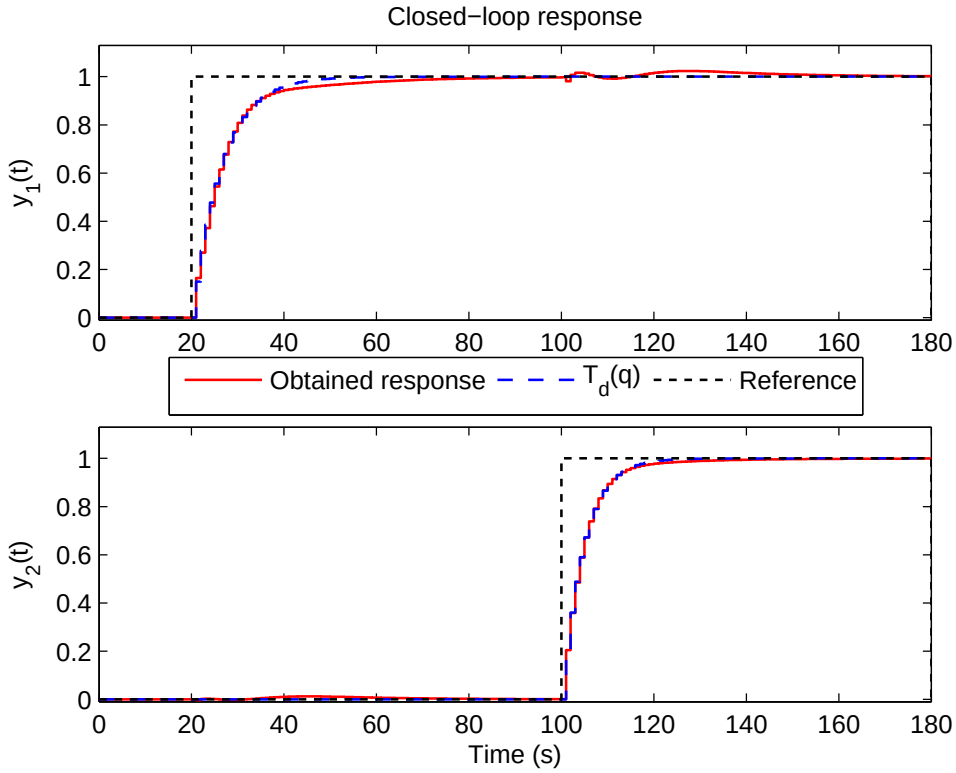

Source: author.

3.4.3 The noisy unmatched-case

Consider again system (111) in closed-loop with controller (113). We applied a PRBS with amplitude 1 and length of 1260 samples in the reference and the output is corrupted

by white noise with $\sigma^2 = 0.025$ (SNR ≈ 25 dB), which represents $v(t)$ in (25). Consider also the parametrized reference model (114), representing the unmatched-case – which happens in most practical situations – in order to show how our methodology works in such case.

We performed 1001 Monte Carlo experiments (in order to estimate 1000 controllers using instrumental variables), with 70 iterations each and the estimated zero is portrayed in Figure 10. From the experiments, 29 applications of the proposed methodology resulted in estimations of the NMP transmission zero with error larger than 5%; 225 resulted in estimations of the NMP transmission zero with error between 2–5%; and 746 resulted in estimations of the NMP transmission zero within a 2% margin around the actual value. From this batch we get a mean value of $\mu_{\hat{z}_{nm}} = 1.21$, which is almost equal to the one obtained in the noiseless case. The standard deviation of the estimate was $\sigma_{\hat{z}_{nm}} = 0.0224$.

Figure 10 – Identified transmission zeros in 1000 Monte Carlo experiments; the 2% and 5% error margins are shown by the red and black horizontal lines, respectively.

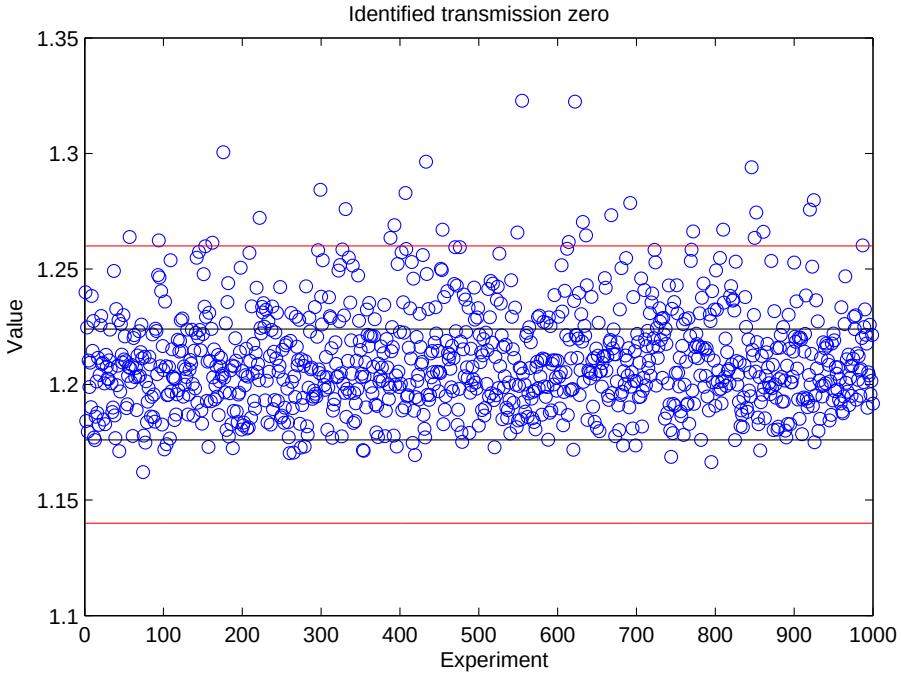

Source: author.

We took at random one experiment from this batch, which output is portrayed in Figure 11, and obtained the following reference model and controller:

$$T_d(q, \hat{\eta}^{(70)}) = \begin{bmatrix} \dfrac{-0.224(q-1.179)}{(q-0.8)(q-0.8)} & 0 \\ 0 & \dfrac{-0.224(q-1.179)}{(q-0.8)(q-0.8)} \end{bmatrix},$$

$$C(q,\hat{P}^{(70)}) = \begin{bmatrix} \dfrac{0.3231(q-0.6044)(q-0.9248)}{q(q-1)} & \dfrac{-0.4553(q-0.6128)(q-0.9282)}{q(q-1)} \\ \dfrac{-0.2619(q-0.5962)(q-0.9258)}{q(q-1)} & \dfrac{0.2184(q-0.4494)(q-0.8301)}{q(q-1)} \end{bmatrix}. \tag{127}$$

Figure 11 – Output signal $y(t)$ of the closed-loop system with initial controller (113) of one noisy experiment.

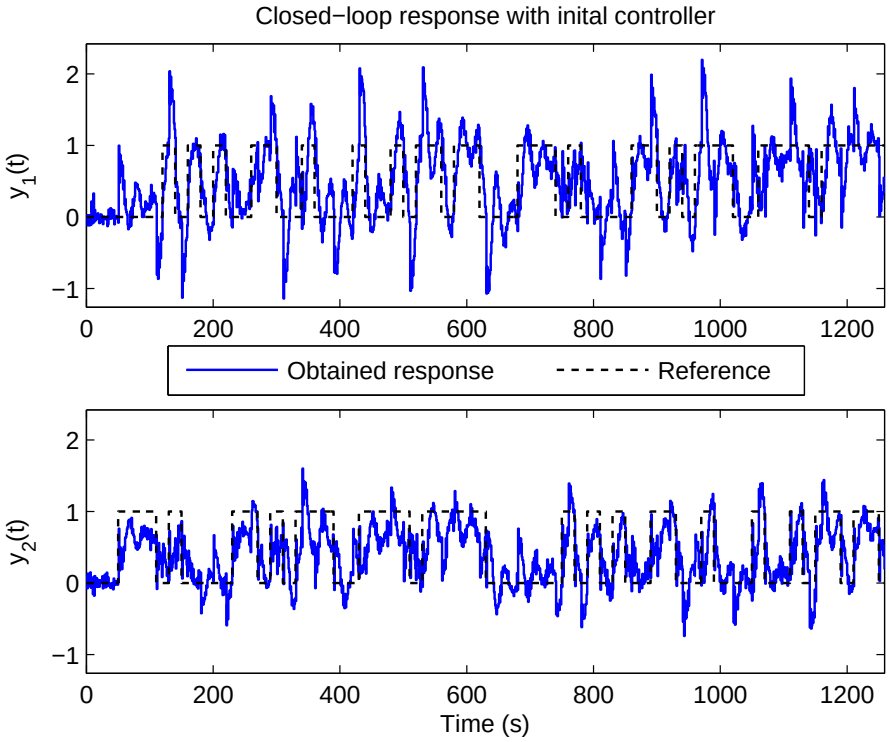

Source: author.

The closed-loop response with the controller (127) is shown in Figure 12. Notice that apart from the noise the overall response resembles the one obtained in Figure 4, even though the identified zero is not exactly the same. In this case, the cost function evaluated $J^{MR}(\hat{P}) = 1.05$, a value greater than that of obtained in Subsection 3.4.1.1 with controller (115) due to additive noise.

3.4.4 OCI with flexible criterion

Consider again system (111), now operating with the initial controller

$$C_0(q) = \begin{bmatrix} \dfrac{0.1(q-0.9)}{q-1} & \dfrac{-0.1(q-0.9)}{q-1} \\ \dfrac{-0.1(q-0.9)}{q-1} & \dfrac{0.2(q-0.9)}{q-1} \end{bmatrix}. \tag{128}$$

Figure 12 – Closed-loop response of system (111) with controller (127).

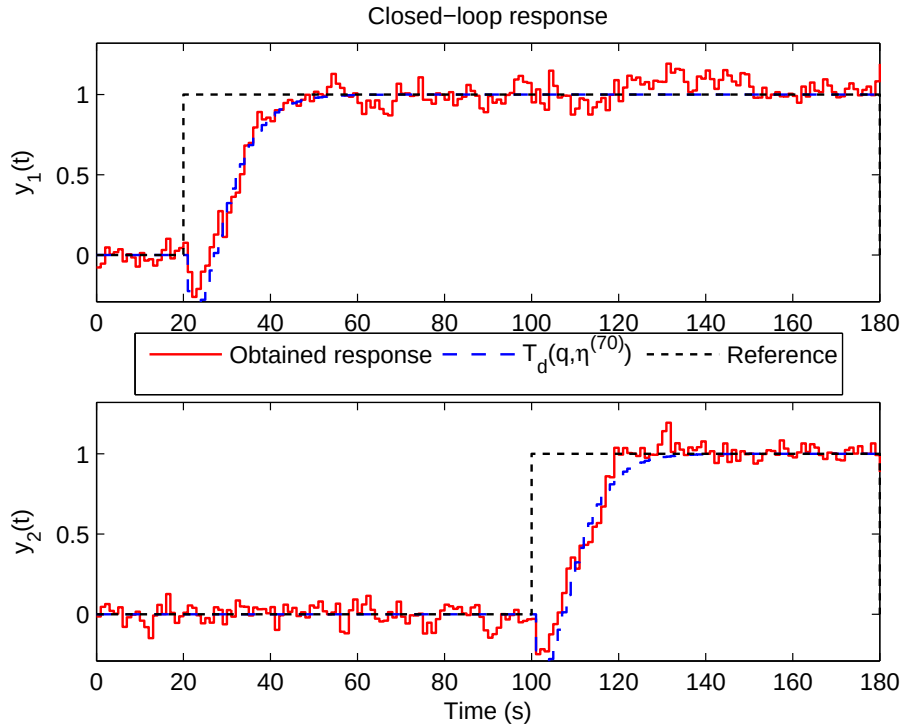

Source: author.

Let the parametrized reference model be given by

$$T_d(q,\eta) = \begin{bmatrix} \dfrac{\eta_1 q - \eta_2}{(q-0.6)(q-0.8)} & \dfrac{\eta_3 q - \eta_4}{(q-0.6)(q-0.75)(q-0.8)} \\ 0 & \dfrac{0.25}{q-0.75} \end{bmatrix}. \tag{129}$$

with respective parametrized loop function

$$L_d(q,\eta) = \begin{bmatrix} \dfrac{\eta_1 q - \eta_2}{q-\eta_5} & \dfrac{\eta_3 q - \eta_4}{q-\eta_5} \\ 0 & 0.25 \end{bmatrix} \frac{1}{q-1}. \tag{130}$$

This reference model satisfies Assumption 3.1 for a centralized PID controller class, and also moves the NMP transmission zero effect to output 1. We set $\eta_3 = 4/3$.

In order to collect data from the system, we set a closed-loop experiment where the reference $r(t)$ is a PRBS with amplitude ± 5 and measure signals $u(t)$ and $y(t)$. We also consider the case where the output is corrupted by white Gaussian noise such that $SNR \approx 8.5$ dB at the closed-loop output $y(t)$ for both loops. Notice that the SNR value is much lower than the one used in VRFT, as this approach is cast in a prediction error framework, so it is supposed to cope better with a larger amount of noise. The result of the experiment is shown in Figure 13.

Figure 13 – Closed-loop experiment of system (111) with initial controller (128).

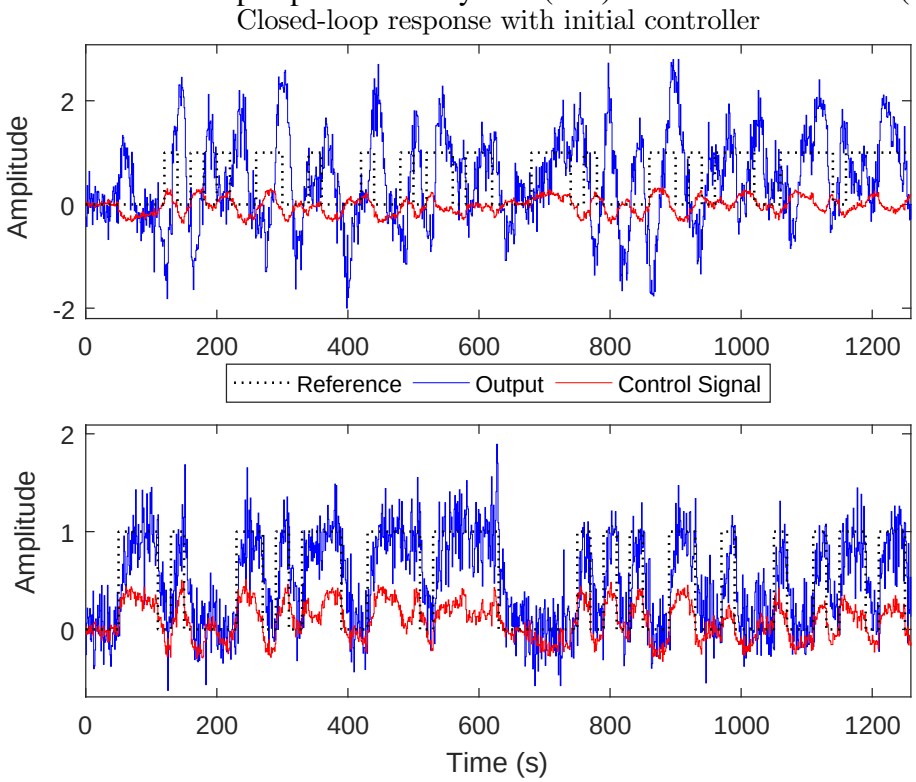

Source: author.

We then apply the proposed methodology for both cases. For the noise-free case we obtained

$$C_1(q,\hat{P}) = \begin{bmatrix} \dfrac{0.593(q-0.798)(q-0.9)}{q(q-1)} & \dfrac{-1.45(q-0.797)(q-0.9)}{q(q-1)} \\ \dfrac{-0.497(q-0.799)(q-0.9)}{q(q-1)} & \dfrac{1.39(q-0.786)(q-0.805)}{q(q-1)} \end{bmatrix} \tag{131}$$

$$T_{d_1}(q,\hat{\eta}) = \begin{bmatrix} \dfrac{-0.40(q-1.2)}{(q-0.6)(q-0.8)} & \dfrac{1.33(q-0.896)(q-1)}{(q-0.6)(q-0.75)(q-0.8)} \\ 0 & \dfrac{0.25}{(q-0.75)} \end{bmatrix}, \tag{132}$$

and for the noisy case

$$C_2(q,\hat{P}) = \begin{bmatrix} \dfrac{0.718(q^2-1.73q+0.752)}{q(q-1)} & \dfrac{-1.24(q-0.829)(q-0.903)}{q(q-1)} \\ \dfrac{-0.569(q-0.834)(q-0.885)}{q(q-1)} & \dfrac{1.26(q-0.762)(q-0.831)}{q(q-1)} \end{bmatrix} \tag{133}$$

$$T_{d_2}(q,\hat{\eta}) = \begin{bmatrix} \dfrac{-0.38(q-1.21)}{(q-0.6)(q-0.8)} & \dfrac{1.33(q-0.854)(q-1)}{(q-0.6)(q-0.75)(q-0.8)} \\ 0 & \dfrac{0.25}{(q-0.75)} \end{bmatrix}. \tag{134}$$

Notice that even with a low SNR, we obtained a good estimation of the NMP transmission zero in $T_{d_2}(q, \hat{\eta})$. Even though the controllers' gains differ from each other, their respective closed-loop response does not as much. Figure 14 portrays the closed-loop response obtained with controllers (131) and (133) to a sequence of steps. Notice that the inverse response to a step appears only in loop 1 (as designed) whereas loop 2 is unaffected by the NMP behavior. For controller $C_1(q)$ the Model Reference cost function evaluated to $J^{MR}(\hat{P}) = 0.09857$, and for controller $C_2(q)$ it was obtained $J^{MR}(\hat{P}) = 2.3769$.

Figure 14 – Closed-loop response of system (111) with controllers (131) and (133).

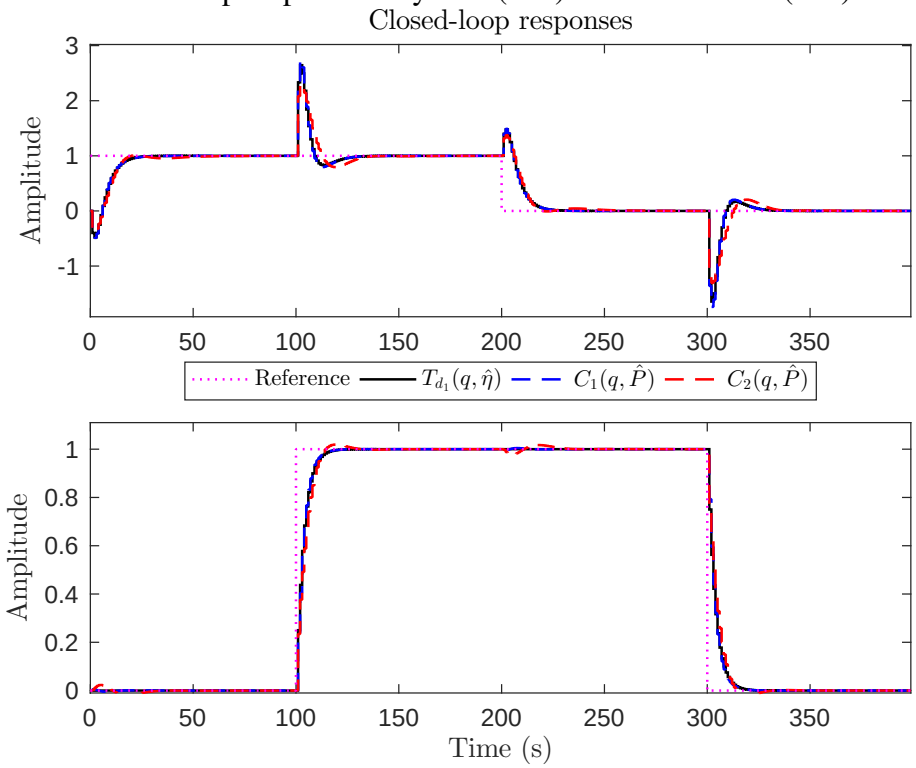

Source: author.

Consider now the parametrized reference model

$$T_d(q,\eta) = \begin{bmatrix} \dfrac{\eta_1 q - \eta_2}{(q-0.8)^2} & \dfrac{\eta_3 q - \eta_4}{(q-0.75)(q-0.8)^2} \\ 0 & \dfrac{0.25}{q-0.75} \end{bmatrix}, \tag{135}$$

which does not satisfy Assumption 3.1 for a PID controller class and where $\eta_3 = 4/3$ has been fixed. We applied the same OCI procedure with the noisy data set collected previously and obtained

$$C_3(q,\hat{P}) = \begin{bmatrix} \dfrac{0.277(q-0.701)(q-0.91)}{q(q-1)} & \dfrac{-0.91(q-0.668)(q-0.918)}{q(q-1)} \\ \dfrac{-0.261(q-0.743)(q-0.902)}{q(q-1)} & \dfrac{1.03(q-0.625)(q-0.858)}{q(q-1)} \end{bmatrix} \tag{136}$$

$$T_{d_3}(q,\hat{\eta}) = \begin{bmatrix} \dfrac{-0.2825(q-1.142)}{(q-0.8)^2} & \dfrac{1.333(q-0.8829)(q-1)}{(q-0.75)(q-0.8)^2} \\ 0 & \dfrac{0.25}{(q-0.75)} \end{bmatrix}. \tag{137}$$

Even though the estimated NMP transmission zero in $T_{d_3}(q,\hat{\eta})$ is not as accurate as in the previous designs, controller (136) still yields a stable closed-loop response that resembles the identified reference model as portrayed in Figure 15. For controller $C_3(q)$ the Model Reference cost function evaluated to $J^{MR}(\hat{P}) = 2.1211$.

Figure 15 – Closed-loop response of system (111) with controller (136).

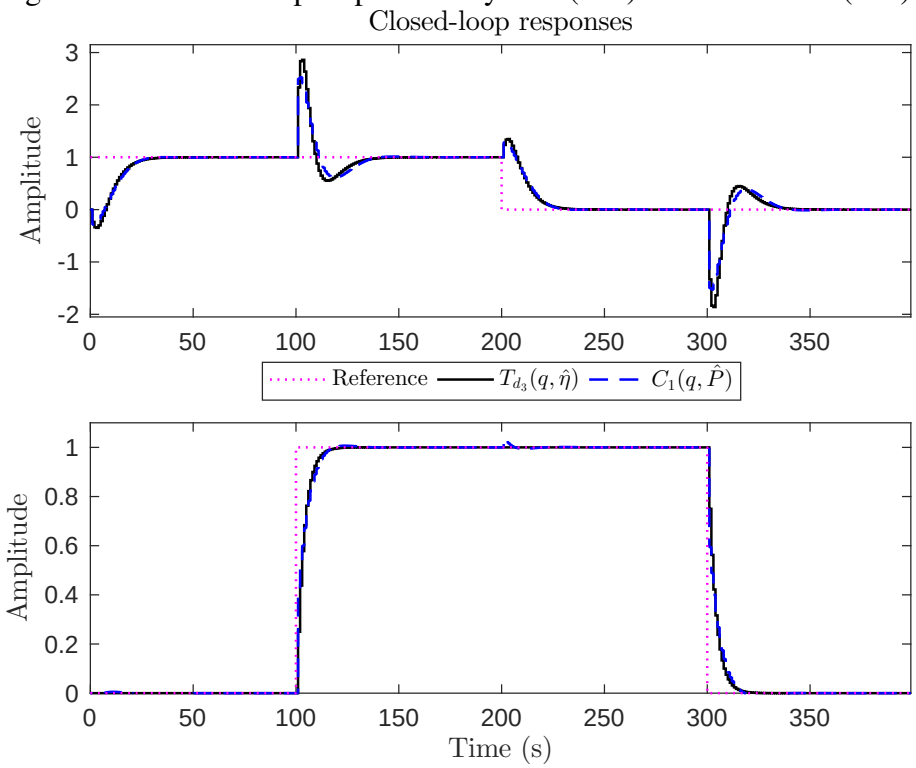

Source: author.

3.5 Chapter conclusions

Based on a previous procedure elaborated for SISO systems, we have extended the MIMO-VRFT method to cope with NMP multivariable plants. By means of a flexible reference model, the optimization is able to both identify NMP transmission zeros and include them in the reference model to find the optimal controller parameters. The formulation however requires that the same transient performance is specified for all loops – that is, the reference model must be diagonal with the same transfer function at all its diagonal elements. This limitation is overcome with a two-step procedure: in the first step the NMP transmission zero location is estimated and, if the closed-loop response obtained in Step 1 is not satisfactory, then Step 2 is performed, which consists of a MIMO-VRFT

design for NMP plants with previously known transmission zeros (GONÇALVES DA SILVA; CAMPESTRINI; BAZANELLA, 2016). However, the NMP effect is still present in all outputs.

To alleviate this constraint we explored the idea of a flexible criterion with the MIMO-OCI method. In this case, instead of parametrizing the reference model directly, the idea was used in a *desired* loop function, which is a function of the reference model. The solution uses a block diagonal structure for the reference model, which allows to move the NMP effect to a desired output. Simulation examples showed the effectiveness of the proposed methodologies.

4 DATA-DRIVEN LQR CONTROL

It is two over there, two over here.

João Bosco

This chapter deals with a data-driven approach to the discrete-time infinite horizon Linear Quadratic Regulator (LQR) problem. Previous approaches to this problem consider an iterative finite horizon case where the state variables are not measurable and the computation yields a closed-loop control signal, and not the (sub-)optimal gain. Also, on-line implementation issues have been reported due to increasing size of matrices, but mainly because their computed control signal is always delayed. In this chapter we change the perspective in order to find the optimal infinite horizon LQR gain only after a large batch of data has been collected. The results of this chapter have been published in (GONÇALVES DA SILVA *et al.*, 2019).

The LQR design is a classical control problem whose analysis and solution can be found in most textbooks on control theory. It requires the solution of a Riccati equation which is a function of the plant's state-space model, or the plant's Markov parameters when the solution is given in closed-form (also called *batch-form*) (LEWIS, 1981; FURUTA; WONGSAISUWAN, 1993). Whether applying the classical approach of explicitly solving the Riccati equation, or using a plant's state-space description to calculate the Markov parameters and then feed them into the closed-form solution, this is a *model-based* design approach.

Data-Driven optimal control design methods that start from the LQR/LQG formulation have also been developed, based on these closed-form solutions of the Riccati equation (SKELTON; SHI, 1994; FURUTA; WONGSAISUWAN, 1995; AANGENENT *et al.*, 2005). However, they directly estimate the optimal control input at each time instant. Thus, they can not be said to solve the LQR problem in its classical formulation, and can mainly be cast within a predictive control framework.

Motivated by applications in which a state-feedback is to be designed but a good enough model is not available and is of no interest *per se*, we present in this chapter a DD approach to the solution of the LQR design. Otherwise stated, we provide a DD solution for the computation of the optimal state-feedback gain. In a DD control design,

the controller structure is defined *a priori* and the controller's parameters are tuned with the use of a large batch of data, usually after such data are acquired. As we have shown in previous chapters, in most of the DD control literature, the controller structure consists of output feedback with a predefined transfer function with parameters to be tuned considering a Model Reference approach.

The infinite-horizon LQR problem fits this formulation perfectly: one has a fixed controller structure (the state-feedback gain) with a few parameters to tune, and the controller must minimize a given quadratic performance criterion. The plant's model is just an intermediate step in the design and often has no interest in itself, the controller being the final and only objective. Thus, we provide a method to compute the LQR state-feedback gain from data without the intermediate step of identifying a model of the system.

This chapter is organized as follows: the LQR design problem is presented in Section 4.1, along with its closed-form solution. It is shown that the computation of the LQR state-feedback gain by the closed-form solution requires knowledge of two large matrices: an extended observability matrix and a Toeplitz matrix of the plant's Markov parameters. Then, in the ensuing sections 4.2 and 4.3, algorithms to estimate these two matrices directly from data collected from the plant are provided. In Section 4.4 we briefly review the Internal Model principle and the formulation of reference tracking as a state-feedback problem. Two simulation examples are given in Section 4.5 to illustrate the method's properties. One of our motivating applications – the control of uninterruptible power sources – is explored in Section 4.6, where we present a practical application of the design methodology. It will be seen in the experimental results that our design compares favorably with previously presented model-based solutions to this same practical problem.

4.1 Problem statement

Consider the state-space representation (2) of a strictly-proper linear time-invariant discrete-time system, reproduced here

$$\begin{aligned} x(t+1) &= Ax(t) + Bu(t) + E\nu(t) \\ y(t) &= Cx(t) + Fw(t). \end{aligned} \tag{138}$$

For the time being, let $E = F = 0$, and we shall also assume that A is *stable*.

The *infinite horizon* LQR control problem can be summarized as follows: find the optimal state-feedback gain K of the control law

$$u(t) = -Kx(t) \tag{139}$$

such that the quadratic cost function

$$J = \sum_{t=0}^{\infty} \left(y(t)^T Q y(t) + u(t)^T R u(t) \right) \tag{140}$$

is minimized subject to system (138), where Q and R are positive definite symmetric weighting matrices. The optimal gain is given by

$$K = (R + B^T X B)^{-1}(B^T X A) \tag{141}$$

where X is the unique positive definite solution to the discrete time algebraic Riccati equation (DARE)

$$X = A^T X A - (A^T X B)(R + B^T X B)^{-1}(B^T X A) + C^T Q C. \tag{142}$$

A closed-form solution to the DARE (142) has been reported in (LEWIS, 1981; FURUTA; WONGSAISUWAN, 1993). For a sufficient large N_m, this solution can be written as

$$X = \mathbf{O}^T(\mathbf{Q}_{N_m+1}^{-1} + \mathbf{S}\mathbf{R}_{N_m+1}^{-1}\mathbf{S}^T)^{-1}\mathbf{O}, \tag{143}$$

where

$$\mathbf{O} = \begin{bmatrix} C \\ CA \\ CA^2 \\ \vdots \\ CA^{N_m} \end{bmatrix}, \tag{144}$$

$$\mathbf{S} = \begin{bmatrix} 0 & \cdots & \cdots & \cdots & 0 \\ CB & 0 & \ddots & & \vdots \\ CAB & CB & \ddots & \ddots & \vdots \\ \vdots & \vdots & \ddots & \ddots & \vdots \\ CA^{N_m-1}B & CA^{N_m-2}B & \cdots & CB & 0 \end{bmatrix},$$

$$\mathbf{R}_j \triangleq \text{diag}(R, R, \ldots, R), \;\; \mathbf{Q}_j \triangleq \text{diag}(Q, Q, \ldots, Q),$$

with $\mathbf{R}_j$ and $\mathbf{Q}_j$ containing $j = N_m + 1$ diagonal blocks each.

The matrix $\mathbf{O}$ is an *extended observability matrix* for system (138) and $\mathbf{S}$ is a Toeplitz matrix of its Markov parameters (22):

$$M_i = CA^{(i-1)}B, \;\; i = 1, 2, \ldots, N_m. \tag{145}$$

As shown in (LEWIS, 1981), using (143) in (141) and rearranging some terms, the LQR state-feedback gain K can be computed as a function of the Markov parameters as

$$K = [R + \mathbf{M}^T(\mathbf{Q}_{N_m}^{-1} + \mathbf{S}\mathbf{R}_{N_m}^{-1}\mathbf{S}^T)^{-1}\mathbf{M}]^{-1}\mathbf{M}^T(\mathbf{Q}_{N_m}^{-1} + \mathbf{S}\mathbf{R}_N^{-1}\mathbf{S}^T)^{-1}\mathbf{O}^+, \tag{146}$$

where

$$\mathbf{M} = \begin{bmatrix} M_1 \\ M_2 \\ \vdots \\ M_{N_m} \end{bmatrix} \in \Re^{lN_m \times p}, \tag{147}$$

$$\mathbf{S} = \begin{bmatrix} 0 & \cdots & \cdots & \cdots & 0 \\ M_1 & 0 & \ddots & & \vdots \\ M_2 & M_1 & \ddots & \ddots & \vdots \\ \vdots & \vdots & \ddots & \ddots & \vdots \\ M_{N_m-1} & M_{N_m-2} & \cdots & M_1 & 0 \end{bmatrix} \in \Re^{lN_m \times pN_m}, \tag{148}$$

$$\mathbf{O}^+ = \begin{bmatrix} (CA)^T & (CA^2)^T & \cdots & (CA^{N_m})^T \end{bmatrix}^T \in \Re^{lN_m \times n}. \tag{149}$$

Notice that the gain K in (141) is a function of A, B, and X, which is also a function of system matrices A, B and C. Now we have an expression that depends basically on $\mathbf{S}$ and $\mathbf{O}^+$. If these quantities can be obtained from data, then a data-driven method can be formulated. So, in order to succeed in this data-driven approach, we need to identify the system's Markov parameters – the matrix $\mathbf{S}$ – and an extended observability matrix $\mathbf{O}^+$. Since a state-feedback control is to be implemented, we can assume that the state is measurable, so are the inputs and outputs. Thus, let us pose the problem formally:

Given the data set

$$Z^N = [u(0), u(1), \ldots, u(N), y(0), y(1), \ldots, y(N), x(0), x(1), \ldots, x(N)], \tag{150}$$

find the optimal state-feedback gain K as in (146)*. To do so, a sequence of N_m Markov parameters and the N_m extended observability matrix must be estimated from data.*

In the sequel we present a procedure to obtain both the Markov parameters and the extended observability matrix without using a model for the system.

4.2 Markov parameters estimation

The estimation of the system Markov parameters via the so-called ARMarkov/Toeplitz models is reviewed next. Notice that estimating the system's Markov parameters is equivalent to identifying an N_m-th order Finite Impulse Response (FIR) representation for the system. We now follow the description in (VAN OVERSCHEE; DE MOOR, 2012).

The main idea behind the algorithm is to observe $N_m + 1$ future data so the state variable can be eliminated and an ARMarkov/Toeplitz model can be identified. We summarize the procedure next.

Let the state be repeatedly substituted $N_m + 1$ times in (138); then

$$\begin{aligned} x(t + N_m + 1) &= A^{N_m+1}x(t) + \mathbf{T}\mathbf{u}_m(t) \\ \begin{bmatrix} y(t) \\ y(t+1) \\ \vdots \\ y(t+N_m) \end{bmatrix} &= \mathbf{O}x(t) + \mathbf{S} \underbrace{\begin{bmatrix} u(t) \\ u(t+1) \\ \vdots \\ u(t+N_m) \end{bmatrix}}_{\mathbf{u}_m(t)} \end{aligned} \tag{151}$$

where $\mathbf{T} = [A^{N_m}B \ \ldots \ AB \ B]$, $\mathbf{O}$ is given in (144) and $\mathbf{S}$ in (148).

According to (LIM; PHAN; LONGMAN, 1998), as long as $(N_m + 1)l \geq m$, it is guaranteed for an observable system that there exists a matrix $\mathbf{F}$ such that $A^{N_m+1} + \mathbf{FO} = 0$, which ensures that there exists an expression where the state is eliminated from (151). This allows to write a predictor for the system's output as follows.

Let the Hankel matrix of a given signal – say $e(t)$ – be defined as

$$H(e(t)) \triangleq \begin{bmatrix} e(t) & e(t+1) & \cdots & e(t+L-1) \\ e(t+1) & e(t+2) & \cdots & e(t+L) \\ \vdots & \vdots & \ddots & \vdots \\ e(t+N_m-1) & e(t+N) & \cdots & e(t+N_m+L-2) \end{bmatrix}. \tag{152}$$

Define the set of data matrices

$$\begin{aligned} U_p &= H(u(0)) \qquad U_f = H(u(N_m)) \\ Y_p &= H(y(0)) \qquad Y_f = H(y(N_m)). \end{aligned} \tag{153}$$

Then a predictor of the system output can be written as (VAN OVERSCHEE; DE MOOR, 2012)

$$Y_f = \underbrace{[\mathbf{O}(\mathbf{C} + \mathbf{FS}) \ \ -\mathbf{OF} \ \ \mathbf{S}]}_{\mathbf{W}} \underbrace{\begin{bmatrix} U_p \\ Y_p \\ U_f \end{bmatrix}}_{\mathbf{\Phi}}. \tag{154}$$

Thus, an estimate $\widehat{\mathbf{W}}$ of $\mathbf{W}$ can be obtained by solving the least-squares problem ;

$$\widehat{\mathbf{W}} = Y_f \mathbf{\Phi}^\dagger \tag{155}$$

with $[\cdot]^\dagger$ denoting the Moore-Penrose pseudo-inverse, and extract an estimate $\widehat{\mathbf{S}}_m$ from the rightmost pN_m columns of the estimated $\widehat{\mathbf{W}}$. In a parallel with the classical parametric identification problem, N_m plays the role of the number of parameters to be identified and L accounts for the amount of data used in identification; so larger L yields better estimates. If the system has a feedthrough term, i.e., $D \neq 0$ (and therefore $M_0 = D$), than the main diagonal of $\widehat{\mathbf{S}}_m$ will contain this term. Moreover, $\mathbf{M}$ can be extracted from the first column of $\widehat{\mathbf{S}}$. This estimation has been shown to be consistent for the Markov parameters only (KAMRUNNAHAR; HUANG; FISHER, 2000).

Remark 4.1. *When data is corrupted with noise, then the upper triangular part of* $\widehat{\mathbf{S}}_m$ *is not necessarily composed of zeros, but one can forcibly set those values after the estimation is done.*

4.3 Extended observability matrix estimation

Since a state-feedback control is to be implemented, we can assume that the state is measurable. Hence, in this section we present two original algorithms to identify an extended observability matrix in the same state coordinates we are measuring and later we discuss their properties. We define the vector of measured state by

$$\mathbf{X} \triangleq [x(0) \;\; x(1) \;\; x(2) \;\; \cdots \;\; x(L-1)]. \tag{156}$$

4.3.1 Algorithm 1

The output equation (151) can also be written with Hankel matrices without eliminating the state vector. It can be put in an extended output matrix equation as (VAN OVERSCHEE; DE MOOR, 2012)

$$Y_p = \mathbf{O}\mathbf{X} + \mathbf{S}U_p. \tag{157}$$

Since an estimate $\widehat{\mathbf{S}}$ can be obtained using the algorithm provided in Section 4.2, and U_p and Y_p can be formed with collected data, we can then solve the system of equations in (157) for $\mathbf{O}$:

$$\widehat{\mathbf{O}} = (Y_p - \widehat{\mathbf{S}}U_p)\mathbf{X}^{\dagger}. \tag{158}$$

To obtain $\mathbf{O}^{+}$, one simply removes the first l rows of $\mathbf{O}$.

4.3.2 Algorithm 2

First, define U_{po} as the geometric operator that projects the row space of a matrix onto the orthogonal complement of the row space of the matrix U_p in (153)

$$U_{po} \triangleq I_L - U_p^T(U_pU_p^T)^{-1}U_p \tag{159}$$

where I_L is an identity matrix of size L. Then by post-multiplying the extended output matrix (157) by U_{po}, we have

$$\begin{aligned} Y_pU_{po} &= \mathbf{O}\mathbf{X}U_{po} + \mathbf{S}U_pU_{po} \\ Y_pU_{po} &= \mathbf{O}\mathbf{X}U_{po} \end{aligned} \tag{160}$$

Notice that by using the projection U_{po} we eliminate the need to know, or estimate, $\mathbf{S}$.

An estimator of the extended observability matrix can thus be computed as

$$\widehat{\mathbf{O}} = (Y_pU_{po})(\mathbf{X}U_{po})^{\dagger}. \tag{161}$$

4.3.3 Estimates properties

The estimates just provided allow the computation of the state-feedback gain according to (146) and, as shown in (LEWIS, 1981), in the noise-free case the gain thus computed converges asymptotically, as the number of Markov parameters $N_m \to \infty$, to the optimal LQR state-feedback. A simulation example in Section 4.5 illustrates this property.

On the other hand, when the state measurement is corrupted by noise, one can expect some bias in the estimates of the extended observability matrix, since both solutions presented are of a least-squares nature. We now briefly discuss the bias and covariance of these estimates. Consider the system state-space representation (138) with the noise terms. We can write the extended output equation as

$$Y_p = \mathbf{O}\mathbf{X} + \mathbf{S}U_p + \mathbf{S}_E V_p + FW_p \tag{162}$$

where $V_p = H(\nu(0))$ and $W_p = H(w(0))$ are Hankel matrices of the noise sequences $\nu(t)$ and $w(t)$ respectively, and $\mathbf{S}_E$ has the same structure as $\mathbf{S}$ with E *in lieu* of B. We can also write

$$\mathbf{X} = \mathbf{X}^o + E\mathbf{V} \tag{163}$$

where $\mathbf{V}$ is a row vector of the noise sequences $\nu(t)$. We also assume the sequence $u(t)$ uncorrelated with $\nu(t)$, as open-loop experiments are being carried out to collect data.

4.3.3.1 Algorithm 1

Let $\mathcal{E}[\cdot]$ denote the expected value function. The bias of the first algorithm is given by

$$\mathcal{B}(\widehat{\mathbf{O}}) = \mathcal{E}[\widehat{\mathbf{O}}] - \mathbf{O} = \mathcal{E}[(Y_p - \widehat{\mathbf{S}}U_p)\mathbf{X}^\dagger - \mathbf{O}]. \tag{164}$$

Inserting (162) into (164)

$$\begin{aligned}\mathcal{B}(\widehat{\mathbf{O}}) &= \mathcal{E}[(\mathbf{O}\mathbf{X} + \mathbf{S}U_p + \mathbf{S}_E V_p + FW_p - \widehat{\mathbf{S}}U_p)\mathbf{X}^\dagger - \mathbf{O}] \\ &= \mathcal{E}[\mathbf{O}(\mathbf{X}\mathbf{X}^\dagger - I) + (\mathbf{S} - \widehat{\mathbf{S}})U_p\mathbf{X}^\dagger + \mathbf{S}_E V_p\mathbf{X}^\dagger + FW_p\mathbf{X}^\dagger]\end{aligned} \tag{165}$$

First term of (165) is null when $\mathbf{X}$ is full row rank – a constraint not so hard to satisfy (so that $\mathbf{X}\mathbf{X}^\dagger = I$), and the expectation of the second term is null either if $\widehat{\mathbf{S}} = \mathbf{S}$ or because $u(t)$ is uncorrelated with $\nu(t)$. We then have

$$\mathcal{B}(\widehat{\mathbf{O}}) = \mathbf{S}_E\mathcal{E}[V_p\mathbf{X}^\dagger] + F\mathcal{E}[W_p\mathbf{X}^\dagger]. \tag{166}$$

If we further assume that $\nu(t)$ is uncorrelated with $w(t)$, then

$$\mathcal{B}(\widehat{\mathbf{O}}) = \mathbf{S}_E\mathcal{E}[V_p\mathbf{X}^\dagger]. \tag{167}$$

The covariance of the first algorithm is given by

$$\begin{aligned}\mathcal{V}(\widehat{\mathbf{O}}) &= \mathcal{E}[(\widehat{\mathbf{O}} - \mathcal{E}[\widehat{\mathbf{O}}])(\widehat{\mathbf{O}} - \mathcal{E}[\widehat{\mathbf{O}}])^T] \\ &= \mathcal{E}[((\mathbf{S} - \widehat{\mathbf{S}})U_p\mathbf{X}^\dagger + \mathbf{S}_E V_p\mathbf{X}^\dagger + FW_p\mathbf{X}^\dagger - \mathbf{S}_E\mathcal{E}[V_p\mathbf{X}^\dagger] - F\mathcal{E}[W_p\mathbf{X}^\dagger]) \\ &\quad \times ((\mathbf{S} - \widehat{\mathbf{S}})U_p\mathbf{X}^\dagger + \mathbf{S}_E V_p\mathbf{X}^\dagger + FW_p\mathbf{X}^\dagger - \mathbf{S}_E\mathcal{E}[V_p\mathbf{X}^\dagger] - F\mathcal{E}[W_p\mathbf{X}^\dagger])^T]\end{aligned} \tag{168}$$

which after some algebraic manipulation results in

$$\begin{aligned}\mathcal{V}(\widehat{\mathbf{O}}) = \mathcal{E}\Big\{&[(\mathbf{S} - \widehat{\mathbf{S}})U_p\mathbf{X}^\dagger + \mathbf{S}_E V_p\mathbf{X}^\dagger + FW_p\mathbf{X}^\dagger]\Lambda_1^T + \\ &[(\mathbf{S} - \widehat{\mathbf{S}})U_p\mathbf{X}^\dagger + \Lambda_1][(\mathbf{S} - \widehat{\mathbf{S}})U_p\mathbf{X}^\dagger]^T\Big\}\end{aligned} \tag{169}$$

$$\Lambda_1 = \mathbf{S}_E(V_p\mathbf{X}^\dagger - \mathcal{E}[V_p\mathbf{X}^\dagger]) + F(W_p\mathbf{X}^\dagger - \mathcal{E}[W_p\mathbf{X}^\dagger]) \tag{170}$$

4.3.3.2 Algorithm 2

Following the same steps as in Algorithm 1, the following expressions are obtained for the bias of the estimates given by Algorithm 2.

$$\begin{aligned}\mathcal{B}(\widehat{\mathbf{O}}) &= \mathcal{E}[(Y_pU_{po})(U_{po}\mathbf{X})^\dagger - \mathbf{O}] = \mathcal{E}[(\mathbf{O}\mathbf{X} + \mathbf{S}U_p + \mathbf{S}_E V_p + FW_p)U_{po}(\mathbf{X}U_{po})^\dagger - \mathbf{O}] \\ &= \mathcal{E}[\mathbf{O}((\mathbf{X}U_{po})(\mathbf{X}U_{po})^\dagger - I) + \mathbf{S}_E V_pU_{po}(\mathbf{X}U_{po})^\dagger + FW_pU_{po}(\mathbf{X}U_{po})^\dagger] \\ &= \mathbf{S}_E\mathcal{E}[V_pU_{po}(\mathbf{X}U_{po})^\dagger] + F\mathcal{E}[W_pU_{po}(\mathbf{X}U_{po})^\dagger].\end{aligned} \tag{171}$$

If we further assume that $\nu(t)$ is uncorrelated with $w(t)$, then

$$\mathcal{B}(\widehat{\mathbf{O}}) = \mathbf{S}_E\mathcal{E}[(V_pU_{po})(\mathbf{X}U_{po})^\dagger]. \tag{172}$$

For the covariance, one obtains

$$\mathcal{V}(\widehat{\mathbf{O}}) = \mathcal{E}\left\{[\mathbf{S}_E(V_pU_{po})(\mathbf{X}U_{po})^\dagger + F(W_pU_{po})(\mathbf{X}U_{po})^\dagger]\Lambda_2^T\right\} \tag{173}$$

$$\begin{aligned}\Lambda_2 = \mathbf{S}_E&[(V_pU_{po})(\mathbf{X}U_{po})^\dagger - \mathcal{E}[(V_pU_{po})(\mathbf{X}U_{po})^\dagger]] + \\ &F[(W_pU_{po})(\mathbf{X}U_{po})^\dagger - \mathcal{E}[(W_pU_{po})(\mathbf{X}U_{po})^\dagger]\end{aligned} \tag{174}$$

Notice that, as expected, the bias of both estimates is inversely proportional to the signal to noise ratio and the estimates will be unbiased only if there is no noise in the measurement. We provide an illustrative example in Section 4.5.3 to compare the bias, covariance and – most importantly – the mean square error resulting from the two algorithms.

4.4 Internal model principle and augmented state space

The internal model principle is a well-known concept in control theory. The core idea from a control design perspective is to insert a stabilizing compensator in feedback on the main loop such that its modes include the ones that are the goal for reference

tracking or disturbance rejection (FRANCIS; WONHAM, 1976), mainly constant and sinusoidal references. With some abuse of nomenclature, we shall refer to an internal model *controller* (IMC) as a controller that incorporates the internal model principle (not to be confused with internal model *control* as defined in (MORARI, 1983)). Thus, in this section we show how to use open-loop data to obtain an augmented state and output vectors in order to adjust the gains also for reference tracking considering a feedback loop with an internal model controller.

Let

$$\mathcal{C} = (A_c, B_c) \tag{175}$$

denote the discrete-time state and input matrices of the internal model controller equation, whose n_c states are measurable and B_c has p_c inputs. Assume that every output of the system has to follow a reference represented by the internal model controller. Then the augmented open-loop space-state representation of system (138) with controller (175) is given by

$$\begin{aligned} x_a(t+1) &= \underbrace{\begin{bmatrix} A & \mathbf{0}_{m,n_c\times l} \\ -C\otimes(B_c\mathbf{1}) & I\otimes A_c \end{bmatrix}}_{A_a} x_a(t) + \underbrace{\begin{bmatrix} B \\ \mathbf{0}_{n_c\times l,p} \end{bmatrix}}_{B_a} u(t) \\ y_a(t) &= \underbrace{\begin{bmatrix} C & \mathbf{0}_{l,n_c\times l} \\ \mathbf{0}_{n_c\times l,m} & I_{n_c\times l} \end{bmatrix}}_{C_a} x_a(t) \end{aligned} \tag{176}$$

where $\otimes$ is the Kronecker product, $\mathbf{1}$ is a column vector of size p_c with 1 as elements, and I is an identity matrix of size l. From partition $(2,1)$ of A_a we see that the open-loop IMC state vector needed to compute the gain K can be obtained by simply filtering the plant outputs by $-\mathcal{C}$.

For example, the *state equation* of the integrator $\frac{1}{q-1}$ can be represented by

$$x_c(t+1) = \underbrace{1}_{A_c} x_c(t) + \underbrace{1}_{B_c}(r(t) - y(t)) \tag{177}$$

and a resonant controller at frequency ω_n with a pre-warping Tustin representation can be realized as

$$x_c(t+1) = \underbrace{\begin{bmatrix} 0 & 1 \\ -1 & 2\cos(\omega_n T_s) \end{bmatrix}}_{A_c} x_c(t) + \underbrace{\begin{bmatrix} 0 \\ 1 \end{bmatrix}}_{B_c}(r(t) - y(t)) \tag{178}$$

where T_s is the sampling time.

Let $x_{IMC}(t)$ represent the state of the open-loop IMC[1] , and the augmented output and state vector be given by $y_a(t) = [y(t)\ x_{IMC}(t)]^T$ and $x_a(t) = [x(t)\ x_{IMC}(t)]^T$, respectively. Thus, these are the vectors that should be used, along with $u(t)$, to estimate the Markov parameters and the extended observability matrix.

[1] which can be obtained with MATLAB command `lsim`; for instance, `xIMC=-lsim(IMC,y)`.

4.5 Simulation examples

4.5.1 Regulation control

In this first example we illustrate the convergence of the proposed method. Consider a system as in (138) whose matrices are given by

$$\begin{aligned} A &= \begin{bmatrix} 1 & 0.15 \\ -0.2 & 0.6 \end{bmatrix} \quad B = \begin{bmatrix} 0.04 & 0.01 \\ 0.02 & -0.01 \end{bmatrix} \\ C &= \begin{bmatrix} 1 & 2 \\ 0 & 1 \end{bmatrix} \qquad\qquad E = F = 0\cdot \end{aligned} \tag{179}$$

Also, let the performance requirements be given by

$$R = 0.2I_2 \quad Q = 20I_l, \tag{180}$$

where I_l is the identity matrix of size l (number of outputs), that is, we are valuing more the evolution of the state than the control effort. The *model-based* optimal LQR controller is given by

$$K = \begin{bmatrix} 4.6491 & 7.5226 \\ 1.4461 & -1.9886 \end{bmatrix}\cdot \tag{181}$$

In order to apply the proposed methodology we set an open-loop experiment where the input signal is a PRBS with amplitude 1 and length 1022 samples, and both $y(t)$ and $x(t)$ data were collected. Table 2 shows the convergence of the state-feedback gain as we choose to identify more Markov parameters.

Table 2 – Convergence of the state-feedback gain (146) with increasing identified Markov parameters

N_m	$\hat{K}$
3	$\begin{bmatrix} 2.9766 & 7.9269 \\ 0.060133 & -1.5126 \end{bmatrix}$
5	$\begin{bmatrix} 3.4144 & 7.887 \\ 0.48589 & -1.7033 \end{bmatrix}$
10	$\begin{bmatrix} 4.2314 & 7.644 \\ 1.127 & -1.8959 \end{bmatrix}$
30	$\begin{bmatrix} 4.6463 & 7.5234 \\ 1.444 & -1.988 \end{bmatrix}$
50	$\begin{bmatrix} 4.6491 & 7.5226 \\ 1.4461 & -1.9886 \end{bmatrix}$

At $N_m = 50$, a value close to the system's open-loop settling time (approximately 45 samples), $\hat{K}$ equals the model-based solution (181) up to the fifth significant digit. Figure

16 shows the closed-loop response with the gain obtained with $N_m = 50$ to an initial state $x_0 = [0.8 \;\; 1.5]^T$.

Figure 16 – Closed-loop response of system (179) for regulation control with state-feedback gain $\hat{K}_{50}$.

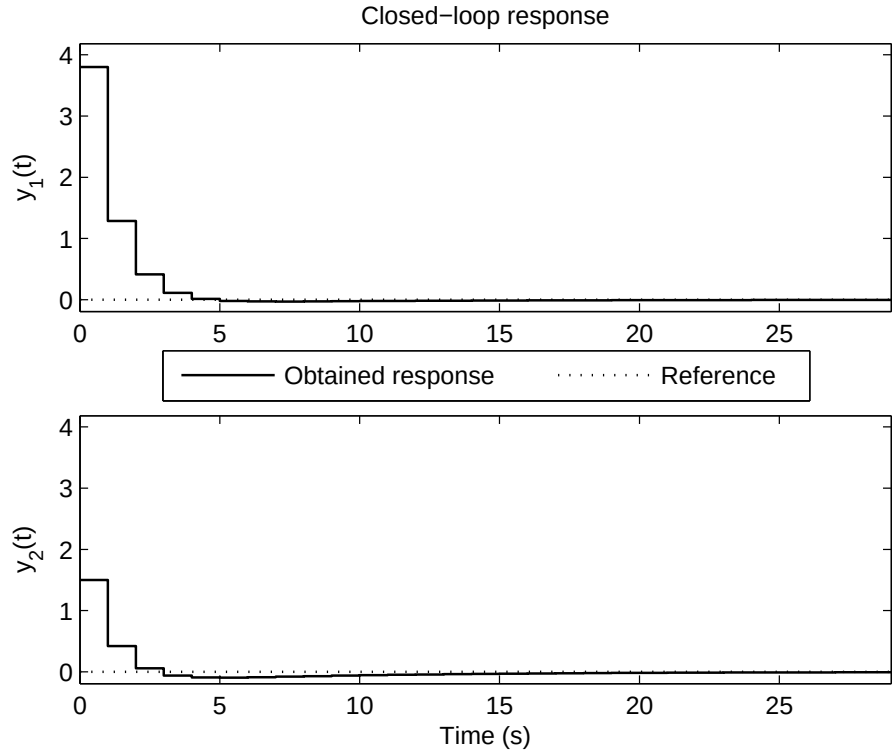

Source: author.

4.5.2 Integral control

Consider again system (179) and assume now we want both outputs to follow constant references, that is, we are aiming for a design with integral control in both outputs. For the sake of completeness, the augmented open-loop state-space representation (176) with compensator (177) is given by

$$A_a = \begin{bmatrix} 1 & 0.15 & 0 & 0 \\ -0.2 & 0.6 & 0 & 0 \\ -1 & -2 & 1 & 0 \\ 0 & -1 & 0 & 1 \end{bmatrix} \quad B_a = \begin{bmatrix} 0.04 & 0.01 \\ 0.02 & -0.01 \\ 0 & 0 \\ 0 & 0 \end{bmatrix}$$
$$C_a = \begin{bmatrix} 1 & 2 & 0 & 0 \\ 0 & 1 & 0 & 0 \\ 0 & 0 & 1 & 0 \\ 0 & 0 & 0 & 1 \end{bmatrix}. \tag{182}$$

In order to apply the proposed method, the output obtained in the open-loop experiment performed before was filtered by $-\mathcal{C}$ as in (177). Notice that now we have $l = 4$, and the

LQR performance is again set as in (180). Again, we estimated 50 Markov parameters and the extended observability matrix, and we obtained:

$$\hat{K}_{50} = \begin{bmatrix} 13.088 & 19.214 & -4.8911 & 1.2088 \\ 12.314 & -21.84 & 1.2736 & 8.2577 \end{bmatrix} \tag{183}$$

which again matches the model-based LQR gain up to the fifth significant digit. Figure 17 shows the closed-loop response to a sequence of steps.

Figure 17 – Closed-loop response of system (179) for integral control with state-feedback gain (183).

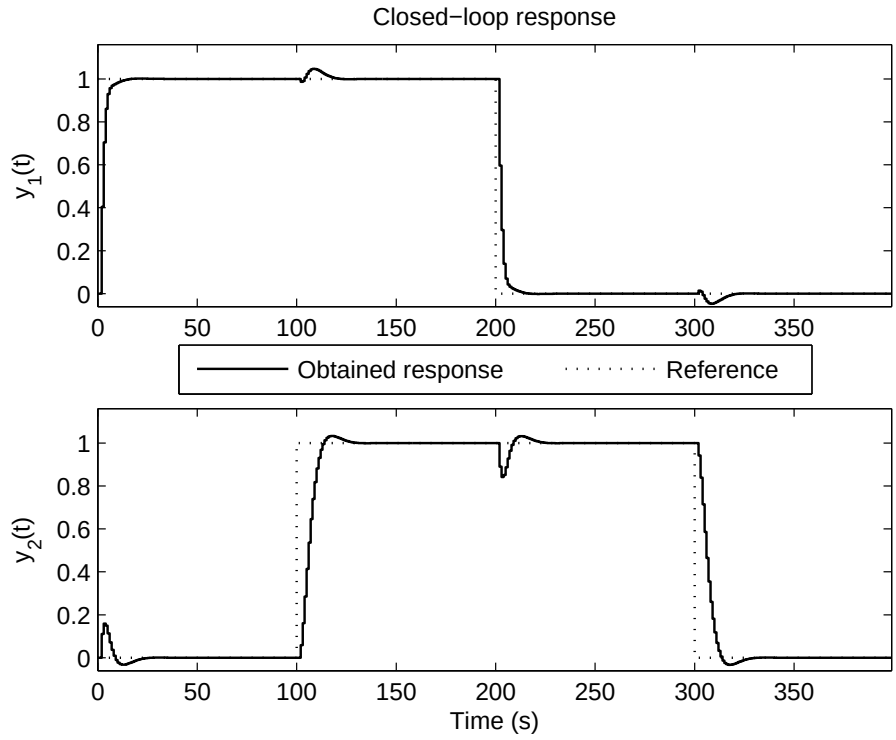

Source: author.

4.5.3 The noisy case: observability matrix statistical properties

We provide now a simple example to illustrate bias and covariance of the observability matrix estimators. Consider a system with state-space matrices

$$A = 0.14, \quad B = 1.72, \quad C = 1, \quad E = 1, \quad F = 0, \tag{184}$$

and let the LQR performance matrices be $R = 0$ and $Q = 1$, so we are aiming for a dead-beat control, and convergence can be found with $N_m = 3$ (due to row removal, that means the extended observability matrix will be of size 2). The actual extended observability matrix is then $\mathbf{O}^+ = [0.14 \;\; 0.0196]^T$.

We set a Monte Carlo experiment with 5000 runs and with a PRBS input of length 1022 samples and $\nu(t)$ as white noise with variance $\sigma^2 = 0.1$. Figure 18 portrays the results obtained with both estimators (158) and (161).

Figure 18 – Estimates of the observability matrix in a Monte Carlo experiment. The ellipses represent the covariance regions around the mean value with 95% confidence.

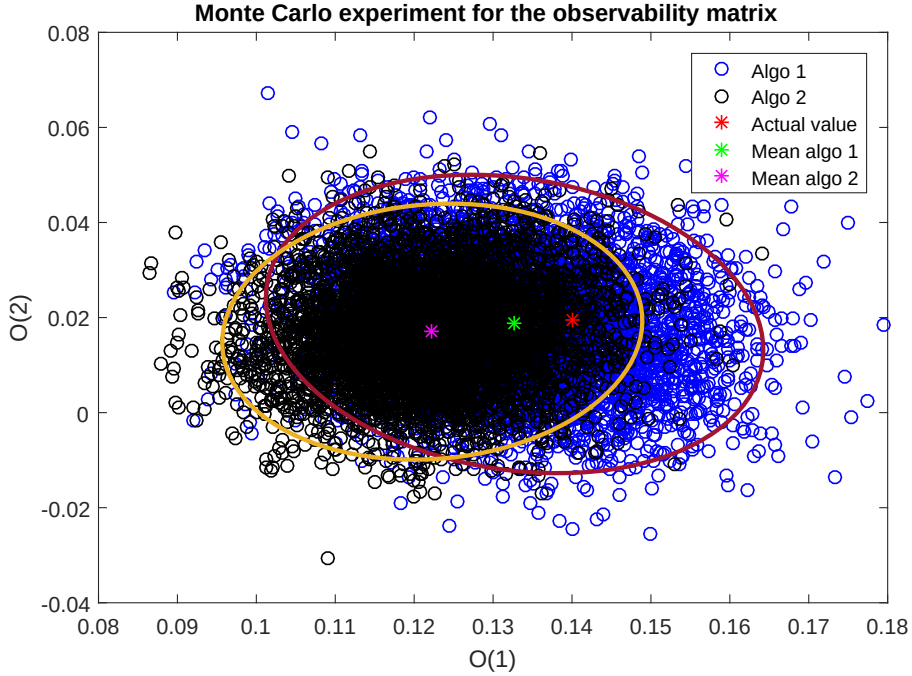

Source: author.

As mentioned before, the estimate bias with Algorithm 1 is smaller, whereas with Algorithm 2 a smaller covariance is achieved. In fact, we obtained $\mathcal{E}(\widehat{\mathbf{O}}_1) = [0.1327 \;\; 0.01865]^T$ and $\mathcal{E}(\widehat{\mathbf{O}}_2) = [0.1223 \;\; 0.01704]^T$, and the eigenvalues λ of the covariance matrices $\lambda[\mathcal{E}(\widehat{\mathbf{V}}_1)] = [1.365 \;\; 1.938]^T \times 10^{-4}$ and $\lambda[\mathcal{E}(\widehat{\mathbf{V}}_2)] = [1.093 \;\; 1.3]^T \times 10^{-4}$. Notice that the largest eigenvalue with Algorithm 2 is approximately the smallest eigenvalue with Algorithm 1.

We also computed the eigenvalues of the MSE matrix of both algorithms and obtained $\lambda(MSE_1) = [1.723 \times 10^{-4} \;\; 1.812 \times 10^{-2}]^T$ and $\lambda(MSE_2) = [1.182 \times 10^{-4} \;\; 1.537 \times 10^{-2}]^T$. Note that Algorithm 2 provides a smaller MSE, even though its bias is larger.

4.5.4 NMP system

Consider the following state-space representation of the NMP system (111)

$$A = \begin{bmatrix} 0.8 & \frac{\sqrt{10}}{10} & 0 & 0 \\ 0 & 0.9 & 0 & 0 \\ 0 & 0 & 0.8 & 0 \\ 0 & 0 & 0 & 0.8 \end{bmatrix} \quad B = \begin{bmatrix} 0 & 0 \\ 1 & 0 \\ 1 & 0 \\ 0 & 2 \end{bmatrix} \tag{185}$$
$$C = \begin{bmatrix} \frac{\sqrt{10}}{10} & 1 & 0 & 1 \\ 0 & 0 & 1.25 & 0.75 \end{bmatrix}.$$

We consider integral control of both outputs and a performance criterion given by

$$Q = \begin{bmatrix} 50 & 0 & 0 & 0 \\ 0 & 50 & 0 & 0 \\ 0 & 0 & 1 & 0 \\ 0 & 0 & 0 & 1 \end{bmatrix} \qquad R = \begin{bmatrix} 0.001 & 0 \\ 0 & 0.001 \end{bmatrix}. \tag{186}$$

In order to obtain data from the system, we set an open-loop experiment with PRBS input of amplitude ± 1 and length 2555 samples. We also considered a state vector noise $\nu(t)$ as in (138) such that $SNR = 12$ dB *at the output* $y(t)$ (noise vector $w(t)$ was set to zero). The output was filtered by (177) to obtain the IMC state vector for our proposed algorithm. We estimated 90 Markov parameters and the extended observability matrix, and we obtained:

$$\hat{K}_{90} = \begin{bmatrix} 0.1929 & 0.2275 & 0.1252 & 0.04293 & -0.02594 & 0.07550 \\ -0.01771 & 0.09016 & 0.09622 & 0.3471 & -0.01777 & -0.08516 \end{bmatrix}. \tag{187}$$

Notice that no adjustments were needed in any step of the estimation process in order to account for the NMP characteristic of the system. Figure 19 shows the closed-loop response to a sequence of steps and with $E = F = 0$, i.e, no noise.

Figure 19 – Closed-loop response of system (111) for integral control with state-feedback gain (187).

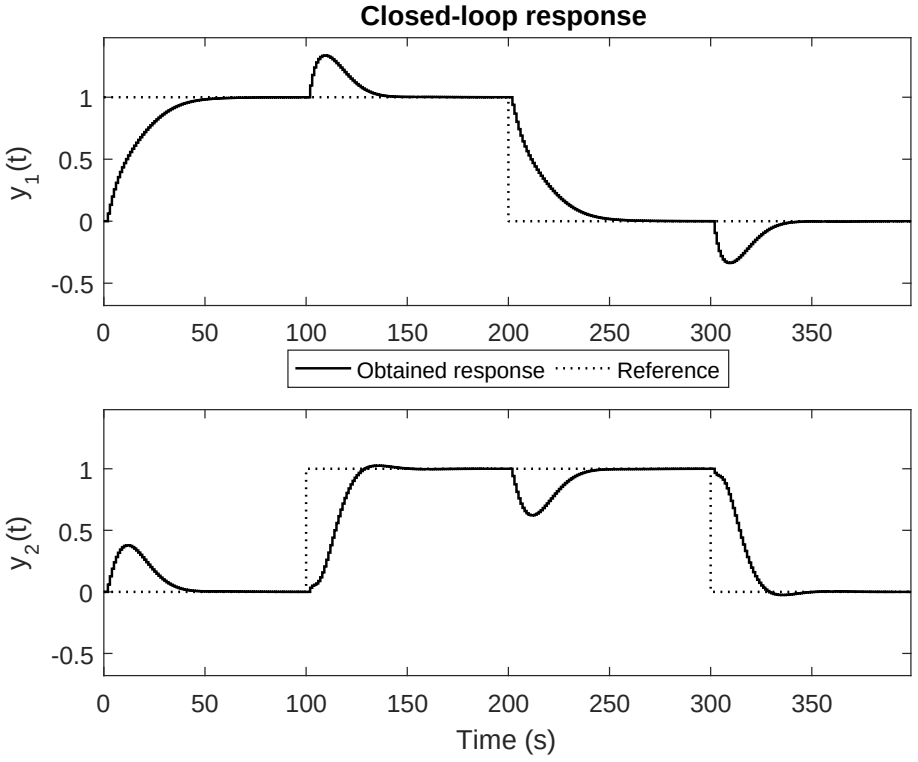

Source: author.

4.6 Control of an UPS

We now consider a practical application of the proposed methodology to an uninterruptible power supply (UPS). This plant has been studied before in a model-based approach in (PEREIRA *et al.*, 2014; LORENZINI *et al.*, 2015).

Consider the simplified electrical diagram of the output stage of a single-phase UPS system, as illustrated in Figure 20. The PWM (Pulse Width Modulation) comparator input drives the switching between S_1 and S_2. The system output is the voltage on the capacitor, where L_f and C_f are the output filter inductance and capacitance respectively, whereas R_{L_f} accounts for the inductor resistance.

Figure 20 – Schematic representation of the UPS with load.

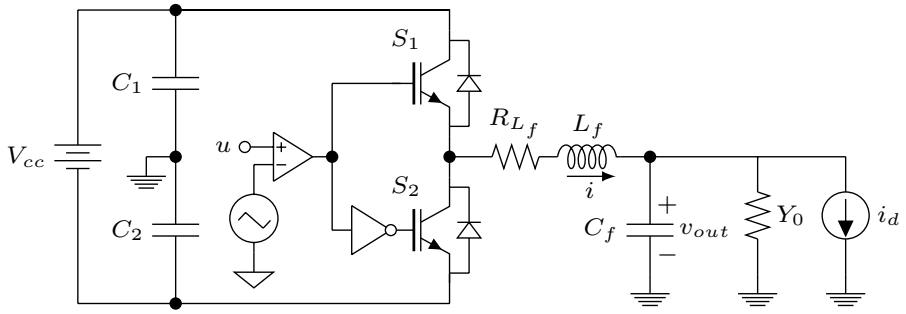

Source: author.

The load effect on the system output is modeled by a parallel connection of an uncertain admittance $Y_0(t)$ and an unknown periodic disturbance given by the current source $i_d(t)$. Switching between S_1 and S_2 with a PWM is modeled by a gain K_{PWM} multiplied by the control input. Also, defining the system state vector as the inductor current and the capacitor voltage, $x(t) = [i(t) \;\; v(t)]^T$, the *continuous-time* state-space representation for the UPS system is given by:

$$\begin{aligned} \dot{x} &= \underbrace{\begin{bmatrix} \frac{-R_{L_f}}{L_f} & \frac{-1}{L_f} \\ \frac{1}{C_f} & \frac{-Y_0}{C_f} \end{bmatrix}}_{A} x + \underbrace{\begin{bmatrix} \frac{K_{PWM}}{L_f} \\ 0 \end{bmatrix}}_{B} u + \underbrace{\begin{bmatrix} 0 \\ \frac{-1}{C_f} \end{bmatrix}}_{B_d} i_d \\ y &= \underbrace{\begin{bmatrix} 0 & 1 \end{bmatrix}}_{C} x \end{aligned} \tag{188}$$

where u is the PWM control input; i_d is the current source representing the exogenous disturbances generated by non-linear loads; and y is the output voltage to be controlled. Admittance Y_0 can be set as an open circuit (no load), as a nominal resistance $R_0 = 6\ \Omega$ and as a non-linear load given by a full-bridge circuit with a capacitor, which represents the input stage of typical UPS's loads.

In closed-loop, the reference signal is typically a sinusoid of frequency 60 Hz and amplitude $127\sqrt{2}$. Since the reference signal is a sinusoid, then the right choice of the

IMC is a resonant controller (178), such that

$$x_c(t+1) = \begin{bmatrix} 0 & 1 \\ -1 & 2\cos(120\pi T_s) \end{bmatrix} x_c(t) + \begin{bmatrix} 0 \\ 1 \end{bmatrix} (r(t) - y(t)) \tag{189}$$

The control design problem can be summarized as: *design a data-driven state-feedback controller for sinusoid reference tracking for the UPS operating with* ***non-linear load***.

In order to obtain meaningful data from the system, we set an open-loop experiment as follows. The sampling time was set to $T_s = 1/15000$ s; the input of the PWM was set as a PRBS with amplitude ± 104 V and with length 75000 samples (i.e., a 5 seconds long signal); current and voltage were measured as portrayed (zoomed time scale) in Figure 21 for the UPS operating with its *non-linear load*. The output voltage was filtered by (189) to obtain the IMC state for our proposed algorithm.

Figure 21 – Open-loop response with nominal non-linear load.

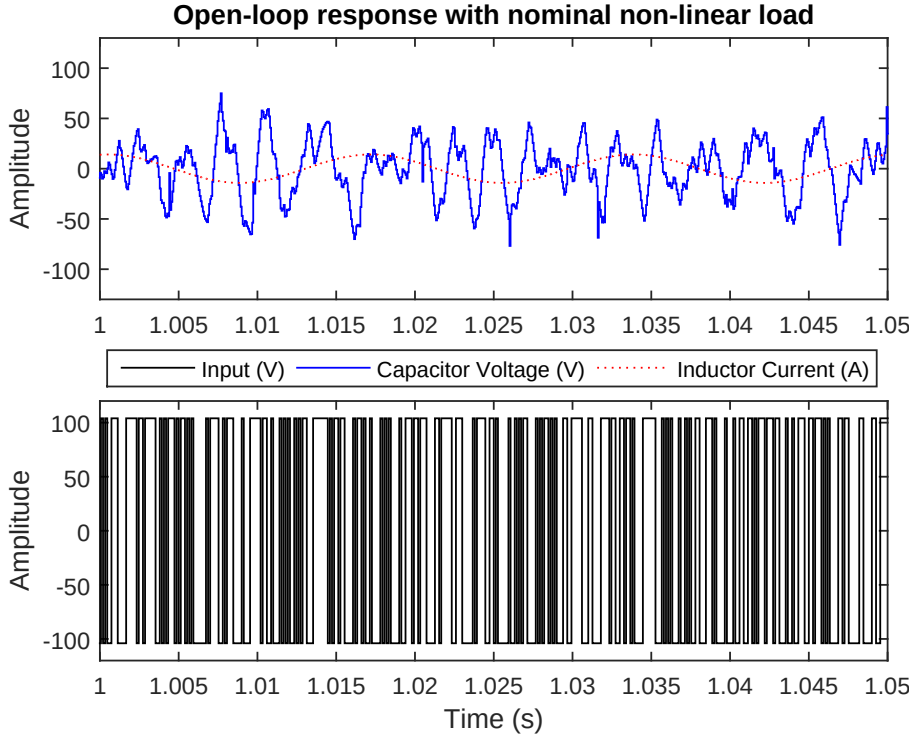

Source: author.

The parameters chosen for the LQR were $Q = 200I_3$ and $R = 5000$, that is, we strongly penalized the control signal as to try to achieve closed-loop stability even when there is no load in the UPS and to reduce sensibility due to noise, specially for the current measurement. Prior to any knowledge about the system settling time, we also selected $N_m = 150$. The obtained LQR gain is

$$K = [4.85548 \;\; 5.54514 \;\; 0.638479 \;\; -0.644019]. \tag{190}$$

Figure 22 shows the closed-loop response for the UPS operating at nominal capacity with non-linear load. Stability and reference tracking were achieved with correspond-

ing Total Harmonic Distortion (THD) of 11.7% – a similar result to the one obtained in (PEREIRA *et al.*, 2014) for the same amount of resonant modes, in which the state-feedback gain was designed using a full plant model and a Linear Matrix Inequality approach.

Figure 22 – Closed-loop response with nominal non-linear load.

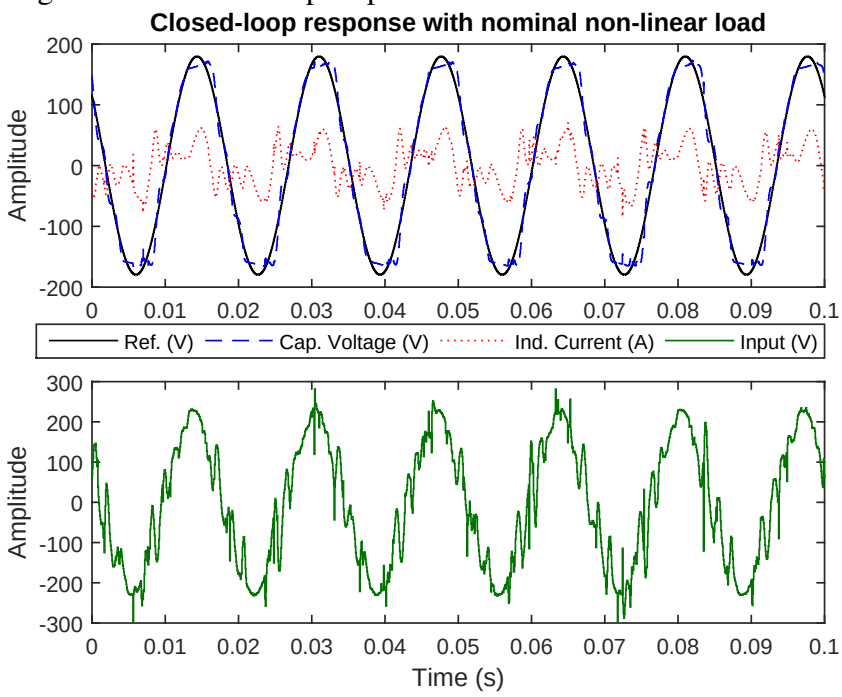

Source: author.

We also applied the obtained controller to different scenarios: (a) the open circuit (no load) case and (b) the nominal linear load R_0. Figure 23 shows the closed-loop responses for cases (a) and (b) respectively. Closed-loop stability was achieved and with very small THD – 1.4% and 1.8% respectively –, even though the controller was not designed with data obtained in these scenarios.

Notice that with this approach we obtained a linear state-feedback gain with only one experiment on the plant, even though the actual plant has a strong nonlinear behavior and a single linear model would not describe the system with reasonable accuracy. If data were used to identify a plant model, then more than one experiment would be necessary in order to evaluate a plant model and an uncertainty matrix. Of course, robustness in this case is not only because of the data-driven methodology, but mainly because of the choices for the matrices Q and R.

4.7 Chapter conclusions

In this chapter we provided a data-driven method to compute the infinite horizon LQR state-feedback gain, without identifying a model of the plant. The idea was based on

Figure 23 – Closed-loop response with no output load and with nominal linear load.

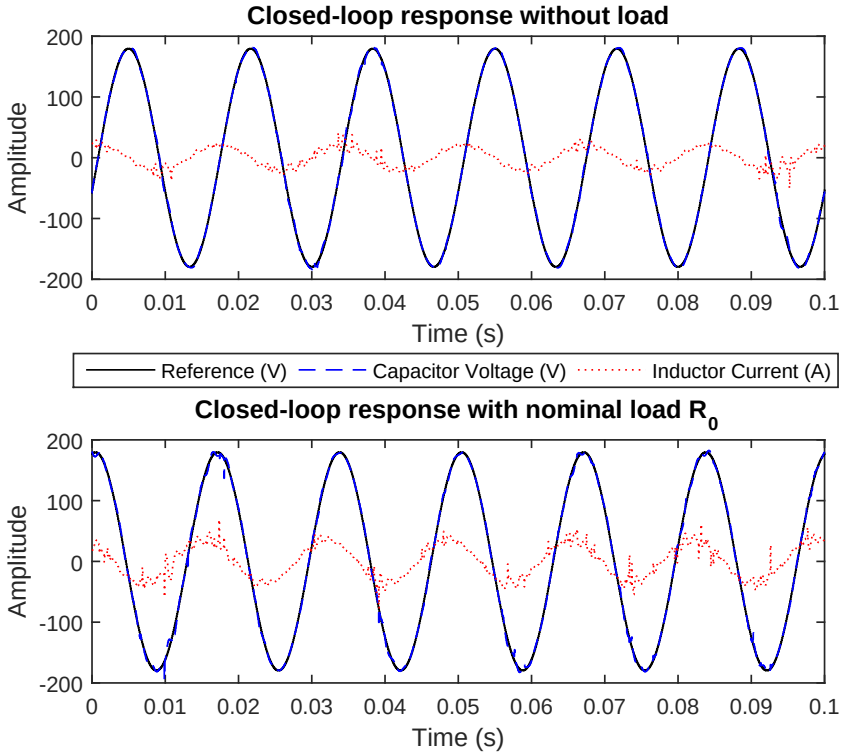

Source: author.

previous works where the system Markov parameters were estimated, but instead of also estimating a generalized system state vector, we estimate an extended observability matrix. In our method, the feedback gain is computed from a batch of data and converges to the infinite horizon LQR gain as the amount of data and, by consequence, the number of estimated Markov parameters grow. The most onerous step of our procedure is performing one experiment in the plant, as the solution is achieved by solving two least-squares problems. Simulation examples illustrated the convergence of the method and an experimental application to an UPS showed its practical applicability.

5 DATA-DRIVEN CONTROLLER CERTIFICATION AND ROBUST PERFORMANCE ASSESSMENT

Shrimp that sleeps, the wave takes away.

Zeca Pagodinho

The standard setup in DD control design is to perform an open-loop experiment to collect data and then tune the controller parameters that, given an appropriate choice of the reference model (GONÇALVES DA SILVA; BAZANELLA; CAMPESTRINI, 2018), will lead to a stable closed loop with given transient characteristics. For the closed-loop case, i.e., when there is an initial stabilizing controller operating on the system, the change in the parameters from the current controller to the one estimated via DD methods can be abrupt, and the user might be suspicious in closing the loop with this new controller. Besides, these DD methodologies usually have no guarantee to yield a stabilizing controller.

An embedded stability constraint in DD methods have been proposed in (VAN HEUSDEN; KARIMI; BONVIN, 2011), using an approach similar to (LANZON *et al.*, 2006), but a number of approximations take place in order to yield a convex optimization problem, sometimes causing the obtained closed-loop response to bear no resemblance to the reference model. The stability criterion is based on $\mathcal{H}_\infty$-norm estimation of a given sensitivity function using spectral estimates.

Data-driven controller certification deals with the problem of establishing through a batch of data if a controller will stabilize a given plant without having the process model. The idea to validate a controller before inserting it in the closed loop is borrowed from the adaptive control version of the problem, the cautious control design. Most previous approaches to the problem derives from Vinnicombe's seminal work (VINNICOMBE, 1993). Vinnicombe introduced the ν-gap metric between two transfer functions (and the conditions in which they are measurable) and showed that when this distance is less than a generalized stability margin (which is also function of the plant model), then the new controller is assured to stabilize the plant. This criterion has shown to convey not only about stability but also about performance of the new controller, and has since then been used as the standard tool in controller certification procedures (PARK; BITMEAD,

2004, 2007; CHEONG; BITMEAD, 2012). However, this constraint can also be too conservative and when the plant is unknown it is hard to be validated.

A different closed-loop configuration is proposed in (DEHGHANI *et al.*, 2009) in order to collect data and validate closed-loop stability with a new controller, circumventing the test via the ν-gap criterion. The proposed data-driven approach however requires many experiments, as the constraint studied depends on the frequency response of a given transfer function. Using the same configuration, the authors proposed other mappings in order to evaluate performance in the same basis of the generalized stability margin (CHA *et al.*, 2014). Nevertheless, all examples provided are exclusively model-based, so all possible frequency dependent outcomes are evaluated, but no technicality about a pure data-driven approach is provided, e.g., which algorithm to use, issues when data is corrupted by noise, possible false-positives outcomes.

In this chapter, we start from the findings in (DEHGHANI *et al.*, 2009; CHA *et al.*, 2014). First, we bring their mappings to the standard closed-loop configuration, not only for stability purposes, but also for robust performance assessment. We then show that a similar procedure can be applied when data are collected in open loop (i.e., there is no initial stabilizing controller), provided that the plant is open-loop stable. All these tests are based on an $\mathcal{H}_\infty$-norm criterion of given transfer functions, whether in the Single-Input Single-Output (SISO) or Multi-Input Multi-Output (MIMO) case. We show that all these mappings can be obtained from one single experiment and present an algorithm to estimate the respective $\mathcal{H}_\infty$-norm directly, without identifying a respective parametrized transfer function (matrix). As far as the author is aware, this is the first one-shot data-driven approach that can be directly applied to the multivariable case without requiring modification nor extra experiment.

NOTATION: In this chapter we present a formulation which actually works for both the continuous and discrete-time domain, although we focus on the latter to derive the data-driven approach, so we drop the argument (q) of the transfer functions, except in the examples.

5.1 Background

Consider a plant G_0 in feedback interconnection with a controller C_i, as in Figure 3 and repeated here for convenience. We denote this interconnection by $[G_0, C_i]$.

Let C_0 be an initial stabilizing controller and let C_1 represent a new controller that is to be put in place of C_0 in the feedback interconnection. The question that the Controller Certification procedure tries to answer is, given *a priori* information on $[G_0, C_0]$ and without inserting C_1 on the closed loop, whether $[G_0, C_1]$ is internally stable or not.

The most common approach to answer this question is via Vinnicombe's ν-gap metric

Figure 24 – Block diagram of the closed-loop system.

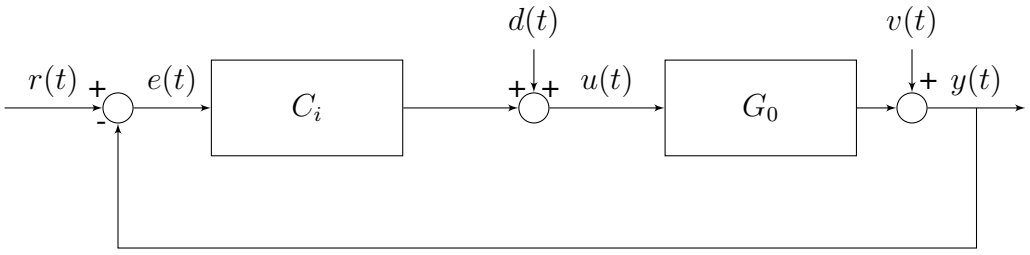

Source: author.

(VINNICOMBE, 1993). Before presenting the result on stability, we need some definitions that are introduced next. We follow the presentation in (DEHGHANI *et al.*, 2009), adapting it to discrete-time.

Definition 5.1. *$\mathcal{H}_\infty$ denotes the space of functions bounded and analytic in the complement of the closed unit disc. We denote by $\mathcal{R}$ the set of real-rational proper transfer functions and hence the real-rational subspace of $\mathcal{H}_\infty$ by $\mathcal{RH}_\infty$.*

Definition 5.2. *The pair $\{E_i, F_i\} \in \mathcal{RH}_\infty$ is a right-coprime factorization (rcf) of $X_i \in \mathcal{R}$ if F_i is invertible in $\mathcal{R}$, $X_i = E_i F_i^{-1}$, and E_i and F_i are right-coprime over $\mathcal{RH}_\infty$. The pair $\{E_i, F_i\}$ is a normalized rcf of X_i if $\{E_i, F_i\}$ is a rcf of X_i and $F_i^* F_i + E_i^* E_i = I$, where $[\cdot]^*$ is the complex conjugate.*

Definition 5.3. *The pair $\{U_i, V_i\} \in \mathcal{RH}_\infty$ is a left-coprime factorization (lcf) of $X_i \in \mathcal{R}$ if V_i is invertible in $\mathcal{R}$, $X_i = V_i^{-1} U_i$, and U_i and V_i are left-coprime over $\mathcal{RH}_\infty$. The pair $\{U_i, V_i\}$ is a normalized lcf of X_i if $\{U_i, V_i\}$ is a lcf of X_i and $V_i V_i^* + U_i U_i^* = I$.*

The right and left coprime factorizations always exist and are unique to within right (left) multiplication by a constant (unitary, for the normalized case) matrix (VINNICOMBE, 2000).

Definition 5.4. *The interconnection $[G_0, C_i]$ in Figure 24 is well-posed if $(I + C_i G_0)$ is invertible in $\mathcal{R}$. The mapping $[y(t)\ u(t)]^T = H(G_0, C_i)[r(t)\ d(t)]^T$ is given by (VINNICOMBE, 1993, modified)*

$$H(G_0, C_i) = \begin{bmatrix} G_0 \\ I \end{bmatrix} (I + C_i G_0)^{-1} \begin{bmatrix} C_i & I \end{bmatrix}. \tag{191}$$

Definition 5.5. *(Generalized Stability Margin) The interconnection $[G_0, C_i]$ is internally stable if it is well-posed and $H(G_0, C_i) \in \mathcal{RH}_\infty$. In this case we say that C_i stabilizes G_0. The Generalized Stability Margin b_{G_0,C_i} is thus defined as*

$$b_{G_0,C_i} = \begin{cases} \|H(G_0, C_i)\|_\infty^{-1}, & \text{if } [G_0, C_i] \text{ is internally stable;} \\ 0, & \text{otherwise.} \end{cases} \tag{192}$$

Definition 5.6. *(Winding Number Condition (WNC)) Two controllers, C_i and C_j, satisfy the WNC if*

$$\begin{aligned} &\det(I + C_j^* C_i)(e^{j\omega}) \neq 0, -\pi \leq \omega \leq \pi \text{ and} \\ &\mathrm{wno}(\det(I + C_j^* C_i)) + \eta(C_i) - \bar{\eta}(C_j) = 0 \end{aligned} \tag{193}$$

where $\mathrm{wno}(\cdot)$ *indicates the winding number of the Nyquist contour (that encircles the area outside the unit disc and is indented at* 1*),* $\eta(C_i)$ *is the number of poles of* $\det(C_i)$ *outside the open unit circle and* $\bar{\eta}(C_j)$ *is the number of poles of* $\det(C_j)$ *outside the closed unit circle.*

Definition 5.7. *(Vinnicombe's ν-gap metric (VINNICOMBE, 1993)) Given two transfer function matrices, $C_i = E_i F_i^{-1}$ and $C_j = V_j^{-1} U_j$, the distance between these two transfer matrices is given by*

$$\delta_\nu(C_i, C_j) = \begin{cases} \left\| \begin{bmatrix} -V_j & U_j \end{bmatrix} \begin{bmatrix} E_i \\ F_i \end{bmatrix} \right\|_\infty, & \text{if (193) is satisfied;} \\ 1, & \text{otherwise.} \end{cases} \tag{194}$$

The metric (194) has then been shown to play an important role for robust stability as presented in the following theorem.

Theorem 5.1. *(VINNICOMBE, 1993) Consider a plant G_0 and two controllers C_i and C_j, with C_i stabilizing G_0. Then $[G_0, C_j]$ is internally stable if*

$$\delta_\nu(C_i, C_j) < b_{G_0, C_i}. \tag{195}$$

Vinnicombe's constraint (195) has, since then, been used as the standard tool to answer the question of controller certification and many verification procedures (PARK; BITMEAD, 2004, 2007; CHEONG; BITMEAD, 2012) derived from this constraint. However, this constraint depends on a model G_0 of the process; and even if b_{G_0,C_i} can be obtained directly from data (using, for example, the algorithm we will provide in Section 5.3), this constraint could still be too conservative. Moreover, relation (195) has also been used to verify if a controller stabilizes a nominal plant and a perturbation around this model, i.e., applying the ν-gap for G_0 and a G_1; this is also related to the small gain theorem.

Based on coprime factorizations and Nyquist conditions, other stability equivalencies have been proposed in (VINNICOMBE, 2000), but they seemed to be overlooked as possible stability tests. Based on definitions 5.2 and 5.3, the following theorem holds.

Theorem 5.2. *(VINNICOMBE, 2000) Define the graph symbols of $G_0 = E_0 F_0^{-1}$ and $C_i = V_i^{-1} U_i$ by*

$$P \triangleq \begin{bmatrix} E_0 \\ F_0 \end{bmatrix}, \quad K_i \triangleq \begin{bmatrix} U_i & V_i \end{bmatrix}. \tag{196}$$

Then the following statements are equivalent:

(a) $[G_0, C_i]$ *is internally stable;*

(b) $(K_iP)^{-1} = [V_i(I + C_iG_0)F_0]^{-1} \in \mathcal{RH}_\infty$*;*

(c) $\det(K_iP)(e^{j\omega}) \neq 0, -\pi \leq \omega \leq \pi$ *and* $\text{wno}(\det(K_iP)) = 0$.

Notice that condition (b) in Theorem 5.2 is equivalent to $H(G_0, C_i) \in \mathcal{RH}_\infty$, and condition (c) is the evaluation of the Nyquist condition. Also, condition (b) shows an interesting twist: BIBO-stability of $(K_iP)^{-1}$ implies internal stability of $[G_0, C_i]$. Stability tests based on Theorem 5.2 have been proposed in (DEHGHANI *et al.*, 2007, 2009), where another setup is proposed based on an "observer-form implementation" of the controller, such that the final test circumvents the need to certify the controller by verifying condition (195), but that still requires the estimation of the $\mathcal{H}_\infty$-norm of a target function. We then present a one-shot algorithm to estimate the norm that can be directly applied to the MIMO case without the need of any additional experiment.

5.2 Experimental setting

Except for some sign changes in the block diagram of Figure 25, as we try to bring the explanation closer to the standard feedback control configuration in Figure 3, the results presented in subsections 5.2.1 and 5.2.2 are given in (DEHGHANI *et al.*, 2009; CHA *et al.*, 2014). We then show in Subsection 5.2.3 how one can apply similar mappings to infer about stability when data are collected in open loop.

5.2.1 Closed-loop stability test setup

Consider the block diagram of Figure 25, where C_0 has been split into its *lcf* with a forward V_0^{-1} and a feedback U_0 factor in the loop, and $z(t)$ is a signal generated by filtering the control signal and the output by the *lcf* of C_1. For now, we shall not consider the exogenous signals $d(t)$ and $v(t)$ as they will not be relevant to the remaining of the discussion. Also, define the mapping $\mathcal{T} : r(t) \mapsto z(t)$:

$$\mathcal{T} = [U_1\ V_1] \begin{bmatrix} G_0(I + C_0G_0)^{-1} \\ (I + C_0G_0)^{-1} \end{bmatrix} V_0^{-1} \tag{197}$$

$$= V_1(I + C_1G_0)(I + C_0G_0)^{-1}V_0^{-1} \tag{198}$$

$$= (K_1P)(K_0P)^{-1}. \tag{199}$$

The following theorem defines the stability tests.

Theorem 5.3. *(DEHGHANI et al., 2009) Let* $[G_0, C_0]$ *be internally stable. Let* $C_0 = V_0^{-1}U_0$ *and* $C_1 = V_1^{-1}U_1$ *be* lcf *over* $\mathcal{RH}_\infty$*. Then the following statements are equivalent:*

(a) $[G_0, C_1]$ *is internally stable;*

Figure 25 – Experimental setting proposed in (DEHGHANI *et al.*, 2009).

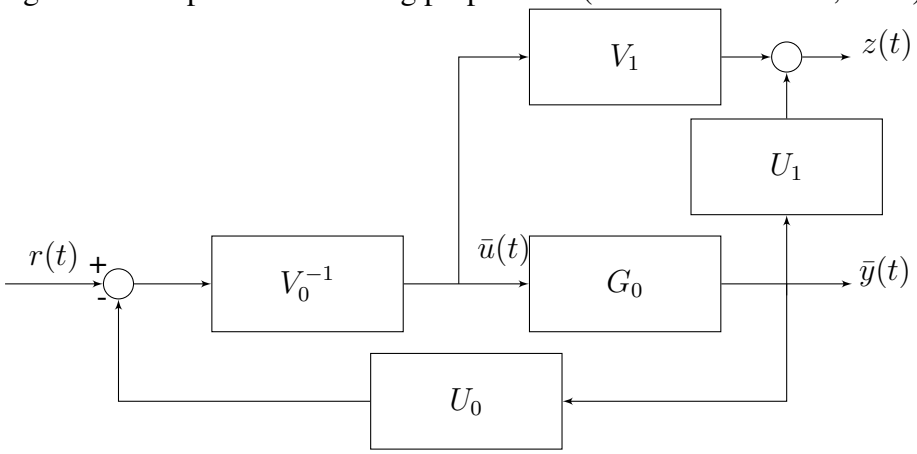

Source: (DEHGHANI *et al.*, 2009).

(b) $\mathcal{T}^{-1} \in \mathcal{RH}_\infty$*;*

(c) $\text{wno}(\det \mathcal{T}) = 0$ *and* $\det \mathcal{T}(e^{j\omega}) \neq 0,\ -\pi \leq \omega \leq \pi$*;*

(d) $\arg\det \mathcal{T}(e^{j\pi}) = \arg\det \mathcal{T}(e^{j0})$ *and* $\det \mathcal{T}(e^{j\omega}) \neq 0,\ -\pi \leq \omega \leq \pi$.

See (DEHGHANI *et al.*, 2009) for a detailed proof, but most equivalences are direct results from Theorem 5.2, given (199). In particular, for condition (b), which is the one we will explore in our certification procedure, it suffices to see that, if $(K_0P)^{-1} \in \mathcal{RH}_\infty$ (Theorem 5.2-(b)) and $(K_0P)(K_1P)^{-1} \in \mathcal{RH}_\infty$ (Theorem 5.3-(b) and Eq. (199)), then by consequence $(K_1P)^{-1} \in \mathcal{RH}_\infty$, which satisfies Theorem 5.2-(b). Also, notice that $\mathcal{T}$ is stable and bi-proper by construction.

Under the assumption that the plant G_0 is unknown, then one can not explicitly compute the transfer function $\mathcal{T}$. Instead, one can set an experiment and use data from the reference $r(t)$ and the filtered signal $z(t)$ in order to analyze one of the conditions in Theorem 5.3.

An experimental setup for testing condition (d) in Theorem 5.3 has been proposed in (DEHGHANI *et al.*, 2007) and further detailed in (DEHGHANI *et al.*, 2009). The stability verification consists of two tests: first, based on a sequence of steps in each input and collecting the steady-state outputs of $z(t)$, they try to falsify controller C_1; if the controller is not falsified then a frequency response must be estimated. They show that instead of estimating the full frequency response of $\mathcal{T}$, one can estimate the frequency response of $\mathcal{T} - I$ up to a certain maximum frequency.

A test to verify condition (b) in Theorem 5.3 was also proposed in (DEHGHANI *et al.*, 2007). The idea consists in finding whether or not $\det(\mathcal{T})$ has a non-minimum phase zero; or, equivalently, if the step response of $\det(\mathcal{T})$ presents an initially inverse. For that, another set of experiments must be conducted with step inputs, and some of them

include connecting one output of $z(t)$ in $r(t)$. It is important to notice that this procedure applies mostly when working in the continuous-time domain, since in discrete-time the zeros outside the unit disc in the left-plane do not necessarily yield an initially inverse response.

In each of the proposed stability tests, many experiments must be conducted in order to certify controller C_1, and carrying them out can be exceedingly onerous in practical applications. In this chapter we propose a procedure to validate condition (b) in Theorem 5.3 with *only one batch of data* collected from the system operating in closed loop as in Figure 3, without the exogenous signal $d(t)$. First, we show how to obtain $z(t)$ from $r(t)$ and $y(t)$ – which is different from signal $\bar{y}(t)$, as can be seeing comparing figures 3 and 25.

Consider the block diagram in Figure 25. One can readily verify from the bottom part of the setting the implicit signal $y(t)$ present in the feedback part, as revealed in Figure 26.

Figure 26 – Block equivalent of bottom part of Figure 25.

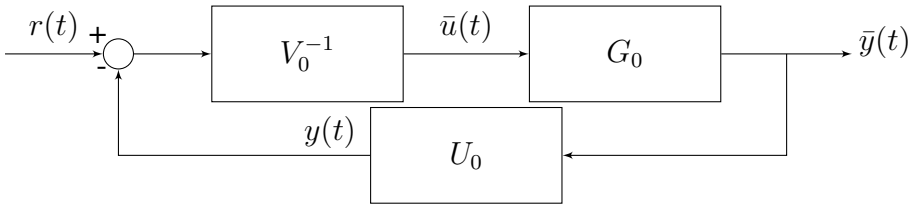

Source: author.

Thus, as depicted in Figure 26, one can obtain $\bar{y}(t)$ by filtering $y(t)$ by the inverse of U_0, i.e.,

$$\bar{y}(t) = U_0^{-1} y(t). \tag{200}$$

If the computations are done off-line, which is typically the case, then causality of U_0 is not required for the computation of $\bar{y}(t)$ in (200). What is required is that U_0 is minimum-phase, so that its inverse is BIBO-stable. Thus, we make use of the following assumption.

Assumption 5.1. The closed-loop case: there is an initial stabilizing controller C_0. C_0 *has no zeros outside the open unit circle.*

Also, note that

$$\bar{u}(t) = V_0^{-1} r(t) - C_0 \bar{y}(t) = V_0^{-1}(r(t) - y(t)). \tag{201}$$

Finally, one can obtain the signal $z(t)$ as

$$\begin{aligned} z(t) &= V_1 \bar{u}(t) + U_1 \bar{y}(t) \\ &= V_1[V_0^{-1}(r(t) - y(t))] + U_1 U_0^{-1} y(t) \\ &= V_1 V_0^{-1} r(t) + (U_1 U_0^{-1} - V_1 V_0^{-1}) y(t) \end{aligned} \tag{202}$$

Since reference $r(t)$ is a signal one sets and $y(t)$ can be measured in closed loop, then one can obtain $z(t)$ and form the data set $\{r(t), z(t)\}$, in order to extract information of $\mathcal{T}$ (respectively $\mathcal{T}^{-1}$) in (198) to verify condition (b) in Theorem 5.3. Notice that this condition is whether the $\mathcal{H}_\infty$-norm of $\mathcal{T}^{-1}$ is bounded or not, i.e., if $\mathcal{T}^{-1}$ is stable, and not about its exact $\mathcal{H}_\infty$-norm. Finding through data if a system is stable, but not exactly where its poles are located, calls more for a nonparametric approach than for a parametric one, and we shall explore this idea in the sequel.

Remark 5.1. *In contrast with (DEHGHANI et al., 2009), where definitions 5.1 and 5.6 and theorems 5.2 and 5.3 were given in continuous-time, we presented here a discrete-time formulation, since we seek for a data-driven approach. We highlight however that our approach can be applied to both continuous and discrete-time controller implementations. For the continuous-time case, though, one is implicitly evaluating a discretized version of the objective function $\mathcal{T}$. We explore this case in Example 5.4.3.*

5.2.2 Data-driven robust performance assessment

We shall see next that we can also establish two mappings from the experimental setting in Figure 25 in order to obtain information about whether the new controller C_1 provides better generalized stability margin b_{G_0,C_i} than controller C_0. Notice that b_{G_0,C_i} only tells us about robust stability, but nothing about transient responses.

Define the following maps

$$r(t) \mapsto \bar{y}(t) \; : \; Y_i \triangleq E_0(K_iP)^{-1} = G_0(I + C_iG_0)^{-1}V_i^{-1}, \tag{203}$$

$$r(t) \mapsto \bar{u}(t) \; : \; W_i \triangleq F_0(K_iP)^{-1} = (I + C_iG_0)^{-1}V_i^{-1}. \tag{204}$$

It is easy to show that (CHA *et al.*, 2014):

$$H(G_0, C_i) = \begin{bmatrix} Y_iU_i & Y_iV_i \\ W_iU_i & W_iV_i \end{bmatrix}. \tag{205}$$

If the pair $\{U_i, V_i\}$ is a normalized *lcf*, then it follows that

$$\|H(G_0, C_i)\|_\infty = \left\| \begin{bmatrix} Y_i \\ W_i \end{bmatrix} \right\|_\infty. \tag{206}$$

For controller C_0 this defines the mapping $\begin{bmatrix} Y_0 \\ W_0 \end{bmatrix} \; : \; r(t) \mapsto \begin{bmatrix} \bar{y}(t) \\ \bar{u}(t) \end{bmatrix}$.

On the other hand, one can verify that, if $\mathcal{T}^{-1} \in \mathcal{RH}_\infty$, then $Y_1 = Y_0\mathcal{T}^{-1}$ and $W_1 = W_0\mathcal{T}^{-1}$, and $Y_1, W_1 \in \mathcal{RH}_\infty$. From the setting in Figure 25, we also have that $Y_1 : z(t) \mapsto \bar{y}(t)$ and $W_1 : z(t) \mapsto \bar{u}(t)$, or shortly, $\begin{bmatrix} Y_1 \\ W_1 \end{bmatrix} \; : \; z(t) \mapsto \begin{bmatrix} \bar{y}(t) \\ \bar{u}(t) \end{bmatrix}$.

Recall that $\bar{y}(t)$ and $\bar{u}(t)$ can be obtained by filtering data from the experimental setting in Figure 24 using relations (200) and (201), thus one can also use a data-driven approach to establish if the new controller provides better stability margin or not.

5.2.3 Open-loop stability test setup

The formulation just presented, which comes from (DEHGHANI *et al.*, 2009; CHA *et al.*, 2014), considers the standard controller certification problem, where a closed-loop experiment is carried out with an initial stabilizing controller. Based on the experimental setting in Figure 25, we now propose an equivalent setting for testing closed-loop stability of controller $C_1 = V_1^{-1}U_1$ when data is obtained in an open-loop experiment on the plant $G_0 = E_0F_0^{-1}$. Such a test shall verify condition (b) in Theorem 5.2 directly. Consider the following block diagram:

Figure 27 – Proposed open-loop experimental setting.

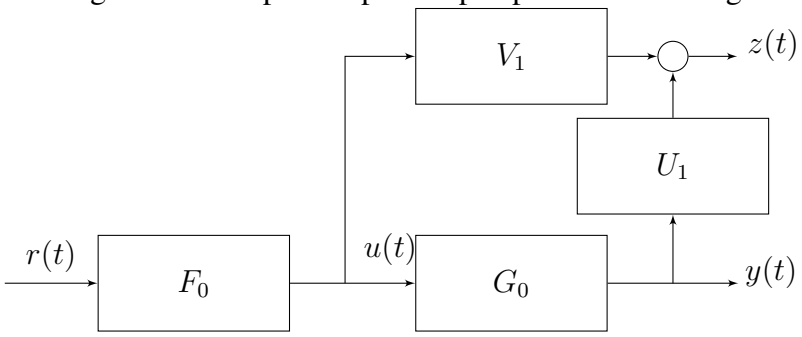

Source: author.

The filtered signal $z(t)$ is given by

$$\begin{aligned} z(t) &= V_1u(t) + U_1y(t) \\ &= V_1F_0r(t) + U_1G_0F_0r(t) \\ &= (V_1 + U_1G_0)F_0r(t) \\ &= V_1(I + C_1G_0)F_0r(t) = (K_1P)r(t). \end{aligned} \tag{207}$$

Thus, in order to establish if condition (b) in Theorem 5.2 holds, one can study the mapping $r(t) \mapsto z(t)$. Notice however that this mapping requires knowledge of F_0, and therefore knowledge of the plant G_0. In order to circumvent this issue, we shall make use of the following assumption, since an open-loop experiment is to be conducted.

Assumption 5.2. The open-loop case: there is no initial stabilizing controller C_0. *The plant G_0 is open-loop stable.*

If G_0 is stable, then $F_0^{-1} \in \mathcal{RH}_\infty$. Thus, evaluating stability through $F_0^{-1}(I + C_1G_0)^{-1}V_1^{-1} \in \mathcal{RH}_\infty$ is equivalent to evaluate if $(I + C_1G_0)^{-1}V_1^{-1} \in \mathcal{RH}_\infty$. Therefore, one can simply set $F_0 = I$ in Figure 27 and carry out the experiment by manipulating directly the signal $u(t)$ (which is the standard open-loop configuration) and then study the mapping $u(t) \mapsto z(t)$. Notice that this is equivalent to set $V_0 = I$ and $U_0 = 0$, such that $C_0 = 0$ in Figure 25, given satisfaction of Assumption 5.2. Also notice that this function equals W_1 as defined in (204).

As for performance assessment, one can readily verify that Y_1 and W_1 are equivalent to the mappings $z(t) \mapsto y(t)$ and $z(t) \mapsto u(t)$, respectively. Thus $\begin{bmatrix} Y_1 \\ W_1 \end{bmatrix} : z(t) \mapsto \begin{bmatrix} y(t) \\ u(t) \end{bmatrix}$.

Notice that both certification and performance assessment procedures are based on an $\mathcal{H}_\infty$-norm result, which is defined for a stable system. Thus, the main tool to be used is an $\mathcal{H}_\infty$-norm estimation from data. We discuss next one possible approach to the estimation problem.

5.3 $\mathcal{H}_\infty$-norm estimation

One of the most common data-based approach to obtain the $\mathcal{H}_\infty$-norm of a system is via Frequency Response Function (FRF) Estimates (PARK, 2008; CHEONG; BITMEAD, 2012), where a large number of experiments is carried out in order to estimate some points of the frequency response, and the function is adjusted with some interpolation points. Bounds on the error using these approaches are also provided.

A different approach is presented in (OOMEN *et al.*, 2014), where the estimate is based on a Toeplitz matrix of the system Markov parameters. This approach is based on a state-space representation of the system and is the one which will be used, but with a different computation approach as the one treated in their article. In that paper, an iterative procedure to estimate the largest eigenvalue $\lambda^{\max}$ via power method is proposed, without needing to identify the Markov parameters. On the other hand, the iterative procedure leads to an estimate of the infinity norm "for a sufficiently large number of iterations and sufficiently long experiments". In the SISO case, each iteration requires one experiment on the true system, but the amount of needed experiments grows for the MIMO case. In their example – a 2×2 case –, 40 iterations (and 80 experiments) of their method were performed on a real-world system. The method nonetheless is able to also identify in which direction (MIMO systems) the worst-case scenario (the $\mathcal{H}_\infty$-norm) occurs.

Carrying out such amount of experiments on a true system may not be attractive from a practical point of view, so it seems reasonable to develop a direct way to determine the $\mathcal{H}_\infty$-norm from one batch of data. Obtaining the Toeplitz matrix of the system Markov parameters is a well-documented procedure in the literature of subspace identification (e.g. (DE MOOR *et al.*, 1988)). Henceforth, we briefly present the main theoretical results.

Consider the system $\mathcal{T}$, which is bi-proper and stable by construction, with a minimal realization described as

$$\begin{aligned} x(t+1) &= Ax(t) + Br(t) \\ z(t) &= Cx(t) + Dr(t). \end{aligned} \tag{208}$$

with $B \in \mathbb{R}^{m \times p}$, $C \in \mathbb{R}^{l \times m}$, $D \in \mathbb{R}^{l \times p}$ and $A \in \mathbb{R}^{m \times m}$ is assumed stable. We shall use

the notation

$$\mathcal{T}_{ss} \triangleq \left[\begin{array}{c|c} A & B \\ \hline C & D \end{array}\right], \tag{209}$$

for referring to a state-space realization of $\mathcal{T}$.

The block representation of the input-output is described by

$$\underbrace{\begin{bmatrix} z(0) \\ z(1) \\ z(2) \\ \vdots \\ z(N_m) \end{bmatrix}}_{\mathbf{z}_m} = \underbrace{\begin{bmatrix} M_0 & \cdots & \cdots & 0 \\ M_1 & M_0 & \ddots & \vdots \\ M_2 & M_1 & \ddots & \vdots \\ \vdots & \vdots & \ddots & \vdots \\ M_{N_m} & M_{N_m-1} & \cdots & M_0 \end{bmatrix}}_{\mathbf{S}_m} \underbrace{\begin{bmatrix} r(0) \\ r(1) \\ r(2) \\ \vdots \\ r(N_m) \end{bmatrix}}_{\mathbf{r}_m}, \tag{210}$$

where $M_i = CA^{(i-1)}B, i = 1, 2, \ldots, N_m - 1$ and $M_0 = D$ are the system's Markov parameters (22).

For the induced norm of $\mathbf{S}$, we have

$$\bar{\sigma}(\mathbf{S}_m) = \|\mathbf{S}_m\|_{i2} = \sqrt{\lambda^{\max}(\mathbf{S}_m^T \mathbf{S}_m)} \tag{211}$$

where $\bar{\sigma}$ is the largest singular value and $\lambda^{\max}$ is the largest eigenvalue. Then it follows that

$$\|\mathcal{T}\|_\infty = \|\mathbf{S}_m\|_{i2} = \|\mathbf{S}_m\|_\infty \text{ as } N_m \to \infty. \tag{212}$$

For simplicity of notation we shall define $\mathbf{S} \triangleq \lim_{N_m \to \infty} \mathbf{S}_m$.

The $\mathcal{H}_\infty$-norm of a system is the largest singular value $\bar{\sigma}$ over its frequency spectrum. From the results above, the $\mathcal{H}_\infty$-norm of the system can be computed as the largest singular value of the *infinity* matrix $\mathbf{S}$. Evidently, one can not obtain an *infinity* matrix, so only an approximation to a certain degree N_m can be achieved for A stable and, from the structure of $\mathbf{S}_m$, it is clear that the computation of the $\mathcal{H}_\infty$-norm via singular value bounds the norm from below.

Recall that condition (b) in Theorem 5.3, which is the one we are trying to verify, is with respect to the $\mathcal{H}_\infty$-norm of $\mathcal{T}^{-1}$, and not $\mathcal{T}$. From (210), it is clear that for the *infinite horizon*, if $\mathbf{z} = \mathbf{S}\mathbf{r}$ then $\mathbf{r} = \mathbf{S}^{-1}\mathbf{z}$. What is not clear at once, and thus must be proved, is that $\mathbf{r}_m = \mathbf{S}_m^{-1}\mathbf{z}_m$, and that $\mathbf{S}_m^{-1}$ has the same structure of $\mathbf{S}_m$ and also contains exactly the Markov parameters of $\mathcal{T}^{-1}$. Before proving it in our next theorem, let us write a realization for $\mathcal{T}^{-1}$.

First, invert the input-output relation in (208)

$$r(t) = -D^{-1}Cx(t) + D^{-1}z(t) \tag{213}$$

and insert it back into the state equation to get

$$\begin{aligned} x(t+1) &= Ax(t) - BD^{-1}Cx(t) + BD^{-1}z(t) \\ &= (A - BD^{-1}C)x(t) + BD^{-1}z(t). \end{aligned} \tag{214}$$

From (213) and (214), we can define a state-space realization of $\mathcal{T}^{-1}$ as

$$\mathcal{T}_{ss}^{-1} \triangleq \left[\begin{array}{c|c} A - BD^{-1}C & BD^{-1} \\ \hline -D^{-1}C & D^{-1} \end{array}\right]. \tag{215}$$

Theorem 5.4. *Consider the system $\mathcal{T}$ bi-proper with minimal realization $\mathcal{T}_{ss}$, as in* (209)*, and corresponding finite Toeplitz matrix $\mathbf{S}_m$ of its firsts N_m Markov parameters as in* (210)*. Then the matrix $\mathbf{S}_m^{-1}$ is a Toeplitz matrix of the firsts N_m Markov parameters of the system $\mathcal{T}^{-1}$ with realization $\mathcal{T}_{ss}^{-1}$, as in* (215)*.*

Proof. We shall derive the proof considering only the first 4 Markov parameters, but it is readily extendable to larger matrices. First, recall one of the many matrix inversion lemma:

$$\begin{bmatrix} X & Y \\ W & Z \end{bmatrix}^{-1} = \begin{bmatrix} X^{-1} + X^{-1}Y(Z - WX^{-1}Y)^{-1}WX^{-1} & -X^{-1}Y(Z - WX^{-1}Y)^{-1} \\ -(Z - WX^{-1}Y)^{-1}WX^{-1} & (Z - WX^{-1}Y)^{-1} \end{bmatrix}, \tag{216}$$

and let $\mathbf{S}_m$ be given by

$$\mathbf{S}_m = \left[\begin{array}{cc|cc} D & 0 & 0 & 0 \\ CB & D & 0 & 0 \\ \hline CAB & CB & D & 0 \\ CA^2B & CAB & CB & D \end{array}\right]. \tag{217}$$

Evaluating (216) with $X = Z$ and $Y = 0$ yields

$$\begin{bmatrix} X & Y \\ W & Z \end{bmatrix}^{-1} = \begin{bmatrix} Z^{-1} & 0 \\ -Z^{-1}WZ^{-1} & Z^{-1} \end{bmatrix}. \tag{218}$$

Finally, applying (218) to (217), where $Z^{-1} = \begin{bmatrix} D^{-1} & 0 \\ -D^{-1}CBD^{-1} & D^{-1} \end{bmatrix}$ yields

$$\mathbf{S}_m^{-1} = \left[\begin{array}{cc|cc} \bar{M}_0 & 0 & 0 & 0 \\ \bar{M}_1 & \bar{M}_0 & 0 & 0 \\ \hline \bar{M}_2 & \bar{M}_1 & \bar{M}_0 & 0 \\ \bar{M}_3 & \bar{M}_2 & \bar{M}_1 & \bar{M}_0 \end{array}\right], \tag{219}$$

where $\bar{M}_0 = D^{-1}$, $\bar{M}_1 = -D^{-1}CBD^{-1}$, $\bar{M}_2 = -D^{-1}CABD^{-1} + D^{-1}CBD^{-1}CBD^{-1}$ and $\bar{M}_3 = -D^{-1}CA^2BD^{-1} + D^{-1}CABD^{-1}CBD^{-1} + D^{-1}CBD^{-1}CABD^{-1} - D^{-1}CBD^{-1}CBD^{-1}CBD^{-1}$. The proof is completed by simply expanding the Markov parameters of representation (215) and by noting the recurrence formula

$$\bar{M}_k = -\sum_{i=1}^{k} \bar{M}_{k-i} M_i \bar{M}_0, \quad k = 1, 2, \ldots \text{ and } \bar{M}_0 = D^{-1}.$$

$\diamond$

We have provided an algorithm to estimate a Toeplitz matrix of the Markov parameters in Section 4.2. In one hand, there we assumed the state matrix A to be stable, as open-loop experiments were considered. This assumption is also a sufficient condition for the convergence of the estimation algorithm itself. On the other hand, here we want to establish stability of a given realization. Since $\mathcal{T}$ is stable and bi-proper by construction, one can apply the provided algorithm to the mapping $r(t) \mapsto z(t)$ and use $\mathbf{S}_m^{-1}$ to obtain the Markov parameters of $\mathcal{T}^{-1}$.

Also, recall that one needs only to establish if the $\mathcal{H}_\infty$-norm of $\mathcal{T}^{-1}$ is bounded, so the best approach here is, for increasing values of N_m, observe the curve $i \times \bar{\sigma}_i(\mathbf{S}_m^{-1}), i = 1, 2, \ldots, N_m$ and check for convergence. Moreover, notice that the Markov parameters themselves provide information about stability characteristics of a system, and they are a byproduct of the estimation procedure. In the SISO case, these parameters correspond to the system's impulse response and if they vanish for $N_m \to \infty$, then the impulse response is absolutely summable, thus the system is BIBO-stable. In the MIMO case, if every entry in the impulse response matrix is absolutely summable, then the system is BIBO-stable (CHEN, 1999).

With all that in mind, let us summarize the certification and performance assessment procedures.

Certification procedure

1. Perform a sufficient large and rich experiment, whether in open loop or in closed loop with controller C_0, as in Figure 3. Collect data $\{u(t), y(t)\}$ (open-loop) or $\{r(t), y(t)\}$ (closed-loop).

2. Compute the normalized left coprime factors $[U_0\ V_0]$ and $[U_1\ V_1]$ of controllers C_0 and C_1, respectively.

3. Compute the signal $z(t) = V_1 u(t) + U_1 y(t)$ (open-loop) or $z(t) = V_1 V_0^{-1} r(t) + (U_1 U_0^{-1} - V_1 V_0^{-1}) y(t)$ (closed-loop).

4. For increasing values of N_m, determine $\widehat{\mathbf{S}}_m$ with (155) and compute $\bar{\sigma}(\widehat{\mathbf{S}}_m^{-1})$.

5. Observe concurrently whether $\bar{\sigma}(\widehat{\mathbf{S}}_m^{-1})$ converges and if each sequence in $\bar{M}_i$ decreases and is bounded. In this case, C_1 is **certified**; otherwise, C_1 is **falsified**.

Note that *only one experiment* is needed with our approach as signal $z(t)$ is obtained filtering data with $[V_0\ U_0]$ and $[V_1\ U_1]$ (in fact, one can test as many controllers C_1 as necessary). Also, we shall formalize the characteristics of the input signal of the first step of the procedure after Example 5.4.1, as this is the most crucial choice to be made with our methodology.

In case controller C_1 is certified, then using the same batch of data, follow the performance assessment procedure.

Performance assessment procedure

1. If data were obtained in open loop, then for increasing values of N_m, determine $\bar{\sigma}(\widehat{\mathbf{S}}_m)$ using algorithm (155) with $r(t) = z(t)$ and $z(t) = [y(t) \;\; u(t)]^T$. This will provide an estimate of b_{G_0,C_1}.

2. If data were obtained in closed loop, then

   (a) for increasing values of N_m, determine $\bar{\sigma}(\widehat{\mathbf{S}}_m)$ using algorithm (155) with $r(t) = r(t)$ and $z(t) = [\bar{y}(t) \;\; \bar{u}(t)]^T$. This will provide an estimate of b_{G_0,C_0}.

   (b) for increasing values of N_m, determine $\bar{\sigma}(\widehat{\mathbf{S}}_m)$ using algorithm (155) with $r(t) = z(t)$ and $z(t) = [\bar{y}(t) \;\; \bar{u}(t)]^T$. This will provide an estimate of b_{G_0,C_1}.

   (c) If $b_{G_0,C_1} > b_{G_0,C_0}$, then controller C_1 provides better stability robustness.

5.4 Illustrative examples

In this section we provide three simulation case studies and an experimental validation. The first case study involves a simple SISO plant and will be extensively worked around in order to illustrate all properties of the proposed approach; a comparison with a parametric system identification approach is also provided. The second example considers a non-minimum phase MIMO system, to show that our approach also works with more complex systems and that it also outperforms the parametric approach. The case of continuous-time controller implementation is considered in the third example. We then present a practical application in a three-tank pilot plant.

5.4.1 A SISO plant

Consider a SISO plant whose model is given by

$$G_0(q) = \frac{0.5}{q - 0.9} \tag{220}$$

which operates in closed loop with controller

$$C_0(q) = \frac{0.2(q - 0.8)}{q - 1}, \tag{221}$$

as in Figure 24, where we consider $d(t) = 0$. Since this is a simulation example, the model is available in our study, so we compute the correct value of the generalized stability margin for comparison purposes, for which $b_{G_0,C_0} = 0.323$ is obtained.

Consider also the following two candidate controllers to be put in place of $C_0(q)$:

$$C_1(q) = \frac{0.3(q - 0.9)}{q - 1}, \tag{222}$$

$$C_2(q) = \frac{4.1(q - 0.9)}{q - 1}, \tag{223}$$

for which it can be easily determined that $\delta_\nu(C_0, C_1) = 0.148 < b_{G_0,C_0}$ and $\delta_\nu(C_0, C_2) = 0.907 > b_{G_0,C_0}$, so controller $C_1(q)$ is *certified* via Vinnicombe's constraint (195), whereas $C_2(q)$ is *falsified*. However, in a more practical situation the model is not available, neither is the initial generalized stability margin, so constraint (195) can not be readily verified.

In order to establish with our data-driven approach whether or not these controllers stabilize the plant in closed loop, we collect data from the following closed-loop experiment: we set the reference $r(t)$ as a PRBS with amplitude ± 4, length 1120 and clock period 20 samples. For each value of N_m we used the maximum L possible (i.e., all data available) as long as the number of columns of $\mathbf{\Phi}$ in (154) is at least four times the number of rows. Thus, in order to use all data available, we can determine a total of $N_m = 80$ Markov parameters.

Simulations were performed both in the noise-free case and in the case were $v(t)$ in Figure 24 is a white Gaussian noise such that the SNR at the output is 20 dB. The evolution of the estimator for increasing values of N_m is shown in Figure 28 for both controllers and for the cases with and without noise, whereas Figure 29 shows the Markov parameters obtained in the final iteration (that is, for $N_m = 80$) for the same cases.

Figure 28 – $\mathcal{H}_\infty$-norm estimates with increasing N_m for the plant (220) with initial controller (221) and candidate controllers (222) and (223).

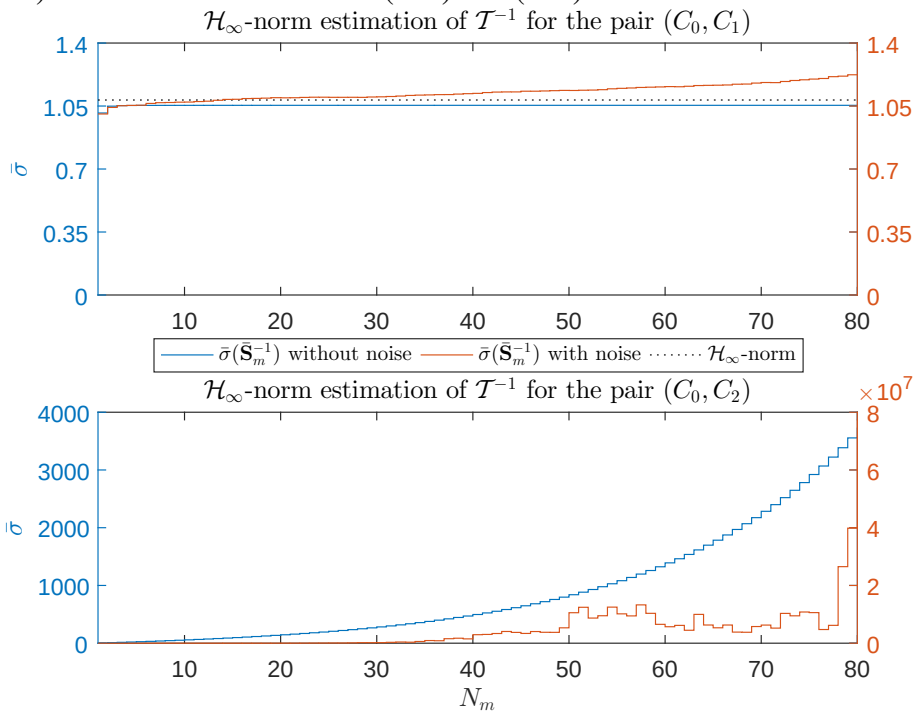

Source: author.

It is clear that for the pair $(C_0(q), C_1(q))$ the $\mathcal{H}_\infty$-norm of $\mathcal{T}^{-1}$ is limited, whereas for the pair $(C_0(q), C_2(q))$ it diverges, so controller $C_1(q)$ is certified and controller $C_2(q)$ is falsified. The same conclusions can be extracted from the estimated Markov parameters in Figure 29, for both noisy and noise-free cases. It is easy to verify, using the plant's

Figure 29 – Final ($N_m = 80$) estimates of the Markov parameters for the candidate controllers (222) and (223).

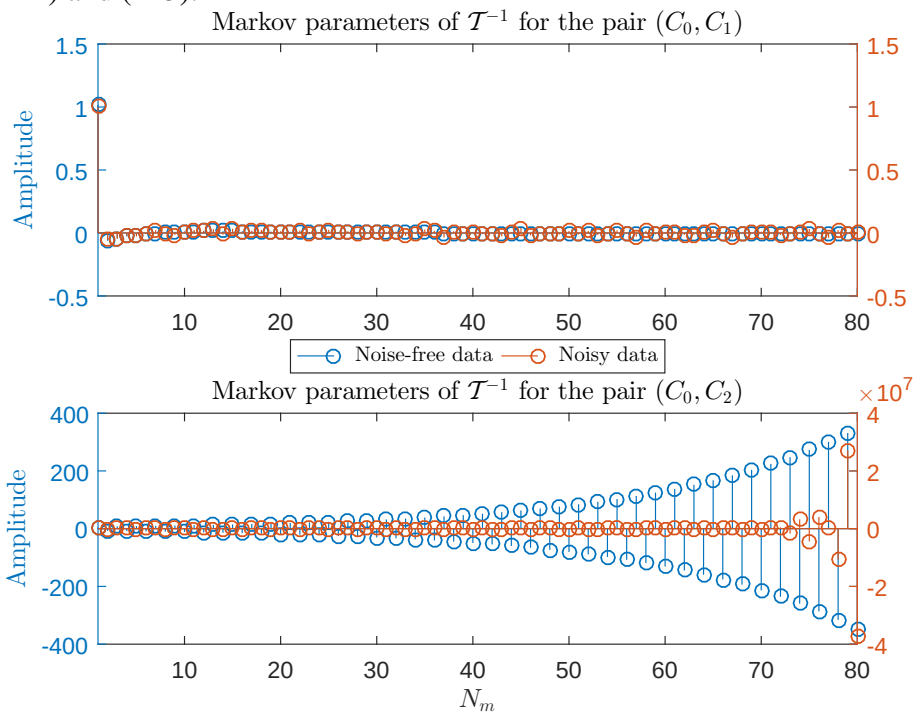

Source: author.

model, that these conclusions are both correct, that is, controller $C_2(q)$ indeed yields an unstable closed loop and controller $C_1(q)$ a stable closed loop.

Consider now an additional candidate controller:

$$C_3(q) = \frac{3.8(q - 0.9)}{q - 1}. \tag{224}$$

This controller actually yields a stable closed loop, but it is falsified under Vinnicombe's constraint because $\delta_\nu(C_0, C_3) = 0.901$. In fact, for the controller structure $C(q, k) = \frac{k(q-0.9)}{q-1}$, Vinnicombe's criterion is verified only for $k \in [0.21, 0.58]$.

We will illustrate, by means of this particular controller candidate, how the quality of the experimental data influences the conservativeness of our certification procedure. We vary the quality of the data by varying the clock period for the PRBS signal and the data length available. The results are given in the following order:

1. we apply the certification procedure for $C_3(q)$ with the same closed-loop data obtained previously;

2. we increase ten times the reference signal length and perform another experiment;

3. we reduce the clock period to 1 but keep the longer reference signal with length 11200 samples.

All tests were performed considering noisy data.

Figure 30 shows the estimated $\mathcal{H}_\infty$-norm for each change in the reference signal whereas Figure 31 shows the corresponding estimated Markov parameters in each case.

Figure 30 – $\mathcal{H}_\infty$-norm estimates with increasing N_m for the plant (220) with initial controller (221) and candidate controller (224) for three different reference signals.

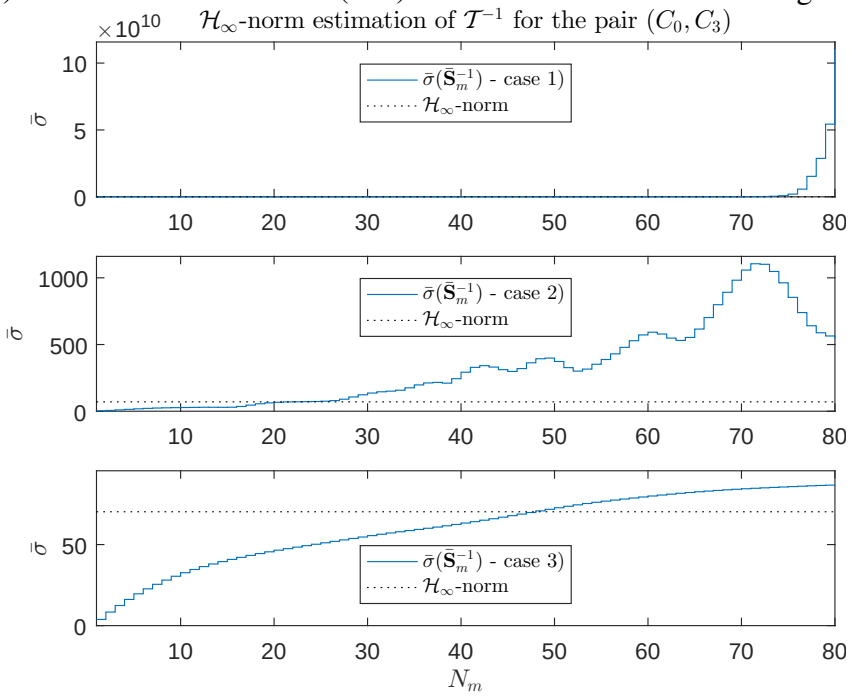

Source: author.

Figure 31 – Final ($N_m = 80$) estimates of the Markov parameters for the candidate controller (224) for each case.

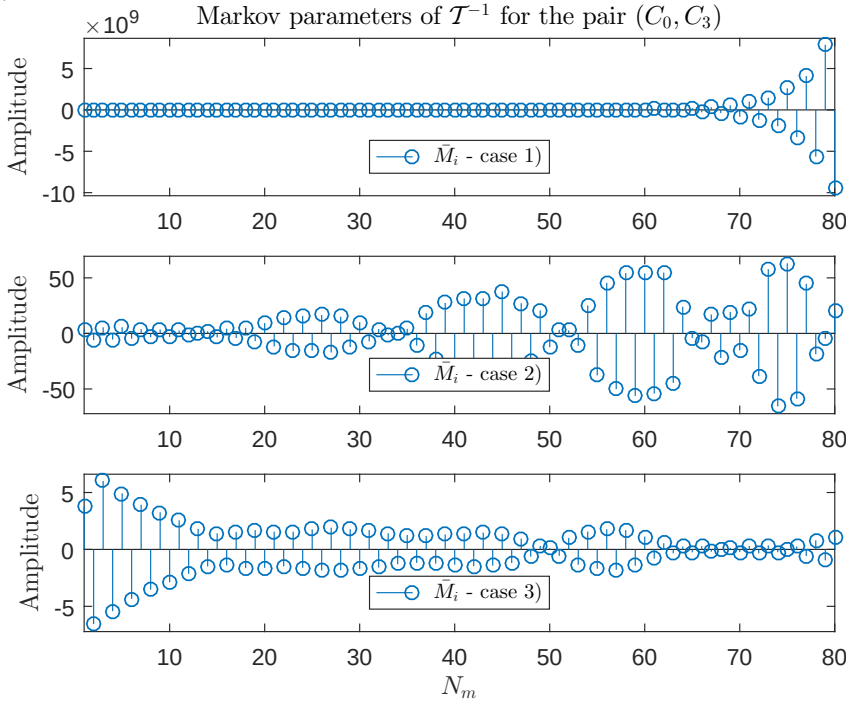

Source: author.

We see that from the first and second experiments controller $C_3(q)$ is falsified, as neither the estimated $\mathcal{H}_\infty$-norm nor the Markov parameters converge. However, with data from the third experiment, controller $C_3(q)$ is certified, as the estimated $\mathcal{H}_\infty$-norm presents convergence (even though to a value above its actual norm) and the Markov parameters initially decrease and stay bounded. For this controller, which is very distant (in the ν-gap sense) from the original controller, a quite rich data set is necessary to solve correctly the certification problem. This is a generic property of the certification problem, that is, the more distant the new controller is from the original one, the more data are necessary to certify or falsify it correctly.

Since a data set is available, one may ask oneself why is a dedicated procedure even necessary; that is, why not use this data to simply identify a parametrized model of $G_0(q)$ and then compute the poles of the corresponding closed-loop transfer function? In the sequel we explore this possibility, and show that this model-based approach is, when fed with the data, outperformed by ours.

5.4.1.1 Comparison with system identification

In what follows we will investigate a model-based approach to try to certify controllers $C_1(q)$ and $C_2(q)$ via parametric identification of the system transfer function $G_0(q)$, i.e., we shall estimate the parameter vector $\theta = [\theta_0 \;\; \theta_1]^T$ of

$$G(q,\theta) = \frac{\theta_0 q^{-1}}{1+\theta_1 q^{-1}}. \tag{225}$$

and then determine the poles of the closed-loop transfer function $\frac{C_i(z)G(q,\theta)}{1+C_i(z)G(q,\theta)}$.

Identification of (225) will be carried out using Output-Error (OE) algorithms (LJUNG, 1999) from MATLAB System Identification Toolbox, that is, prior to any knowledge of the actual noise model, we fix the identification structure as an OE. We compare the Markov parameters approach (computing 80 parameters) with the system identification approach in the following cases. We set a general noise model (i.e, $v(t) = H_0(q)w(t)$, where $w(t)$ is white Gaussian noise), such that the pair $(G_0(q), H_0(q))$ represents a Box-Jenkins (BJ) system with $H_0(q) = \frac{q-0.2}{q-0.8}$, and apply three different inputs signals: PRBS with clock period 1, white Gaussian noise and a sequence of steps. For each case the SNR at the output $y(t)$ is between $12 \sim 16$ dB.

A set of 100 Monte Carlo experiments for each controller in each case was conducted. Due to the amount of certification tests to be performed (a total of 600), we also established a numerical convergence criterion of the Markov parameters *au lieu* of a visual evaluation as follows. We compute a windowed variance of the Markov parameters and then take the average value of the final windows. If this value is less than a specified value, then the controller is certified. In other words, the controller is certified if

$$\frac{1}{3n}\sum_{j=N_m-3n}^{N_m}\left(\frac{1}{n-1}\sum_{i=j}^{n-1+j}(M_i - M_{av})^2\right) \leq \varepsilon, \tag{226}$$

where M_{av} is the average of the respective window and for which we have used $n = 15$ and $\varepsilon = 7.5 \times 10^{-3}$.

Table 3 shows the results of 100 Monte Carlo experiments for each controller in each case. The numbers represent the amount of times the result were correct, i.e., when controller $C_1(q)$ was certified and when controller $C_2(q)$ was falsified.

Table 3 – Results with Markov parameters and system identification for a BJ system structure.

Method/ Input	Markov Param.		System Id.	
	$C_1(q)$	$C_2(q)$	$C_1(q)$	$C_2(q)$
PRBS	100	100	100	60
WN	100	100	100	58
STEPS	100	100	100	0

On one hand, results with both Markov parameters and system identification approaches certified controller $C_1(q)$ all the times. On the other hand, while the proposed methodology was able to always falsify controller $C_2(q)$, the identification procedure yielded many *false positives* – that is, it would recommend to put the destabilizing controller $C_2(q)$ in the loop in most cases!

5.4.1.2 Performance assessment: b_{G_0,C_i} estimation

Once controller $C_1(q)$ has been certified, we can now proceed to the performance assessment via b_{G_0,C_1} before inserting it in the loop, and compare it with the operating controller (221). We shall use data from one of the PRBS experiments in order to compute the largest singular value of the matrix $\mathbf{S}_m$ for the mappings $r(t) \mapsto [\bar{y}(t) \;\; \bar{u}(t)]^T$ and $z(t) \mapsto [\bar{y}(t) \;\; \bar{u}(t)]^T$. Figure 32 portrays the estimation for both cases.

Figure 32 – $\mathcal{H}_\infty$-norm estimates of b_{G_0,C_0} and b_{G_0,C_1} with increasing N_m for the plant (220) with initial controller (221) and candidate controller (222).

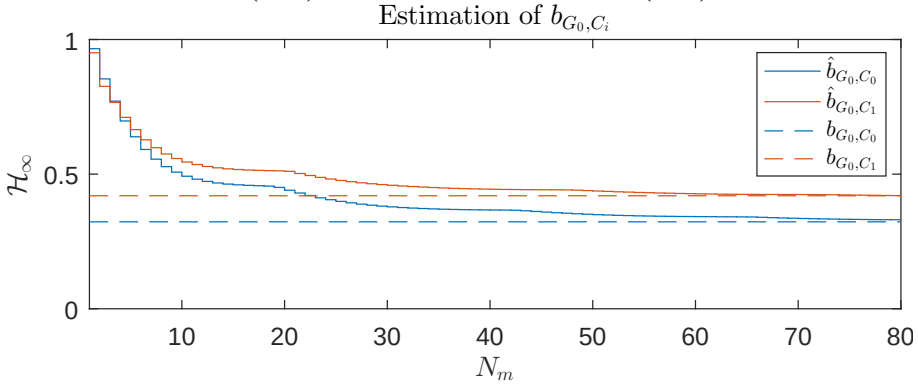

Source: author.

From the estimated b_{G_0,C_i}, we see that controller $C_1(q)$ provides better robust stability than initial controller $C_0(q)$ and should be put in closed loop.

5.4.2 Non-minimum phase multivariable system

In this section we treat a more complex system and compare the proposed certification procedure against the identification approach. We also use this example to illustrate the open-loop case.

Consider again the (by now famous) NMP system (111) of Subsection 3.4.1, which was put in closed loop with an initial stabilizing controller (113). We consider the certification of two controllers tuned in that Subsection, namely controller (115) and controller (112) – herein called $C_1(q)$ and $C_2(q)$, respectively –, and repeated here for convenience:

$$C_1(q) = \begin{bmatrix} \dfrac{0.4057(q-0.7139)(q-0.9168)}{q(q-1)} & \dfrac{-0.5166(q-0.6879)(q-0.922)}{q(q-1)} \\ \dfrac{-0.3166(q-0.6876)(q-0.9205)}{q(q-1)} & \dfrac{0.2805(q-0.6451)(q-0.797)}{q(q-1)} \end{bmatrix},$$

$$C_2(q) = \begin{bmatrix} \dfrac{0.234(q+0.2037)(q-0.9073)}{q(q-1)} & \dfrac{-0.1911(q+0.2666)(q-0.8616)}{q(q-1)} \\ \dfrac{-0.195(q+0.2037)(q-0.9073)}{q(q-1)} & \dfrac{0.2926(q+0.1493)(q-0.8377)}{q(q-1)} \end{bmatrix}.$$

For these controllers we have $\delta_\nu(C_0, C_1) = 0.8974$ and $\delta_\nu(C_0, C_2) = 0.8972$. Notice that both controllers are far from the initial controller $C_0(q)$, and very far from being certified through Vinnicombe's condition (195), as $b_{G_0,C_0} = 0.1037$. Also notice that $C_1(q)$ has also an NMP transmission zero at $q = 1.2672$. Controller $C_1(q)$ stabilizes the plant, whereas controller $C_2(q)$ does not.

In order to compare the proposed methodology with the system identification approach and certify –or falsify –these controllers, we set a batch of Monte-Carlo experiments in different scenarios, just as we showed in the SISO case. We also incorporated system structures OE and ARMAX. For the noise models, we have used

$$H_0(q) = I \qquad \text{for OE;}$$

$$H_0(q) = \begin{bmatrix} \dfrac{(q-0.5)(q-0.7)}{(q-0.8)(q-0.9)} & \dfrac{0.1(q-0.2)}{(q-0.8)(q-0.9)} \\ \dfrac{0.1(q-0.4)}{(q-0.8)(q-0.9)} & \dfrac{(q-0.4)(q-0.6)}{(q-0.8)(q-0.9)} \end{bmatrix} \qquad \text{for ARMAX;}$$

$$H_0(q) = \frac{q-0.2}{q-0.6} I \qquad \text{for BJ.}$$

Reference signals were set with length 5600 samples and for each case the SNR at the output $y(t)$ was approximately 20 dB. For the identification (using OE algorithm) we

selected a structure for $G(q,\theta)$ such that $G(q,\theta^*) = G_0(q)$ and for the Markov approach we estimated 90 parameters and used criterion (226) for each of the four sequences of the Markov parameters.

Tables 4 and 5 show the results of 100 Monte Carlo experiments for each controller in each case. The numbers in these table represent the amount of times the result were correct, i.e., when controller $C_1(q)$ was certified and when controller $C_2(q)$ was falsified.

Table 4 – Results with Markov parameter approach and SNR$\approx 20\ dB$.

Noise/	OE		ARMAX		BJ	
Input	C_1	C_2	C_1	C_2	C_1	C_2
PRBS	100	100	100	100	100	100
WN	100	100	100	100	100	100
STEPS	100	100	100	100	100	100

Table 5 – Results with identification of $G_0(q)$ and computation of closed-loop transfer function with SNR$\approx 20\ dB$.

Noise/	OE		ARMAX		BJ	
Input	C_1	C_2	C_1	C_2	C_1	C_2
PRBS	97	83	89	94	96	94
WN	92	83	95	90	91	83
STEPS	100	100	97	100	93	96

Our methodology gets the correct answer in all cases, avoiding both false positives (which is the gravest of mistakes) and false negatives, regardless of the noise's model structure, whereas the model-based approach fails in a large number of cases, even providing many false positives. Still, it is to be expected that data sets with poor enough quality will cause any method to fail, so we have explored what noise level would lead our method to failure. As lower values of SNR were tried, we have found that the first wrong results appear for a SNR of 14 dB and only with the least rich of signals (a step), as can be seen in Tables 6 and 7, where the results obtained with SNR around 14 dB are presented.

Table 6 – Results with Markov parameter approach and SNR$\approx 14\ dB$.

Noise/	OE		ARMAX		BJ	
Input	C_1	C_2	C_1	C_2	C_1	C_2
PRBS	100	100	100	100	100	100
WN	100	100	100	100	100	100
STEPS	83	99	93	97	96	99

Table 7 – Results with identification of $G_0(q)$ and computation of closed-loop transfer function with SNR$\approx 14\ dB$.

Noise/	OE		ARMAX		BJ	
Input	C_1	C_2	C_1	C_2	C_1	C_2
PRBS	95	80	86	90	93	88
WN	86	77	91	89	73	89
STEPS	100	90	88	100	95	96

5.4.2.1 The open-loop case

We consider now the case of certification of controllers $C_1(q)$ and $C_2(q)$ when data is acquired in open loop. In this case, we set the input $u(t)$ as a PRBS with amplitude ± 1 and clock period 1. The output is corrupted by white Gaussian noise such that SNR $= 15$ dB.

Figures 33 and 34 show, respectively, the estimation of the $\mathcal{H}_\infty$-norm of W_1 for each controller and the estimated sequence of Markov parameters. It is clear that the results are concordant with the closed-loop case, i.e., controller $C_1(q)$ will stabilize the plant whereas controller $C_2(q)$ will not.

Figure 33 – $\mathcal{H}_\infty$-norm estimates with increasing N_m for the plant (111) and candidate controllers (115) and (112).

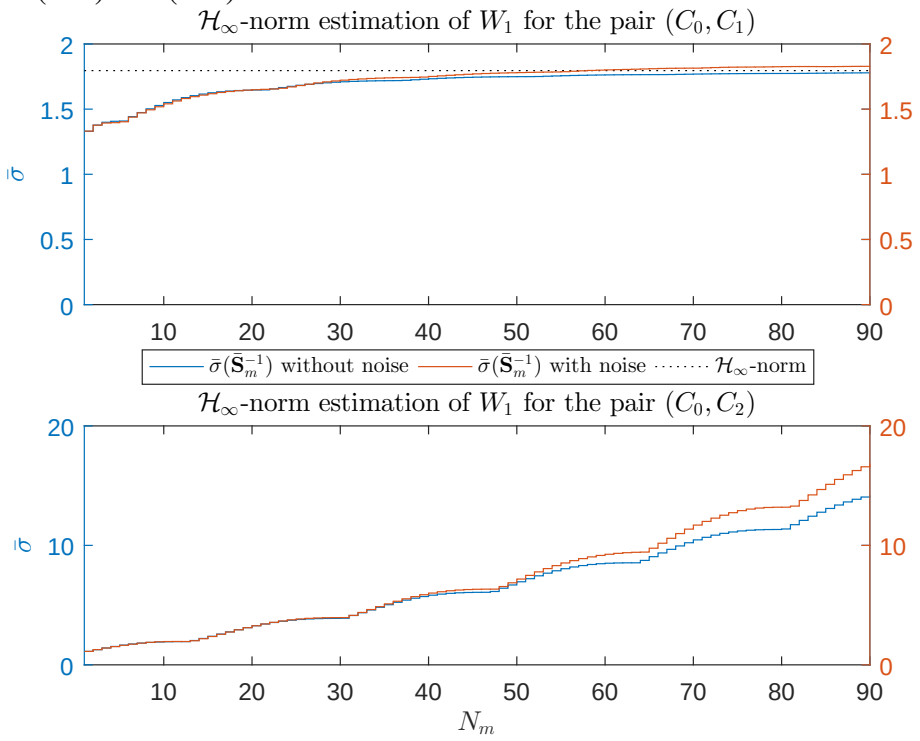

Source: author.

Figure 34 – Estimated Markov parameters at the last iteration for the candidate controllers (115) and (112).

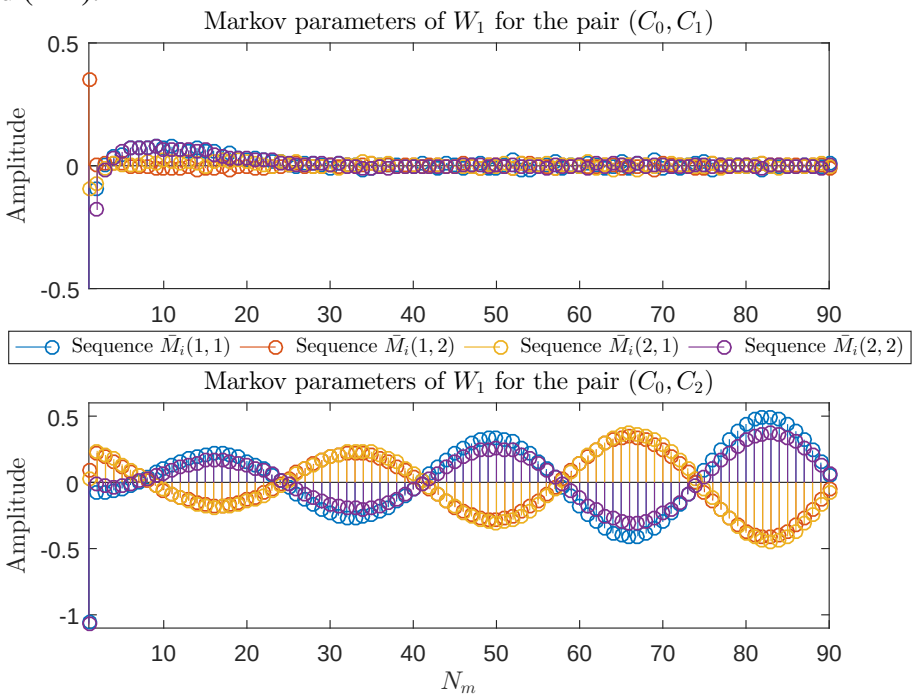

Source: author.

5.4.3 A continuous-time example

Consider a SISO plant whose continuous time model is given by

$$G_0(s) = \frac{4}{s^2 + 5s + 6} \tag{227}$$

which operates in closed loop with controller

$$C_0(s) = \frac{0.3(s+4)}{s}, \tag{228}$$

and the generalized stability margin is $b_{G_0,C_0} = 0.4786$.

Consider also the following two candidate controllers to be put in place of $C_0(s)$:

$$C_1(s) = \frac{(s+5)}{s}, \qquad C_2(s) = \frac{10(s+6)}{s}, \tag{229}$$

where $\delta_\nu(C_0, C_1) = 0.5947$ and $\delta_\nu(C_0, C_2) = 0.9245$, so none of these controllers can be certified via Vinnicombe's constraint (195).

We set a closed-loop experiment just like in Example 5.4.1, only adjusting the PRBS clock period to 1 sample, as one of the controllers to be tested is far from the initial controller (see the discussion right before Subsection 5.4.1.1). Output data is sampled with $T_s = 0.1$ s and the control input considers a Zero-Order-Holder (ZOH).

We then applied steps 2–4 of our procedure and obtained the estimates of $\|\mathcal{T}^{-1}\|_\infty$ for both controllers, as portrayed in Figure 35, and the corresponding Markov parameters,

Figure 35 – $\mathcal{H}_\infty$-norm estimates with increasing N_m for the plant (227) with initial controller (228) and candidate controllers in (229).

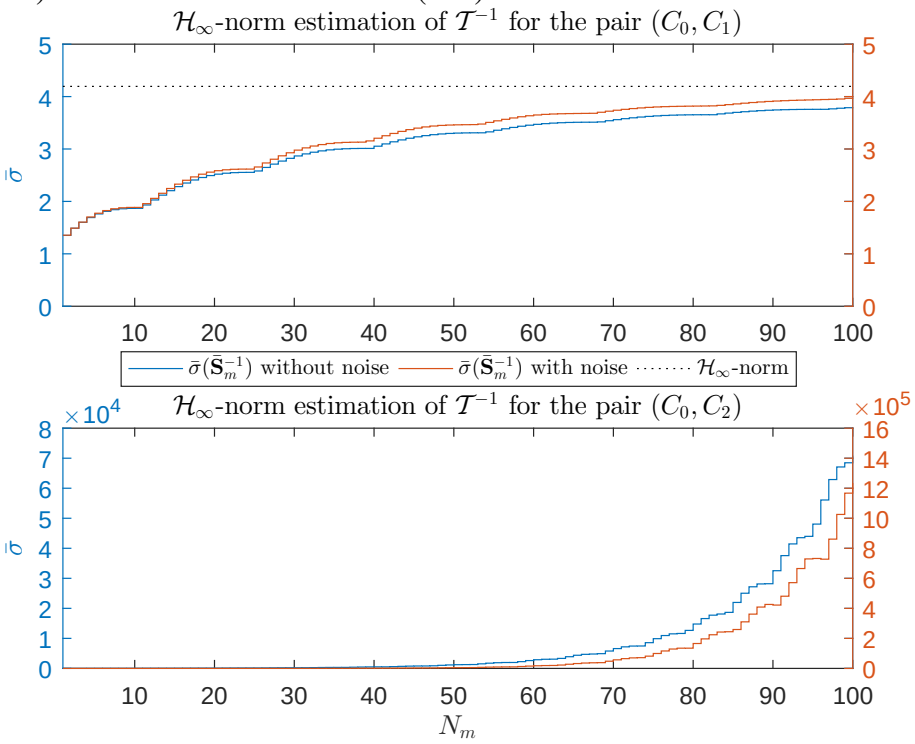

Source: author.

Figure 36 – Final ($N_m = 100$) estimates of the Markov parameters for the candidate controllers in (229).

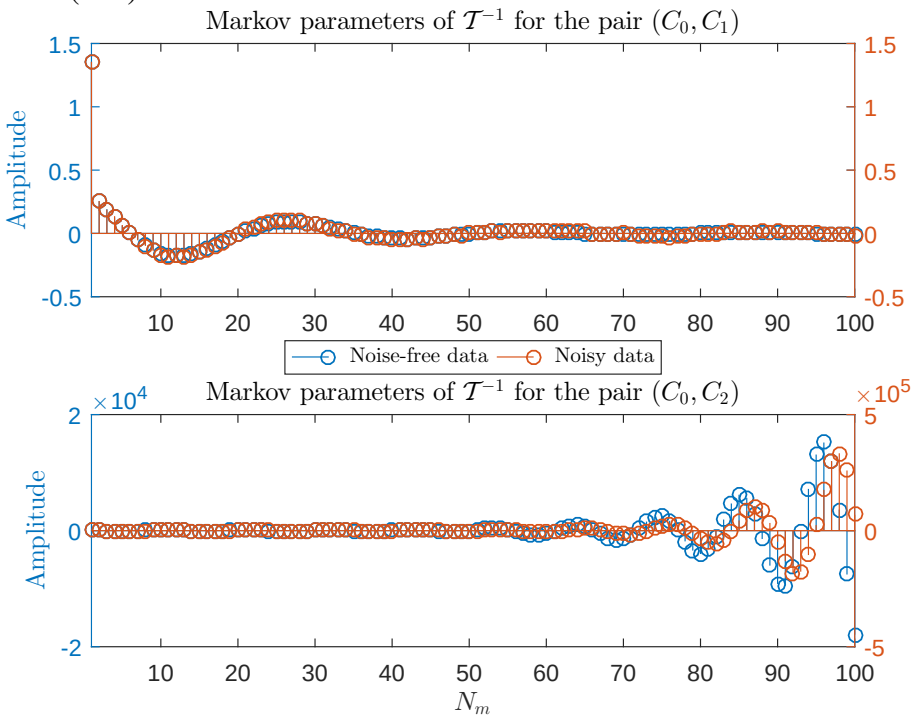

Source: author.

as portrayed in Figure 36. Notice that the referred $\mathcal{T}$ is not the continuous-time transfer function but a discretized version of it.

From these figures we can then certify controller $C_1(s)$, which was not possible with (195), and falsify controller $C_2(s)$, both of which provide the correct answer.

5.4.4 Three-tank pilot plant

Consider the following pilot plant, where the goal is to control the levels, measured in centimeters, of two tanks by the opening, measured in percentage, of two pneumatic valves in a three-tank plant. The schematic diagram in Figure 37 describes the process, which is built with of-the-shelf industrial equipment (pumps, valves, sensors and tanks). Tanks 1 and 2 have a capacity of 70 liters each, while tank 3 is a 250 liters container. The system's variables are sampled with a sampling period $T_s = 5$ s. The same plant has been studied in (CAMPESTRINI *et al.*, 2016) and (LORENZINI *et al.*, 2019).

Figure 37 – Three-tank level control plant schematic.

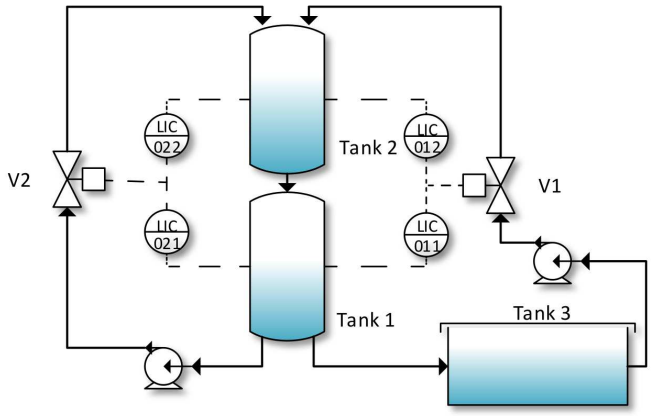

Source: author.

The plant operates with an initial stabilizing decentralized PI controller given by

$$C_0(q) = \begin{bmatrix} \dfrac{2.06(q-0.9636)}{(q-1)} & 0 \\ 0 & \dfrac{6.14(q-0.9712)}{(q-1)} \end{bmatrix}. \tag{230}$$

For this plant, we have two candidate controllers, given by

$$C_1(q) = \begin{bmatrix} \dfrac{5.025(q-0.977)}{(q-1)} & \dfrac{3.954(q-1.001)}{(q-1)} \\ \dfrac{-7.546(q-0.9796)}{(q-1)} & \dfrac{0.3024(q-0.6586)}{(q-1)} \end{bmatrix}, \tag{231}$$

$$C_2(q) = \begin{bmatrix} \dfrac{3(q-0.9612)}{(q-1)} & \dfrac{-4(q-0.9803)}{(q-1)} \\ \dfrac{-6(q-0.9612)}{(q-1)} & \dfrac{-0.1(q+1.413)}{(q-1)} \end{bmatrix}. \tag{232}$$

For these controllers we compute $\delta_\nu(C_0, C_1) = 0.4898$ and $\delta_\nu(C_0, C_2) = 0.5610$, thus both being moderately far from $C_0(q)$. We set a closed-loop experiment in order to collect data from the process, where the reference is a PRBS with clock period 7 samples and amplitude ± 4 cm for both loops. The experiment is portrayed in Figure 38.

Figure 38 – Closed-loop response of the pilot plant with controller (230) with a PRBS reference input.

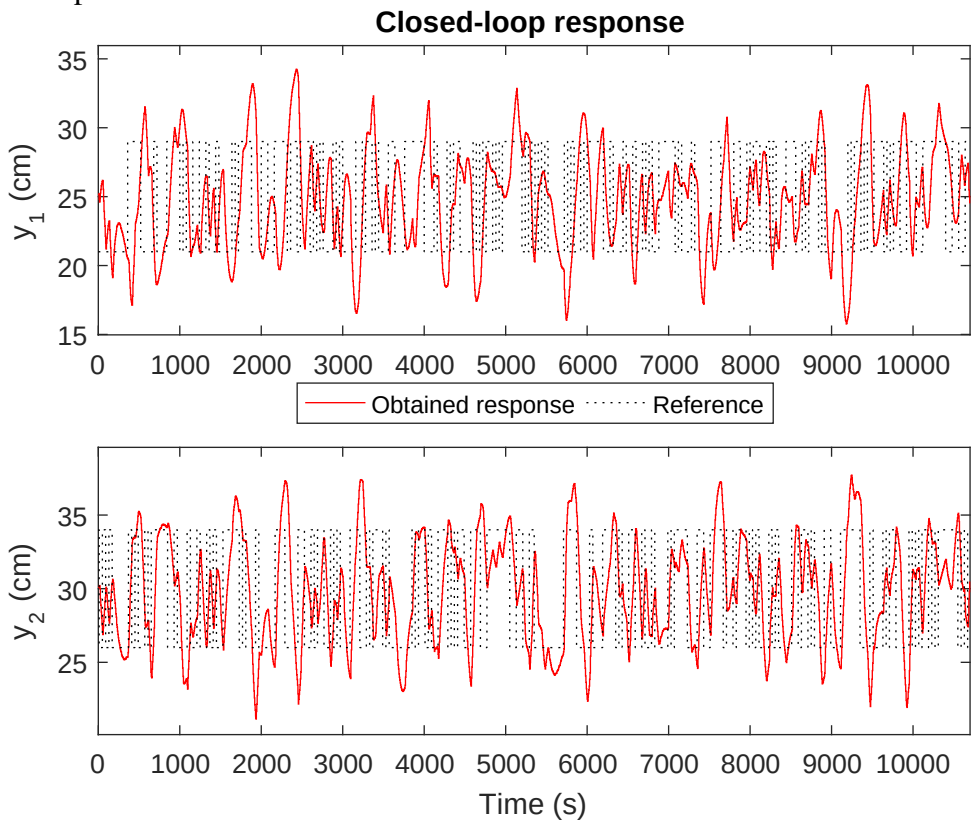

Source: author.

We then proceed with steps 3–5 of our proposed procedure. Figure 39 shows the evolution of the estimates of $\|\mathcal{T}^{-1}\|_\infty$ for both pairs $(C_0(q), C_1(q))$ and $(C_0(q), C_2(q))$, whereas Figure 40 shows the sequences of each Markov parameter at the last iteration.

It is clear from both figures that controller $C_2(q)$ will yield an unstable closed loop. For controller $C_1(q)$ we see in Figure 39 that the norm estimator presents an initial convergence and by the end it starts to increase, which is rather inconclusive, but then in Figure 40 we see that the estimated Markov parameters sequences decrease and converge, so we can confirm that $C_1(q)$ will stabilize the pilot plant. Since controller (231) was certified, we also estimate the respective b_{G_0,C_i}. The result is portrayed in Figure 41.

Figure 39 – $\mathcal{H}_\infty$-norm estimates with increasing N_m for the pilot plant with initial controller (230) and candidate controllers (231) and (232).

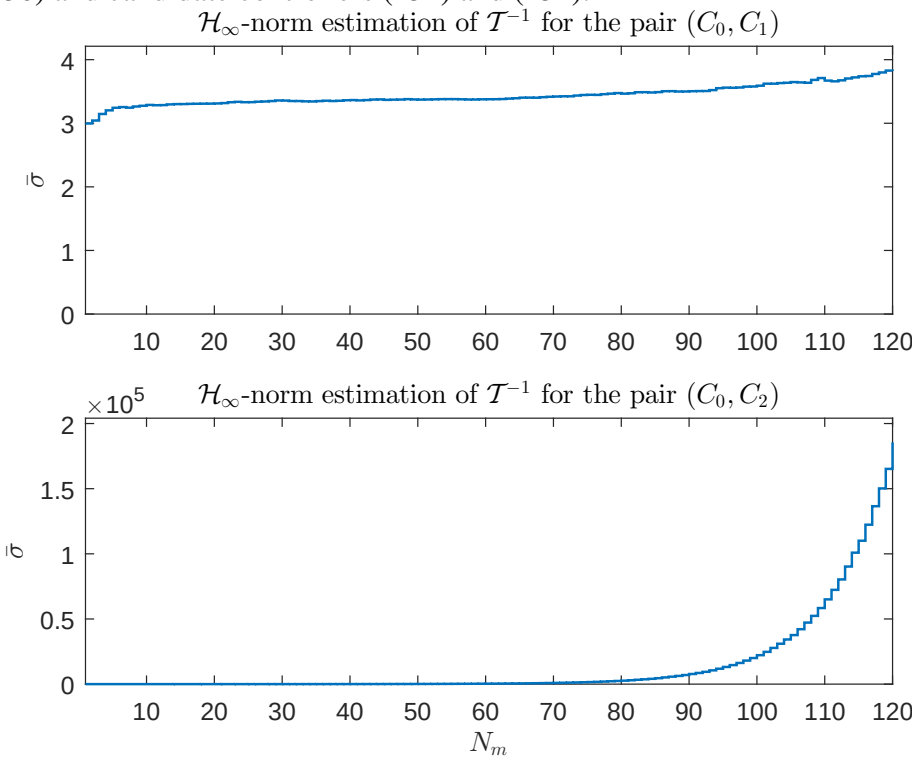

Source: author.

Figure 40 – Final ($N_m = 120$) estimates of the Markov parameters for the candidate controllers (231) and (232).

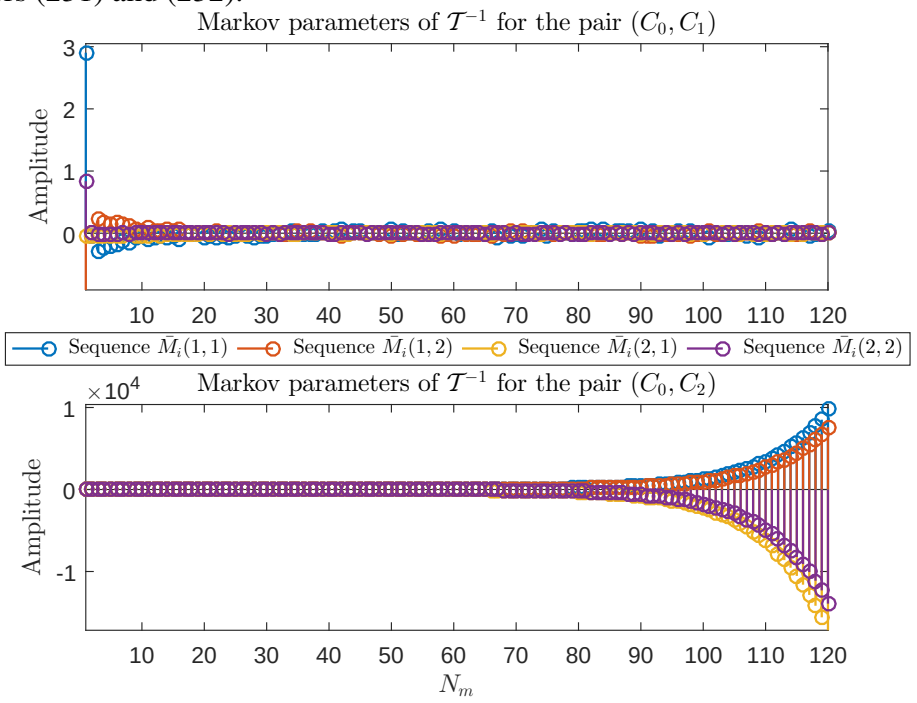

Source: author.

Figure 41 – $\mathcal{H}_\infty$-norm estimates of b_{G_0,C_0} and b_{G_0,C_1} with increasing N_m for the pilot plant with initial controller (230) and candidate controller (231).

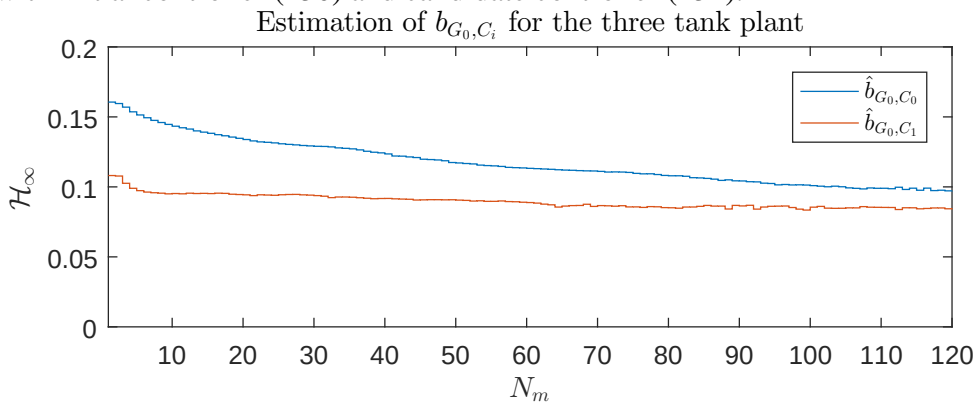

Source: author.

The estimated values of b_{G_0,C_0} and b_{G_0,C_1} tell us that controller $C_1(q)$ is a little less robust than controller $C_0(q)$, but tell us nothing about the transient response. Figure 42 shows the closed-loop behavior with controller $C_0(q)$ to a sequence of steps and Figure 43 the respective control effort.

Figure 42 – Closed-loop response of the pilot plant with controller (230) for a sequence of steps.

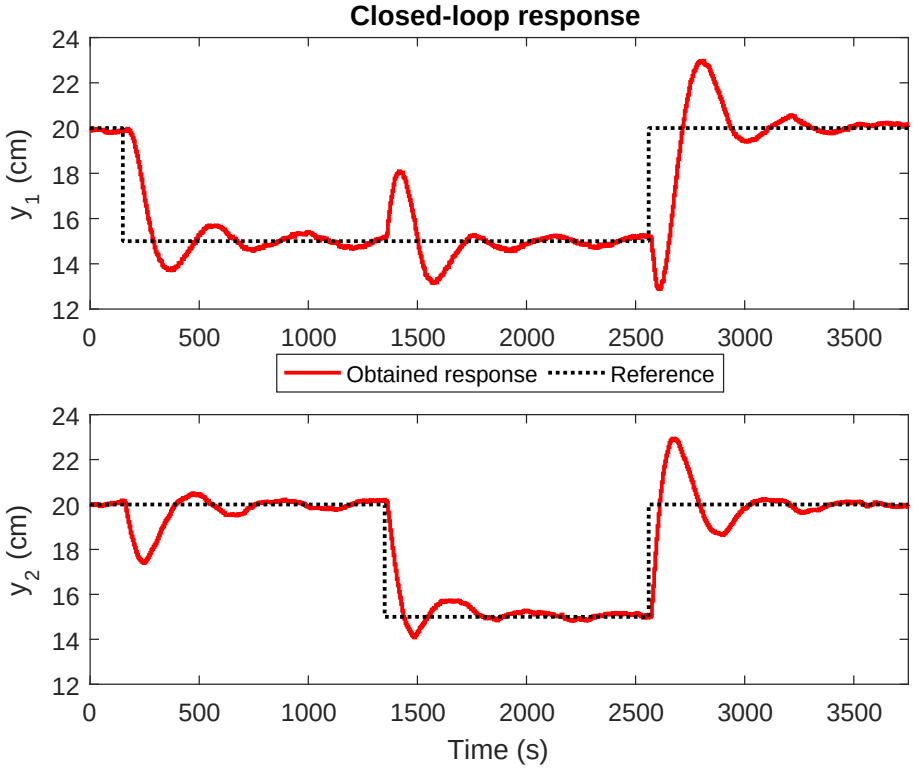

Source: author.

Figure 43 – Control signal of the closed-loop response of the pilot plant with controller (230) for a sequence of steps.

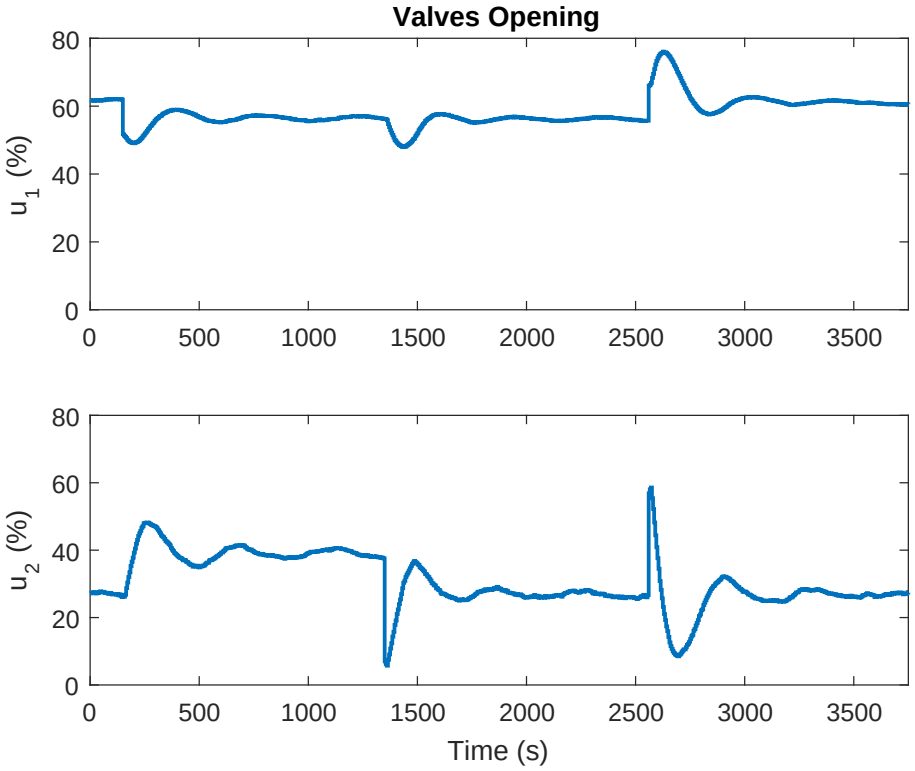

Source: author.

Figures 44 and 45 show the closed-loop behavior and the control effort, respectively, with controller $C_1(q)$ to a sequence of steps. We see that it indeed stabilizes the plant and also provides a faster transient response than that of $C_0(q)$, with almost no overshoot and only a small coupling between loops.

Controller $C_2(q)$ indeed yields an unstable closed loop as portrayed in Figure 46, in which the experiment starts in open loop and at 150 s the loop is closed and the reference for tank 1 is set to 15 cm.

5.5 Chapter conclusions

In this chapter we proposed a one-shot data-driven procedure to determine whether or not a new controller will yield a stable closed loop before inserting it in the actual loop – the so-called controller certification problem. The procedure consists essentially in finding whether a given transfer matrix $\mathcal{T}^{-1}$ is bounded or not.

Two variables play an important role in our proposed procedure: the choice of the input signal – $r(t)$ for a closed-loop test, and $u(t)$ for an open-loop test – and the number of Markov parameters to be estimated. In our examples we showed that Pseudo-Random Binary Signals (PRBS) and white-noise signals yield better results, regardless of the noise model. Also, in Example 5.4.1 we showed that the quality of the data is critical when the

Figure 44 – Closed-loop response of the pilot plant with controller (231) for a sequence of steps.

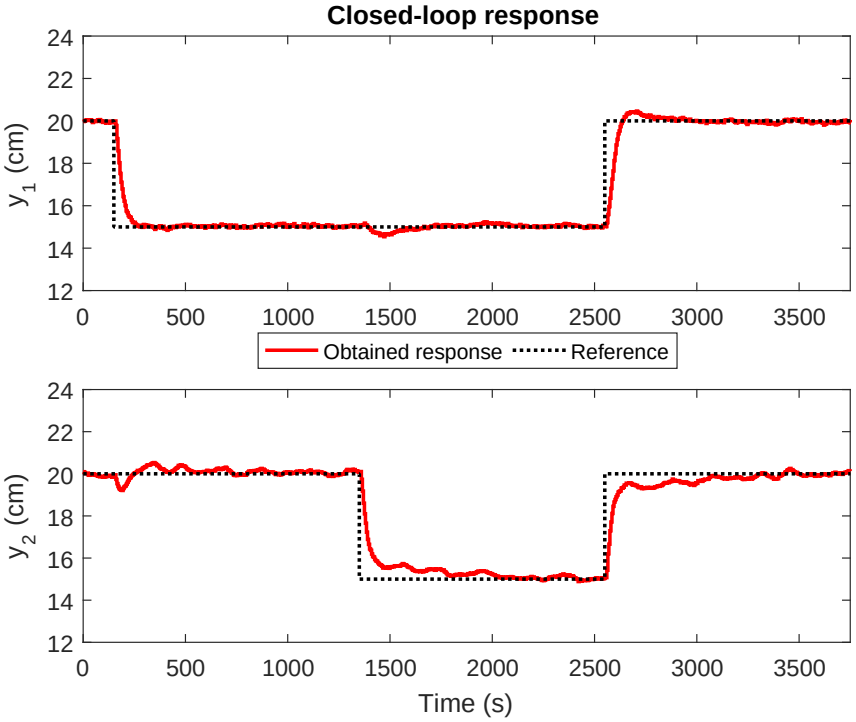

Source: author.

Figure 45 – Control signal of the closed-loop response of the pilot plant with controller (231) for a sequence of steps.

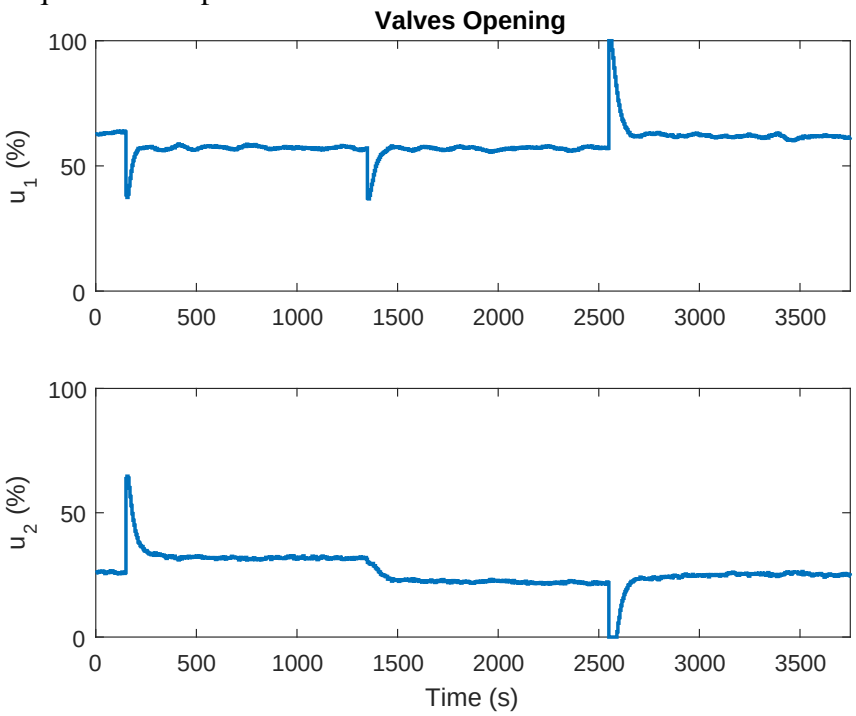

Source: author.

Figure 46 – Closed-loop response of the pilot plant with controller (232), which starts operating at 150 s, when the reference for loop 1 is changed to 15 cm.

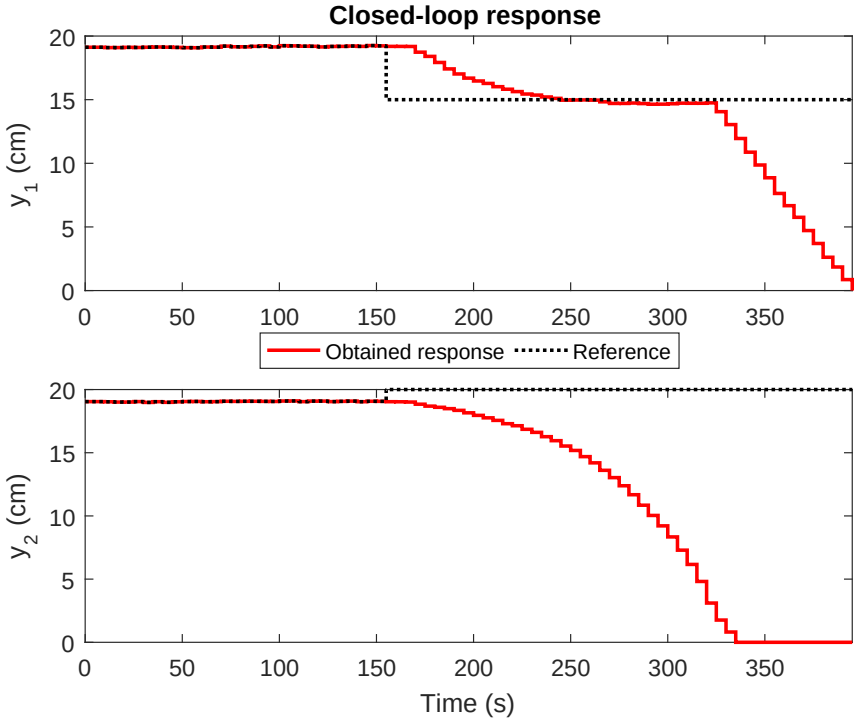

Source: author.

Figure 47 – Control signal of the closed-loop response of the pilot plant with controller (232) for a sequence of steps.

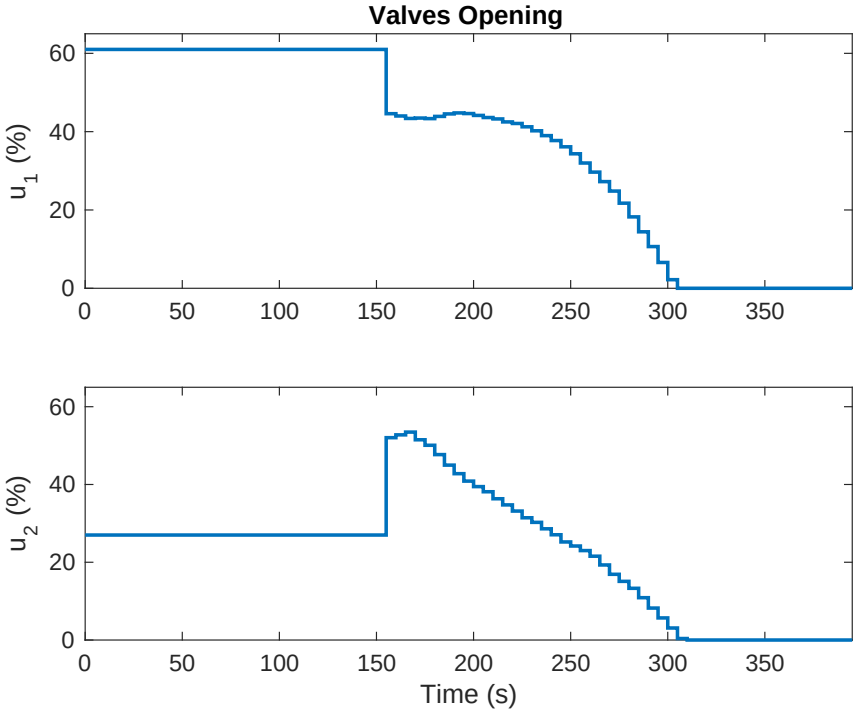

Source: author.

tested controller C_1 is far away (in a ν-gap sense) from the initial controller C_0. On the other hand, even a step input provides good results when the SNR at the output is not too low and for mild distances between the initial and tested controllers. We have also showed that our methodology outperforms the system identification approach, and false positives are often avoided.

Moreover, using other mappings between signals, but with the same estimation algorithm, we have also been able to infer about the performance of a given controller in a robust stability analysis. Nevertheless, this index may not be enough to infer about all properties of the closed-loop response. This was illustrated in our experimental example, where we not only obtained the right certification results, but we observed a better transient response of the new controller to the detriment of robust stability margin. It remains an open question to find another test, or mapping, so one can also evaluate some index related to transient response of this new controller prior to inserting it in the loop.

Even though there are many results in the literature, none can be used as a one-shot data-driven approach for the multivariable case. In this chapter we tried to build a unifying approach, that can be used for both SISO and MIMO systems, for data collected in open loop or closed loop, and even considering discrete and continuous-time system (for data sampled with a given period).

6 CONCLUSIONS

That's it, there's no way. It's over! Good luck.

Vanessa da Mata

In this work we addressed the multivariable Data-Driven control problem with focus on Non-Minimum Phase systems, where extensions to two one-shot data-driven methods were derived; a state-feedback approach, inserted in infinite horizon LQR control framework; and an approach to a one-shot data-driven controller certification and robust performance assessment, both with data from closed or open loop.

In the classical DD approach for the Model Reference control problem, the extensions of two methods with a *flexible criterion* allowed the identification and inclusion of the NMP transmission zero in the reference model along with the controller parameters with an iterative procedure of identification while keeping the methods "one-shot" characteristic. Each method's extension deals with a different structure of the reference model – VRFT with a diagonal one, OCI with a block triangular one –, both having advantages and drawbacks. For the VRFT, the drawback is to have the NMP effect spread through all outputs, but in this case only the zero location needs to be identified. For the OCI, one can move the NMP effect to a specified output, provided the zero location and the ratio between directions are identified; however, the choice of the reference model to cope with more than one NMP transmission zero is more involved.

On the other hand, the proposed DD infinite horizon LQR approach, which results in a static state-feedback gain, needs no modification to deal with NMP systems and can be directly applied as long as the system's states are measured. Critical issues in this case are the choice of the input for data acquisition – recall that the method identifies Markov parameters, which are related to the system impulse response – and, due to the framework from which the solution is derived, the choice of the weighting matrices Q and R.

Furthermore, we have proposed a pure one-shot Data-Driven approach to the controller certification problem, hoping to bring closure to a long-time issue in Data-Driven control methods: the stability guarantee. The procedure is based on a closed-loop configuration where the controller's coprime factorization is split into a feedback and a feedforward path, but we brought the relevant signals mappings into the standard closed-loop

configuration and also showed that similar mappings can be used when data are collected in open loop. This test has been show to be much less conservative than Vinnicombe's criterion and to outperform the system identification approach. Moreover, this approach comes with the bonus of being able to infer about the robust stability performance of a given controller as related to a given plant using the same batch of data.

Finally, it is important to remark the simpleness – algorithmically speaking – of the solutions proposed in this work, even for the more complex problem approached: the controller certification issue. At the expense of an elaborated theory behind it, we can say all problems studied have been solved via a least-squares algorithm, and by combining old and new results in control theory and system identification. Finding simple solutions has been the Ariadne's thread of the research, as we hope our methods to become easily understandable and applicable in practical situations. Simulation and experimental results showed the effectiveness of all the proposed methodologies, so the intended contributions have all been achieved.

As for future work, it remains to test the proposed methodologies against higher order systems and with large delays on the loop. Also, the synthesis of the state-feedback gain using other control designs such as mixed $\mathcal{H}_2/\mathcal{H}_\infty$ performance, pole placement and robust control via LMIs is another interesting subject to be studied. Finally, regarding controller certification, a formulation to test state-feedback gains seems also necessary.

REFERENCES

AANGENENT, W. *et al.* Data-based optimal control. *In*: AMERICAN CONTROL CONFERENCE, 2005, Portland, OR, USA. **Proceedings [...]** New York: IEEE, 2005. v. 2, p. 1460–1465.

BAZANELLA, A. S.; CAMPESTRINI, L.; ECKHARD, D. **Data-driven controller design**: the H2 approach. Netherlands: Springer Science & Business Media, 2011.

BAZANELLA, A. S. *et al.* Iterative minimization of control performance criteria. **Automatica**, Tarrytown, v. 44, n. 10, p. 2549 – 2559, 2008.

BOEIRA, E. *et al.* Comparing MIMO process control methods on a pilot plant. **Journal of Control, Automation and Electrical Systems**, London, v. 29, n. 4, p. 411–425, 2018.

CAMPESTRINI, L. *et al.* Virtual reference feedback tuning for non-minimum phase plants. **Automatica**, Tarrytown, v. 47, n. 8, p. 1778–1784, 2011.

CAMPESTRINI, L. *et al.* Unbiased MIMO VRFT with application to process control. **Journal of Process Control**, Tarrytown, v. 39, p. 35–49, 2016.

CAMPESTRINI, L. *et al.* Data-driven model reference control design by prediction error identification. **Journal of the Franklin Institute**, Tarrytown, v. 354, n. 6, p. 2628–2647, 2017.

CAMPI, M.; LECCHINI, A.; SAVARESI, S. Virtual reference feedback tuning: a direct method for the design of feedback controllers. **Automatica**, Tarrytown, v. 38, n. 8, p. 1337–1346, 2002.

CHA, S. H. *et al.* Verifying stabilizing controllers for performance improvement using closed-loop data. **International Journal of Adaptive Control and Signal Processing**, Sussex, v. 28, n. 2, p. 121–137, 2014.

CHEN, C.-T. **Linear system theory and design**. 3rd. ed. New York, USA: Oxford University Press, 1999.

CHEONG, S.; BITMEAD, R. R. Controller improvement via frequency response function estimates. **IFAC Proceedings Volumes**, Tarrytown, v. 45, n. 16, p. 589–594, 2012.

DE BRUYNE, F. Iterative feedback tuning for MIMO systems. *In*: INTERNATIONAL SYMPOSIUM ON INTELLIGENT AUTOMATION AND CONTROL, 2., 1997, Anchorage, Alaska, USA. **Proceedings [...]** New York: IEEE, 1997.

DE MOOR, B. *et al.* Identification of linear state space models with singular value decomposition using canonical correlation concepts. *In*: INTERNATIONAL WORKSHOP ON SVD AND SIGNAL PROCESSING, 1988, Grenoble. **Proceedings [...]** North Holland: Elsevier Science, 1988. p. 161–169.

DEHGHANI, A. *et al.* Verifying stabilizing controllers via closed-loop noisy data: MIMO case. *In*: DECISION AND CONTROL, 46TH IEEE CONFERENCE ON, 2007, New Orleans, LA, USA. **Proceedings [...]** New York: IEEE, 2007. p. 264–269.

DEHGHANI, A. *et al.* Validating controllers for internal stability utilizing closed-loop data. **IEEE Transactions on Automatic Control**, New York, v. 54, n. 11, p. 2719–2725, 2009.

DU, W. *et al.* Fault diagnosis of non-Gaussian process based on {FKICA}. **Journal of the Franklin Institute**, Tarrytown, v. 354, n. 6, p. 2573 – 2590, 2017.

FORMENTIN, S.; SAVARESI, S. M. Noniterative data-driven design of multivariable controllers. *In*: IEEE CONFERENCE ON DECISION AND CONTROL AND EUROPEAN CONTROL CONFERENCE (CDC-ECC), 50., 2011, Orlando,FL. **Proceedings [...]** New York: IEEE, 2011. p. 5106–5111.

FORMENTIN, S.; SAVARESI, S. M.; DEL RE, L. Non-iterative direct data-driven controller tuning for multivariable systems: theory and application. **Control Theory Applications, IET**, London, UK, v. 6, n. 9, p. 1250–1257, June 2012.

FRANCIS, B. A.; WONHAM, W. M. The internal model principle of control theory. **Automatica**, Tarrytown, v. 12, n. 5, p. 457–465, 1976.

FURUTA, K.; WONGSAISUWAN, M. Closed-form solutions to discrete-time LQ optimal control and disturbance attenuation. **Systems & Control Letters**, Tarrytown, v. 20, n. 6, p. 427–437, 1993.

FURUTA, K.; WONGSAISUWAN, M. Discrete-time LQG dynamic controller design using plant Markov parameters. **Automatica**, Tarrytown, v. 31, n. 9, p. 1317–1324, 1995.

GONÇALVES DA SILVA, G. R.; BAZANELLA, A. S.; CAMPESTRINI, L. On the choice of an appropriate reference model for control of multivariable plants. **IEEE Transactions on Control Systems Technology**, New York, v. 27, n. 5, p. 1937–1949, 2018.

GONÇALVES DA SILVA, G. R.; CAMPESTRINI, L.; BAZANELLA, A. S. Automating the choice of the reference model for data-based control methods applied to PID controllers. *In*: CONGRESSO BRASILEIRO DE AUTOMÁTICA, 20., 2014, Belo Horizonte. **Anais [...]** Campinas: SBA, 2014. p. 1088–1095.

GONÇALVES DA SILVA, G. R.; CAMPESTRINI, L.; BAZANELLA, A. S. Multivariable VRFT: an approach for systems with non-minimum phase transmission zeros. *In*: IEEE CONFERENCE ON CONTROL APPLICATIONS (CCA), 2016, Buenos Aires, Argentina. **Proceedings [...]** New York: IEEE, 2016. p. 1324–1329.

GONÇALVES DA SILVA, G. R.; CAMPESTRINI, L.; BAZANELLA, A. S. Multivariable virtual reference feedback tuning for non-minimum phase plants. **IEEE Control Systems Letters**, New York, v. 2, n. 1, p. 121–126, 2018.

GONÇALVES DA SILVA, G. R. *et al.* Data-driven LQR control design. **IEEE Control Systems Letters**, New York, v. 3, n. 1, p. 180–185, 2019.

GOODWIN, G. C.; GRAEBE, S. F.; SALGADO, M. E. **Control system design**. Upper Saddle River, New Jersey: Prentice Hall, 1984.

GOODWIN, G. C.; SIN, K. S. **Adaptive filtering, prediction and control**. Upper Saddle River, New Jersey: Prentice Hall, 1984.

HAVRE, K. **Studies on controllability analysis and control structure design**. 1998. PhD Thesis — Norwegian University of Science and Technology, Trondheim, 1998.

HAVRE, K.; SKOGESTAD, S. Effect of RHP zeros and poles on performance in multivariable systems. *In*: UKACC INTERNATIONAL CONFERENCE ON CONTROL'96 (CONF. PUBL. NO. 427), 1996, Exeter, UK. **Proceedings [...]** New York: IET, 1996. v. 2, p. 930–935.

HJALMARSSON, H.; BIRKELAND, T. Iterative feedback tuning of linear time-invariant MIMO systems. *In*: IEEE CONFERENCE ON DECISION AND CONTROL, 1998, Tampa, FL. **Proceedings [...]** New York: IEEE, 1998. v. 4, p. 3893–3898.

HJALMARSSON, H.; GUNNARSSON, S.; GEVERS, M. A convergent iterative restricted complexity control design scheme. *In*: IEEE CONFERENCE ON DECISION

AND CONTROL, 33., 1994, Lake Buena Vista, FL. **Proceedings [...]** New York: IEEE, 1994. v. 2, p. 1735 – 1740.

HJALMARSSON, H. *et al.* Iterative feedback tuning: theory and applications. **Control Systems, IEEE**, Piscataway, v. 18, n. 4, p. 26–41, 1998.

HUFF, D. D.; GONÇALVES DA SILVA, G. R.; CAMPESTRINI, L. Data-Driven control design by prediction error identification for a refrigeration system based on vapor compression. *In*: IFAC CONFERENCE ON ADVANCES IN PROPORTIONAL-INTEGRAL-DERIVATIVE CONTROL, 3., 2018, Gent. **Proceedings [...]** Tarrytown: Elsevier, 2018. v. 51, n. 4, p. 704–709.

HUFF, D. D. *et al.* Data-driven control design by prediction error identification for multivariable systems. **Journal of Control, Automation and Electrical Systems**, London, v. 30, n. 4, p. 465–478, 2019.

IOANNOU, P. A.; SUN, J. **Robust adaptive control**. Mineola, NY, USA: Courier Corporation, 2012.

KAMRUNNAHAR, M.; HUANG, B.; FISHER, D. Estimation of Markov parameters and time-delay/interactor matrix. **Chemical Engineering Science**, Tarrytown, v. 55, n. 17, p. 3353–3363, 2000.

KARIMI, A.; MIŠKOVIĆ, L.; BONVIN, D. Iterative correlation-based controller tuning. **International Journal of Adaptive Control and Signal Processing**, Sussex, v. 18, n. 8, p. 645–664, 2004.

KARIMI, A.; VAN HEUSDEN, K.; BONVIN, D. Noniterative data-driven controller tuning using the correlation approach. *In*: EUROPEAN CONTROL CONFERENCE, 2007, Kos Island, Greece. **Proceedings [...]** New York: IEEE, 2007.

KHAKIPOUR, M.; SAFAVI, A.; SETOODEH, P. Bearing fault diagnosis with morphological gradient wavelet. **Journal of the Franklin Institute**, Tarrytown, v. 354, n. 6, p. 2465 – 2476, 2017.

LANDAU, I. D. *et al.* **Adaptive control**: algorithms, analysis and applications. 2nd. ed. London, UK: Springer-Verlag London, 2011. XXII, 590 p.

LANZON, A. *et al.* Checking if controllers are stabilizing using closed-loop data. *In*: DECISION AND CONTROL, 45TH IEEE CONFERENCE ON, 2006, San Diego, CA, USA. **Proceedings [...]** New York: IEEE, 2006. p. 3660–3665.

LECCHINI, A.; GEVERS, M. On iterative feedback tuning for non-minimum phase plants. *In*: DECISION AND CONTROL, PROCEEDINGS OF THE 41ST IEEE

CONFERENCE ON, 2002, Las Vegas, USA. **Proceedings [...]** New York: IEEE, 2002. v. 4, p. 4658–4663.

LEWIS, F. A generalized inverse solution to the discrete-time singular Riccati equation. **IEEE Transactions on Automatic Control**, New York, v. 26, n. 2, p. 395–398, 1981.

LIM, R. K.; PHAN, M. Q.; LONGMAN, R. W. **State estimation with ARMarkov models**. Princeton, NJ: Department of mechanical and aerospace engineering, Princeton University, 1998.

LIU, X.; GAO, Z. Robust finite-time fault estimation for stochastic nonlinear systems with Brownian motions. **Journal of the Franklin Institute**, Tarrytown, v. 354, n. 6, p. 2500–2523, 2017.

LJUNG, L. **System identification**: theory for the user. 2nd. ed. New Jersey: Prentice Hall, 1999.

LORENZINI, C. *et al.* Repetitive controller with low-pass filter compensation applied to uninterruptible power supplies (UPS). *In*: INDUSTRIAL ELECTRONICS SOCIETY, IECON 2015-41ST ANNUAL CONFERENCE OF THE IEEE, 2015, Yokohama, Japan. **Proceedings [...]** New York: IEEE, 2015. p. 003551–003556.

LORENZINI, C. *et al.* The generalized forced oscillation method for tuning PID controllers. **ISA Transactions**, Tarrytown, v. 87, p. 68–87, 2019.

MACFARLANE, A. G. J.; KARCANIAS, N. Poles and zeros of linear multivariable systems: a survey of the algebraic, geometric and complex-variable theory. **International Journal of Control**, London, v. 24, n. 1, p. 33–74, 1976.

MÅRTENSSON, J.; HJALMARSSON, H. Variance-error quantification for identified poles and zeros. **Automatica**, Tarrytown, v. 45, n. 11, p. 2512–2525, 2009.

MIŠKOVIĆ, L. *et al.* Correlation-based tuning of decoupling multivariable controllers. **Automatica**, Tarrytown, v. 43, n. 9, p. 1481–1494, 2007.

MORARI, M. Internal model control - theory and applications. *In*: INTERNATIONAL IFAC/IMEKO CONFERENCE ON THE INSTRUMENTATION AND AUTOMATION IN THE PAPER, RUBBER, PLASTICS AND POLYMERISATION INDUSTRIES, 5., 1983, Antwerp. **Proceedings [...]** Tarrytown: Elsevier, 1983. v. 16, n. 21, p. 1–18.

OOMEN, T. *et al.* Iterative data-driven $\mathcal{H}_\infty$ norm estimation of multivariable systems with application to robust active vibration isolation. **IEEE Transactions on Control Systems Technology**, New York, v. 22, n. 6, p. 2247–2260, 2014.

PARK, J. **Controller certification**: the generalized stability margin inference for a large number of MIMO controllers. 2008. Thesis (Master in Electrical Engineering) — University of California, San Diego, San Diego, CA, USA, 2008.

PARK, J.; BITMEAD, R. R. Vinnicombe's winding number condition is not transitive: impacts for adaptive control. **IFAC Proceedings Volumes**, Tarrytown, v. 37, n. 12, p. 783–787, 2004.

PARK, J.; BITMEAD, R. R. Simultaneous scaling for MIMO controller certification. *In*: DECISION AND CONTROL, 46TH IEEE CONFERENCE ON, 2007, New Orleans, LA, USA. **Proceedings [...]** New York: IEEE, 2007. p. 4409–4414.

PARK, J.; BITMEAD, R. R. Controller certification. **Automatica**, Tarrytown, v. 44, n. 1, p. 167–176, 2008.

PEREIRA, L. F. A. *et al.* Multiple resonant controllers for uninterruptible power supplies – a systematic robust control design approach. **IEEE Transactions on Industrial Electronics**, New York, v. 61, n. 3, p. 1528–1538, 2014.

ROJAS, J. D. *et al.* Application of multivariate virtual reference feedback tuning for wastewater treatment plant control. **Control Engineering Practice**, Tarrytown, v. 20, n. 5, p. 499–510, 2012.

SCHEID FILHO, R. *et al.* Application of Virtual Reference Feedback Tuning to a non-minimum phase pilot plant. *In*: IEEE CONFERENCE ON CONTROL APPLICATIONS (CCA), 2016, Buenos Aires, ARG. **Proceedings [...]** New York: IEEE, 2016. p. 1318–1323.

SKELTON, R. E.; SHI, G. The data-based LQG control problem. *In*: IEEE CONFERENCE ON DECISION AND CONTROL, 33., 1994, Lake Buena Vista, FL, USA. **Proceedings [...]** New York: IEEE, 1994. v. 2, p. 1447–1452.

SKOGESTAD, S.; POSTLETHWAITE, I. **Multivariable feedback control analysis and design**. 2nd. ed. Sussex: John Wiley & Sons, 2005.

VAN HEUSDEN, K.; KARIMI, A.; BONVIN, D. Data-driven model reference control with asymptotically guaranteed stability. **International Journal of Adaptive Control and Signal Processing**, Sussex, v. 25, n. 4, p. 331–351, 2011.

VAN OVERSCHEE, P.; DE MOOR, B. **Subspace identification for linear systems**: theory–implementation–applications. London: Springer Science & Business Media, 2012.

VINNICOMBE, G. Frequency domain uncertainty and the graph topology. **IEEE Transactions on Automatic Control**, New York, v. 38, n. 9, p. 1371–1383, 1993.

VINNICOMBE, G. **Uncertainty and feedback**: $\mathcal{H}_\infty$ loop-shaping and the ν-gap metric. London, UK: Imperial College Press, 2000.

YOUSSEF, T. *et al.* Actuator and sensor faults estimation based on proportional integral observer for TS fuzzy model. **Journal of the Franklin Institute**, Tarrytown, v. 354, n. 6, p. 2524 – 2542, 2017.

YUBAI, K.; USAMI, H.; HIRAI, J. Correlation-based direct tuning of MIMO controllers by least-squares and its application to tension-and-speed control apparatus. *In*: ICCAS-SICE, 2009, Fukuoka, Japan. **Proceedings [...]** New York: IEEE, 2009. p. 931–936.